NASA CR-112160

Technology Development and Demonstration of a Low Thrust Resistojet Thruster

by
G. R. Pfeifer

Prepared Under Contract NAS1-9601
by
The Marquardt Company
Van Nuys, California
for
NATIONAL AERONAUTICS AND SPACE ADMINISTRATION
LANGLEY RESEARCH CENTER

JULY 1972

TECHNOLOGY DEVELOPMENT AND DEMONSTRATION

OF A

LOW THRUST RESISTOJET THRUSTER

By

G. R. Pfeifer

JULY 1972

Prepared under Contract NAS 1-9601 by

THE MARQUARDT COMPANY
16555 Saticoy Street
Van Nuys, California 91409

for

NATIONAL AERONAUTICS AND SPACE ADMINISTRATION
LANGLEY RESEARCH CENTER

TABLE OF CONTENTS

TABLE OF CONTENTS. -Continued

LIST OF FIGURES

LIST OF FIGURES. - Continued

LIST OF FIGURES. -Continued

LIST OF TABLES

TECHNOLOGY DEVELOPMENT AND DEMONSTRATION OF A LOW THRUST RESISTOJET THRUSTER

By: G. R. Pfeifer

The Marquardt Company
Van Nuys, California

SUMMARY

Under NAS 1-8090, resistojet thrusters incorporating high temperature rhenium technology completed high temperature (2400°K) cycling tests on experimental configuration development units. On this contract, NAS 1-9601, that technology has been extended to greatly improve the thruster thermal performance, reproducibility and structural reliability in a "Ruggedized" thruster assembly.

Three thrusters were fabricated to definitized thruster drawings using new rhenium vapor deposition technology. Two of the thrusters were operated using ammonia as propellant and one was operated using hydrogen propellant for performance determination. All demonstrated consistent operational specific impulse performance while demonstrating thermal performance better than the development units from which they evolved. Two of the thrusters were subjected to environmental structural testing including vibration, acceleration and shock loading to specifications considered applicable to future launch and space vehicle environmental considerations. Both of the thrusters subjected to the environmental tests passed all required tests. However, one was subsequently damaged during an off-limits, high level, random vibration test which was conducted to assess its design margin's capability.

The third, spare, thruster was introduced into the life test portion of the program. Two thrusters were then subjected to a life cycling test program under typical spacecraft operating power levels. During the life test sequence, the hydrogen thruster accrued 720 operating life test cycles, more than 370 on-off cycles and 365 hours of powered up time. The ammonia accrued approximately 380 on-off cycles and 392.2 on time hours of operation during the 720 cycling hour test. Both thrusters completed the scheduled operational life test in reasonably good condition, structurally integral and capable of indefinite further operation.

Completion of the life test program did uncover several deficiencies which will require minor redesign of the thruster structure to avoid future potential problem areas. Included in these problems was a requirement to further improve the electron beam weld quality control techniques to avoid minute thruster leakage and potential premature structural failure as experienced during the thruster vibration test. In addition, an anomaly was experienced with the hydrogen thruster where the inner heater element touched the adjacent heater element resulting in an inability to apply full power to the thruster under spacecraft operational conditions. These problems are considered relatively minor but must be corrected prior to submitting the thruster design to formal flight qualification test.

The program demonstrated considerable thermal and structural improvement over previously tested development units. Extended scope tests performed after the required portion of the program had been completed demonstrated structural and operational margins of the thruster. During these tests, more than 700 seconds I_{sp} was demonstrated using hydrogen as the propellant and 359 seconds I_{sp} was demonstrated using ammonia as the propellant. In addition, the valves developed and designed for use with the resistojet and used during the life test program were tested to more than 100,000 operational cycles with no deterioration in sealing or response characteristics.

Based on the favorable program results, the program should be extended to incorporate the design modifications determined necessary to avoid the minor design problems encountered and the thruster should be subjected to a flight qualification program.

INTRODUCTION

Program Objectives

The objectives of this program were to define the areas of development required to "ruggedize" a development configuration resistojet thruster unit, redesign the structure to be compatible with realistic environmental loading, and test the redesigned structure to both the defined structural loads and to a 720 hour life cycle test. An ancillary objective included the design, development and test of a bi-stable latching valve suitable for thruster propellant control. The basic objectives of the program were met and in general exceeded.

Program Organization

This program originated from the NASA Langley Research Center under Contract NAS 1-9601. Mr. Earl Van Landingham was the Technical Monitor for the Applied Rocket Research Section at Langley. The program was completed under the direction of Mr. T. Linton, Manager of Rocket Programs. The Program Manager at The Marquardt Company was Mr. Al Belsley and Mr. G. Pfeifer was the Project Engineer. Other Marquardt personnel and their areas of significant contribution to successful completion of the program included: G. Reed, Coordination of Thruster Design and Fabrication; I. C. Dickens, Structural Design; M. Wilson, Thermal Analysis; A. Malek and E. Austin, Thruster Design; R. Lynch and R. Loustau, Valve Design; J. Peterson, Thruster Fabrication and J. Haden, Experimental Laboratory Control.

Program Description

The design, fabrication and testing of the "ruggedized" resistojet thrusters described in this report represents a significant advancement in the development of a microthrust propulsion system for space application. Initial definition of a resistojet propulsion control system was developed during the MORL, Ref. 1. During that program and in follow-on programs, development configuration rhenium resistojet thrusters were fabricated and operated in long duration tests to demonstrate concept practicality. Structural and other deficiencies in the development design, however, prevented direct application of the development configuration units to a space operational mission. The present program was directed toward evaluation of potential useage environments, redesigning the thruster structure to be compatible with those environments and testing the thruster to assure that the design goals had been met. This report presents the results of that program.

Initial steps in the program were directed toward determination of realistic potential environmental loads from handling, launch vibration, acceleration, space vibration and shock. After practical definition of the loads, the thruster structure was redesigned to be compatible by repackaging the heating element system. In addition, a valve suitable for the intended usage was designed and developed and the valve and thruster integrated into a suitable mounting arrangement. Other design sophistications such as tapering the inner heating element to provide better thermal distribution were incorporated into the redesigned thruster structure.

Three thrusters were fabricated to the production type thruster drawings developed during the program. During the fabrication phase, vendors were developed for vapor deposition fabrication of all of the rhenium heating element tubes used in the thruster. Previous units were primarily made using tube stock made from rolled rhenium sheet stock. Development of controlled rhenium fabrication processes was a significant step in the thruster evolution to a producible configuration.

Two of the three thrusters fabricated, together with their valves, were subjected to environmental tests including shock, acceleration and various random and sine wave vibration environments. The thrusters passed all required tests satisfactorily, however, one of the thrusters was damaged during a high level off limits vibration test.

The third thruster was substituted for the damaged thruster and the test program was continued into the operational life test portion of the program to document life performance on hydrogen and ammonia propellants. During the life test program, the two thrusters were operated at nominally expected power levels for 720 hours of one-half hour on, one half hour off duty cycles. The hydrogen thruster experienced an anomaly wherein a portion of the innermost heating element touched the second heater element and became inactive. The test was continued under equivalent spacecraft operating conditions to determine the ultimate effect of such an anomaly on the ability to complete a typical space mission. Both thrusters completed the test in excellent structural condition. The only effect of the anomaly experienced was to reduce the amount of power which could be absorbed by the affected thruster, thereby only affecting the total mission impulse available.

After completion of all required testing, a series of off limit tests was performed on the thruster used for ammonia testing to determine reasonable upper limit performance levels for hydrogen and ammonia operation. During this test phase, more than 700 seconds specific impulse was developed using hydrogen as the propellant and 359 seconds was developed using ammonia as the propellant. These performance levels were developed well within the thermal capability limits of the thruster. In addition, the valves used on the two thrusters which completed the life test were separately tested to determine their life characteristics. After more than 100,000 cycles accrued on each of the valves, no valve leakage or anomalous operation was found.

As expected in evolution of a new design, minor design deficiencies were uncovered during the program. These included the anomalous touching phenomena previously discussed and the damage incurred to the environmental test thruster resulting from incomplete weld penetration. These occurences require further minor design iterations to preclude recurrence of the problem. With incorporation of the minor design changes required to correct the problems encounted, the thruster is ready for and should be subjected to a flight qualification program.

THRUSTER DESIGN BACKGROUND

The "Ruggedized" Resistojet Thruster, Model 110 described in this report is the product of an evolutionary development program at The Marquardt Company supported by NASA Contract NAS 1-9601. Elementary design concepts including general structural layout were developed during a NASA program conducted under Contract NAS 1-8090 to provide definition of a resistojet control system for the Manned Orbital Research Laboratory, (Reference 1). That program served to define the basic material systems compatible with the intended high performance propellants, hydrogen and ammonia, as well as mission analyses based on predicted performance obtainable with the development thruster design. The final portion of that program resulted in production of six development configuration thrusters which were ultimately tested for in excess of 7000 hours in a cycling mode to demonstrate feasibility of the resistojet concept for long term space missions where microthrust reaction control systems such as the resistojet are applicable.

The design of the thruster is based on the use of a three pass inductively heated, concentric tube heat exchanger having the following advantages: (1) gas temperatures closely approaching that of the heater wall, and (2) high heater efficiencies. Figure 1 shows the 10 millipound size concept. It consists basically of two functional parts: an electric-gas heat exchanger and a nozzle for accelerating the resulting high temperature gas to produce thrust. The electrical flow is through the outer case, case end, nozzle, and inner heating element. A strut connector provides an electrical path between the inner heating element and the second of the heater exchanger tubes while allowing gas to flow through the thruster. The gas flow between the inner and outer case, intercepts the radial-thermal flow and carries much of the heat back toward the center of the device. The gas then passes through the annulus between the inner and outer heating elements where a significant amount of gas heating takes place. The final pass is through the center tube or inner heater element, where the gas temperature very closely approximates the inner element wall temperature. The gas is then exited through the nozzle producing thrust.

The development unit life test program, (Reference 2) uncovered a number of mechanical and thermal design deficiencies required to be corrected.

Although thermal performance of the development units produced was excellent, internal design of the flow passages resulted in a non-optimum thruster temperature distribution. This caused the maximum gas temperature to be reduced prior to approaching the exit nozzle. This effect caused internal thruster temperatures to be significantly higher than desired to produce acceptable exit gas temperature and performance and to reduce the temperature safety operating margin of the thruster for a given performance level. The primary problem, however, with the development units was a structural one. Basic program objectives had been to develop a thruster structure which would

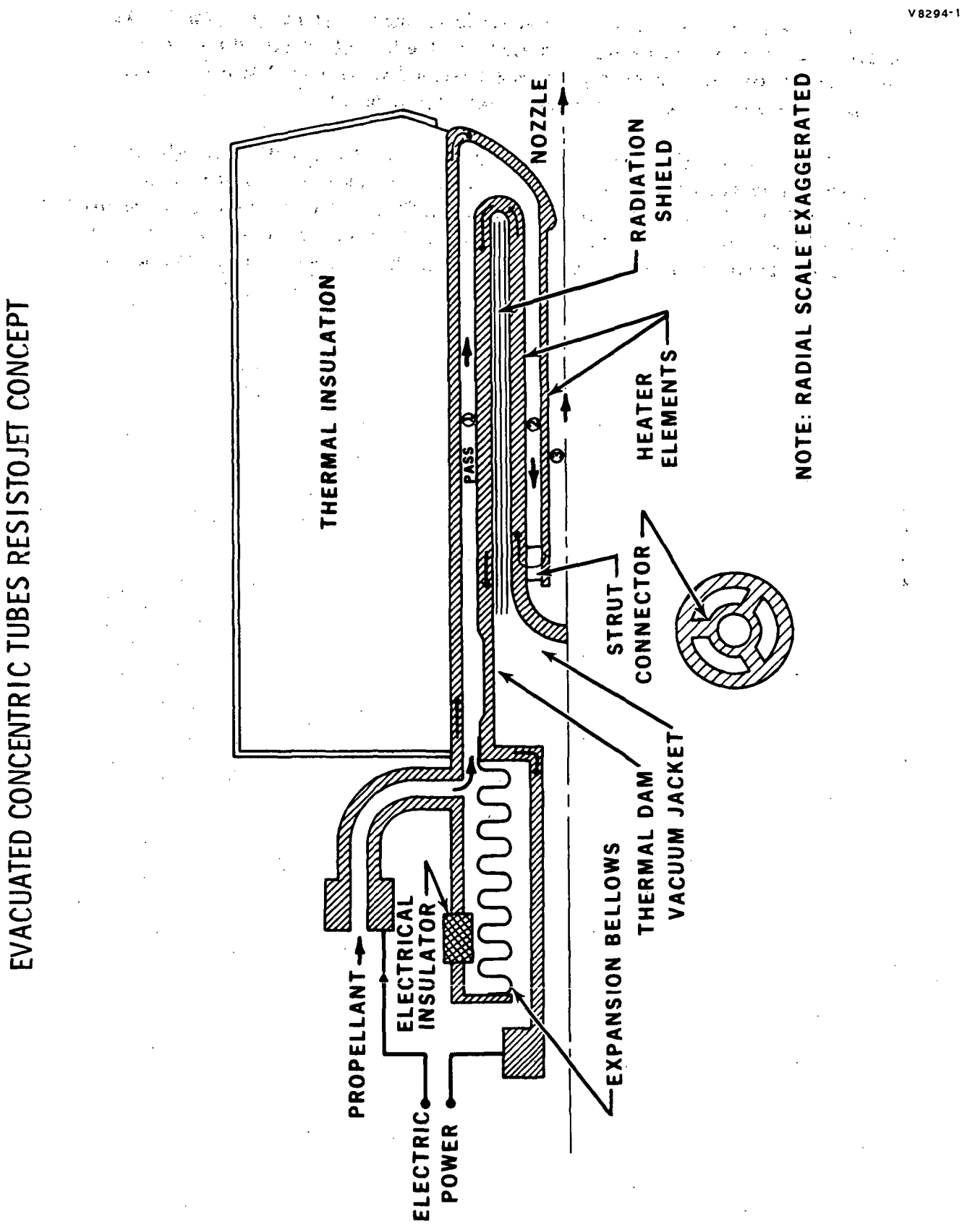
EVACUATED CONCENTRIC TUBES RESISTOJET CONCEPT
V8294-1
NOZZLE
RADIATION SHIELD
THERMAL INSULATION
PASS
HEATER ELEMENTS
NOTE: RADIAL SCALE EXAGGERATED
STRUT CONNECTOR
THERMAL DAM
VACUUM JACKET
EXPANSION BELLOWS
PROPELLANT
ELECTRICAL INSULATOR
ELECTRIC POWER

FIGURE 1.

provide the thermal performance desired from such a resistojet system. The development resistojet thruster structure evolved, while meeting the primary thermal performance objective, was not designed to withstand severe launch imposed vibration loads as a prime criteria for success.

The program discussed in this report is then the result of a NASA-funded program performed at The Marquardt Company of Van Nuys, California to "ruggedize" the thruster to withstand launch and flight environments. A secondary objective was to improve thermal performance through incorporation of design changes in the basic thruster heat exchanger passages and thermal insulation.

THRUSTER DESIGN CHANGES

The first task of the program was to analyze the Model R-100 developmental resistojet thruster (Figure 2 and Table I) previously tested on the NAS 1-8090 life test program for its ability to withstand launch conditions and space environments which are expected to be encountered by future space applications and to revise the structure to withstand those loads. A structural analysis was completed (Reference 3) and detailed redesign of the thruster structure was initiated to accommodate the design changes required. The analysis considered vibration and shock loads, environmental thermal loads, and electrical power surges from the operating power supply. Specific design changes incorporated into the Model R-110 ruggedized thruster as shown in Figure 3 were as follows:

(a) Increase in diameter of the inner heater element by approximately 30% from 0.030 inch to 0.040 inch to obtain greater column strength. Buckling of inner heating elements had been a problem noted in the development units. A further change was to increase the radial clearance between the inner and outer heating elements from a nominal 0.0123 to 0.015 inch at the minimum clearance point to eliminate potential transient touching caused by buckling of the inner heater element during either pressure or electrical transients.

(b) In order to improve the thermal distribution of the thruster by providing a higher temperature exit gas with lower thruster metal temperatures, the inner element was redesigned to vary the inner element wall thickness. The inner element wall was thinned as it approached the thruster nozzle exit. This provided increased ohmic heating of the inner heater element for obtaining a more near uniform axial temperature distribution. This design change improved the heater element's expected life at a given performance level by lowering the maximum element temperature required to obtain a given exit gas temperature.

As part of the thruster redesign, a thermal model of the thruster including its insulation system, was prepared to determine thermal gradients and to establish the most desirable thermal design approach. Radial temperature distribution was calculated for the system using John Mansville Dynaquartz and Min-K-2000. In addition, the effect of outer case surface condition was considered. A fixed inside surface temperature of 1110°K was chosen before the overall resistojet thermal circuit was run to show lower first pass wall temperatures. Two cases were considered, one with a steel case ($\epsilon = 0.45$) and the other with a gold plated and polished case ($\epsilon = 0.05$). Without plating, a case temperature

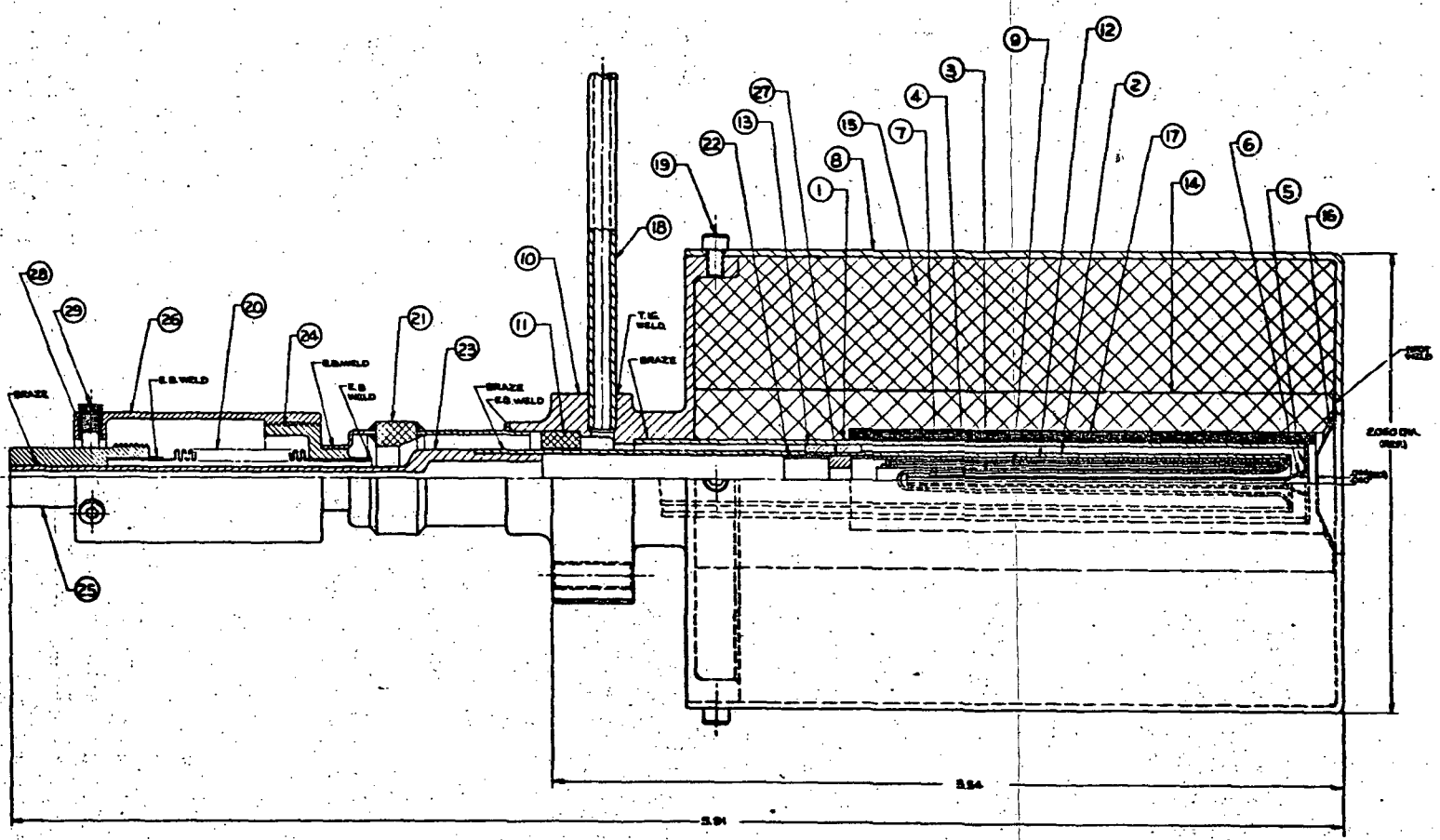

LEGEND: FOR KEY TO PARTS LABELED (1) TO (29) SEE TABLE I

FIGURE 2. MODEL-100 RESISTOJET ASSEMBLY DRAWING

TABLE I

PART LISTING FOR MODEL R-100 RESISTOJET THRUSTER

Part number and name	
1.	Outer case
2.	Inner case
3.	Outer heater
4.	Inner heater
5.	Case cover
6.	Nozzle
7.	Strut connector
8.	Housing
9.	Radiation shield, inner
10.	Housing mount
11.	Spacer ring
12.	Electrical insulator
13.	Spacers (3)
14.	Thermal insulation
15.	Thermal insulation
16.	Exit shield
17.	Radiation shield, outer
18.	Propellant tube
19.	Screws (4)
20.	Bellows
21.	Insulator fitting
22.	Snap tube
23.	Inner case stem
24.	Fitting
25.	Fitting
26.	Guard
27.	Electrical insulator
28.	Guide pins (3)
29.	Set screws (3)

RUGGEDIZED RESISTOJET THRUSTER ASSEMBLY DRAWING

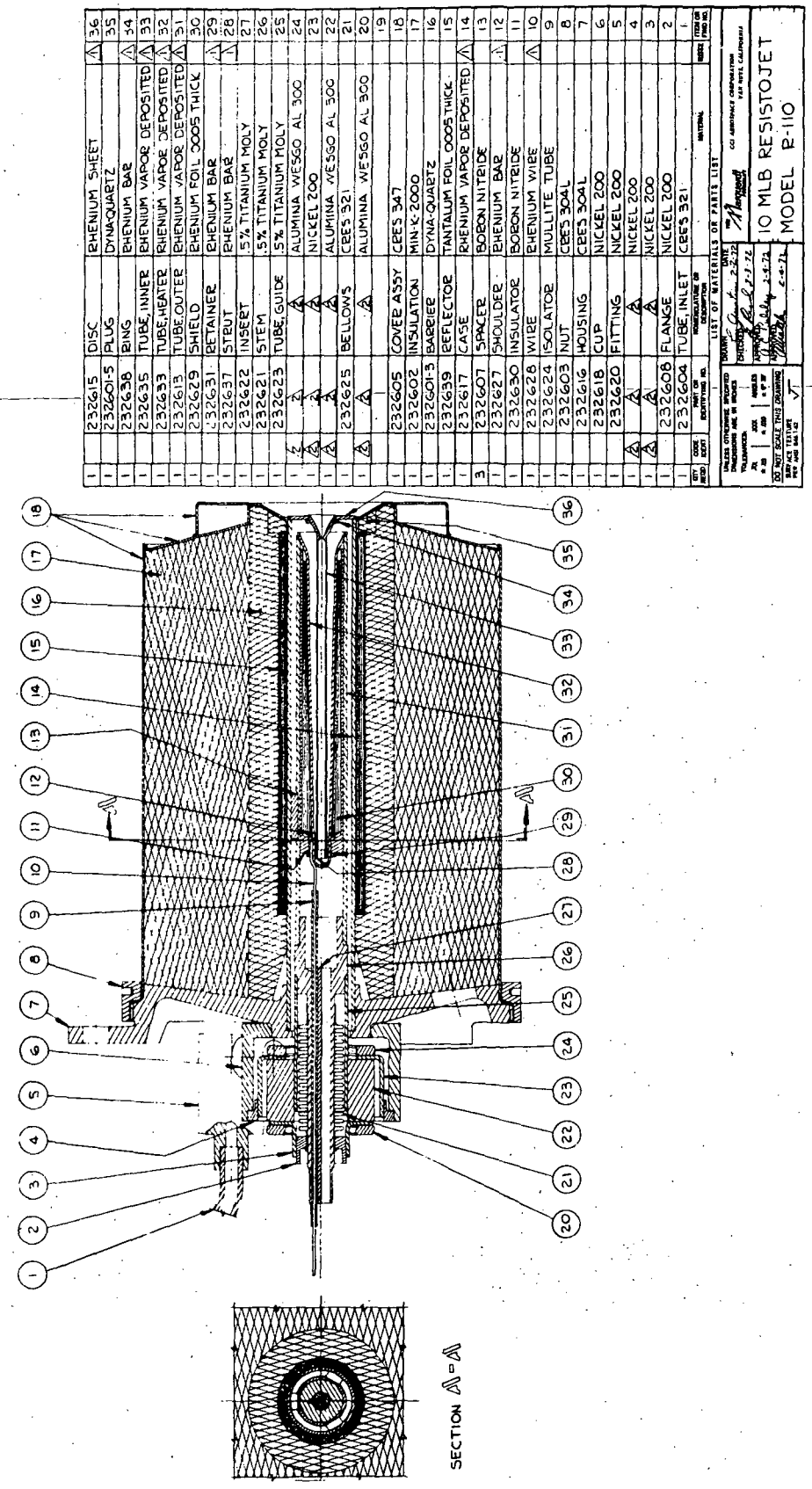

QTY	CODE IDENT	PART OR IDENTIFYING NO.	NOMENCLATURE OR DESCRIPTION	MATERIAL	ITEM OR FIND NO.
1		232615	DISC	RHENIUM SHEET	36
1		232601-5	PLUG	DYNA-QUARTZ	35
1		232638	RING	RHENIUM BAR	34
1		232635	TUBE, INNER	RHENIUM VAPOR DEPOSITED	33
1		232633	TUBE, HEATER	RHENIUM VAPOR DEPOSITED	32
1		232613	TUBE, OUTER	RHENIUM VAPOR DEPOSITED	31
1		232629	SHIELD	RHENIUM FOIL .0005 THICK	30
1		232631	RETAINER	RHENIUM BAR	29
1		232637	STRUT	RHENIUM BAR	28
1		232622	INSERT	5% TITANIUM MOLY	27
1		232621	STEM	5% TITANIUM MOLY	26
1		232623	TUBE, GUIDE	5% TITANIUM MOLY	25
1				ALUMINA WESGO AL 300	24
1				NICKEL 200	23
1				ALUMINA WESGO AL 300	22
1		232625	BELLOWS	CRES 321	21
1				ALUMINA WESGO AL 300	20
1					19
1		232605	COVER ASSY	CRES 347	18
1		232602	INSULATION	MIN-K 2000	17
1		232601-3	BARRIER	DYNA-QUARTZ	16
1		232639	REFLECTOR	TANTALUM FOIL .0005 THICK	15
1		232617	CASE	RHENIUM VAPOR DEPOSITED	14
3		232607	SPACER	BORON NITRIDE	13
1		232627	SHOULDER	RHENIUM BAR	12
1		232630	INSULATOR	BORON NITRIDE	11
1		232628	WIRE	RHENIUM WIRE	10
1		232624	ISOLATOR	MULLITE TUBE	9
1		232603	NUT	CRES 304L	8
1		232616	HOUSING	CRES 304L	7
1		232618	CUP	NICKEL 200	6
1		232620	FITTING	NICKEL 200	5
1				NICKEL 200	4
1				NICKEL 200	3
1		232608	FLANGE	NICKEL 200	2
1		232604	TUBE, INLET	CRES 321	1

LIST OF MATERIALS OR PARTS LIST

UNLESS OTHERWISE SPECIFIED TOLERANCES ARE IN INCHES
.XX ± .03 .XXX ± .010
DO NOT SCALE THIS DRAWING
REVISIONS

DRAWN DATE 2-2-72
CHECKED
APPROVED
MFG APPROVAL

GENERAL ELECTRIC COMPANY
VALLEY FORGE SPACE TECHNOLOGY CENTER

10 MLB RESISTOJET
MODEL R-110

FIGURE 3.

analytically reached 480°K, but radiative losses were reduced more than 36 percent. Based on this study, a high temperature bulk insulation (Min-K-2000) was chosen for insulation with a gold plated cover added to reduce radiation losses from the thruster.

(c) In order to improve thruster structural capability to withstand the expected launch vibration and other environmental loads, the entire thruster structure was made more compact by recessing the thermal expansion compensator within the thruster housing.

(d) As a prelude to preparation for eventual qualification test of the thruster, the thruster drawings were "productionized" i.e., converted from development sketches to checked production-type drawings. This change alone provided capability to convert the ultimate design from a single piece-custom built item, to a more producable structure with appropriate quality controls for reliable reproducibility.

In general, the productionizing process was extremely successful in that three thrusters which were made to the new drawings were virtually identical in both thermal and mechanical performance characteristics. As is usual in development of a redesigned structure, the test program uncovered areas of design requiring further minor improvement, however, on the whole, the program should be considered an unqualified success.

CONCEPT AND CONSTRUCTION

Basic Thruster

The resistojet is basically a highly efficient, multi-pass inductively heated, heat exchanger shown conceptually in Figure 1. Cold gas, either hydrogen or ammonia, enters the thruster inlet and is progressively heated as it passes through the hot heater elements. As the gas nears the thruster exit, it approached maximum metal temperature and then passes through the thruster nozzle and is accelerated in the nozzle exit trumpet creating useful thrust. The ruggedized thruster features a heat exchanger in which all heating parts are made of rhenium. This material is compatible with long term exposure to both hydrogen and ammonia at extremely high temperature. Use temperatures of 2400°K are entirely feasible and have been demonstrated resulting in extremely high gas temperatures and resultant specific impulse.

Previous development units fabricated at The Marquardt Company had been made primarily of rhenium tube either procured as tubing or as tubes made up from rolled rhenium sheet material. Vapor deposition fabrication techniques had been used to a limited extent. Parts which had been made by the vapor deposition process included the following:

(a) Thruster nozzle and strut for inner heater element - these parts were made by vapor deposition and then electron beam welded to the inner heater element.

(b) Dome transition from inner heater element to second tube - this part was fabricated by vapor deposition and then finish machined for welding into the final assembly.

The remainder of the parts were either fabricated from procured tubing (inner heater element tube) or made up from rolled sheet stock (remainder of the thruster tubes). Planning for fabrication of the ruggedized thrusters was predicated on use of prefabricated tube stock made up to size for all tubes except the inner heating element including nozzle and the dome transition section between the inner heater element and the second tube. After the start of this program, rhenium tubing became unavailable and the decision was subsequently made to fabricate all thruster tubing by the vapor deposition process.

Rather sophisticated shapes can be formed by the vapor deposition method with rhenium. Rhenium may be deposited (at a temperature 975°K) on a sacrificial material, such as titanium or molybdenum which is later removed by exposure to a hydrofluoric acid solution. The vapor deposition is usually done by passing H_2 and $ReCl_5$ over the

induction heated mandrel. The reaction,

$$5H_2 + 2ReCl_5 \longrightarrow 2Re + 10\ H\ Cl$$

takes place depositing the rhenium on the mandrel. A flow chart showing the order of steps in the rhenium fabrication process is shown in Figure 4.

Since tubing was unavailable the vapor deposition process was developed to produce the extremely tiny critical parts of the ruggedized resistojets tested during this program.

A photograph of the inner heater element vapor deposition mandrel and the vapor deposited part is shown in Figure 5. The finished part is shown in Figure 6. Comparable photographs of the second (from the inner element) heater tube mandrel, vapor deposited part and the final finished part after grinding is shown in Figures 7 and 8. The process of fabrication is one of progressive welding of the concentric tube assemblies together with appropriate pressure tests between steps to determine and prove weld integrity.

An overall view of the parts and order of assembly is given by Figure 9, a view of S/N 003 thruster after disassembly. It consists of:

(a) Inner heater element (tapered toward nozzle)
(b) Second tube (tapered outward toward nozzle joint
(c) Rhenium radiation shielding
(d) Alumina insulation shield
(e) Third tube
(f) Fourth tube which forms outer pressure case of the thruster
(g) Tantalum radiation shield
(h) Gold plated cover which contains the dyna quartz heat barrier and outer layer of Min-K insulation for reduction of external heat losses.

Within the housing subassembly shown in Figure 10 is included a stem subassembly shown in Figure 11, which incorporates the thermal compensator used to take up differential thermal expansion between the inner heater elements and outer pressure case. Isolation of the correct electrical path through the assembly is provided by an insulator located in the rear portion of the thruster housing.

The electrical insulator fitting designed for the ruggedized thruster, consisting of a metal shell brazed to an alumina tube was not commercially available at the start of the program. Therefore, a materials and braze alloy evaluation was conducted to obtain a leak-tight brazed joint. Ninety-nine percent pure alumina was selected for the insulation and Nickel 200 with expansion characteristics similar to alumina was selected for the shell. A one-half inch diameter alumina bar was metallized on the

RHENIUM CHEMICAL VAPOR DEPOSITION FABRICATION CYCLE

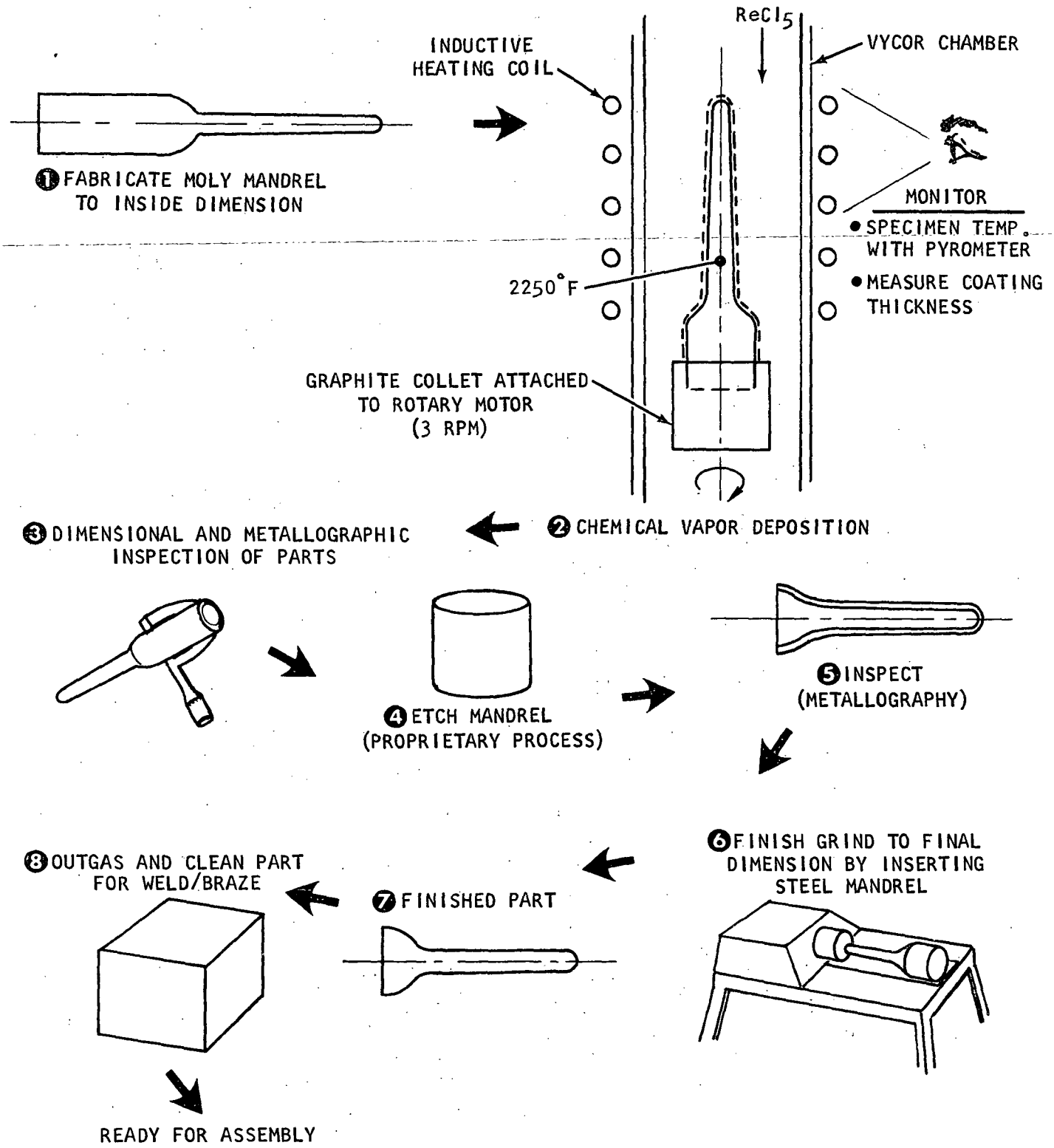

FIGURE 4.

RUGGEDIZED RESISTOJET MODEL R-110
232636 INNER TUBE MANDREL AND VAPOR DEPOSITED PART

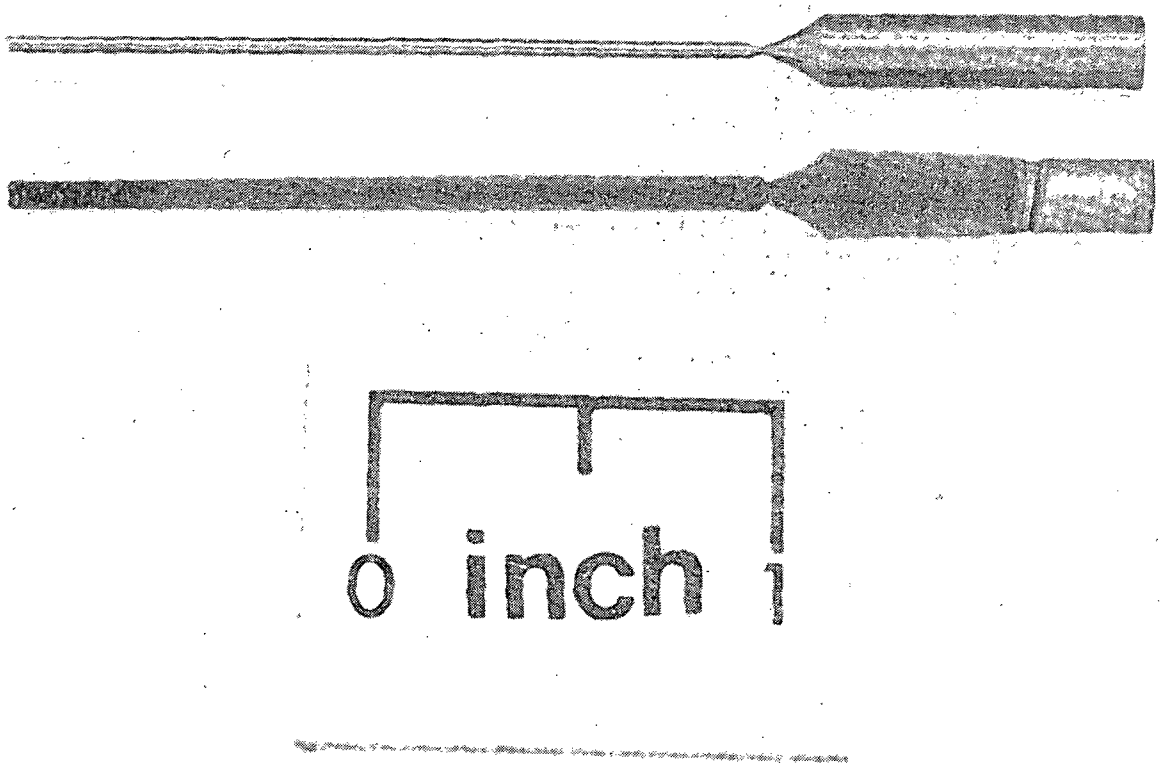

NEG. 9939-4A

FIGURE 5.

RUGGEDIZED RESISTOJET MODEL R-110
232632 TUBE SUBASSEMBLY-INNER

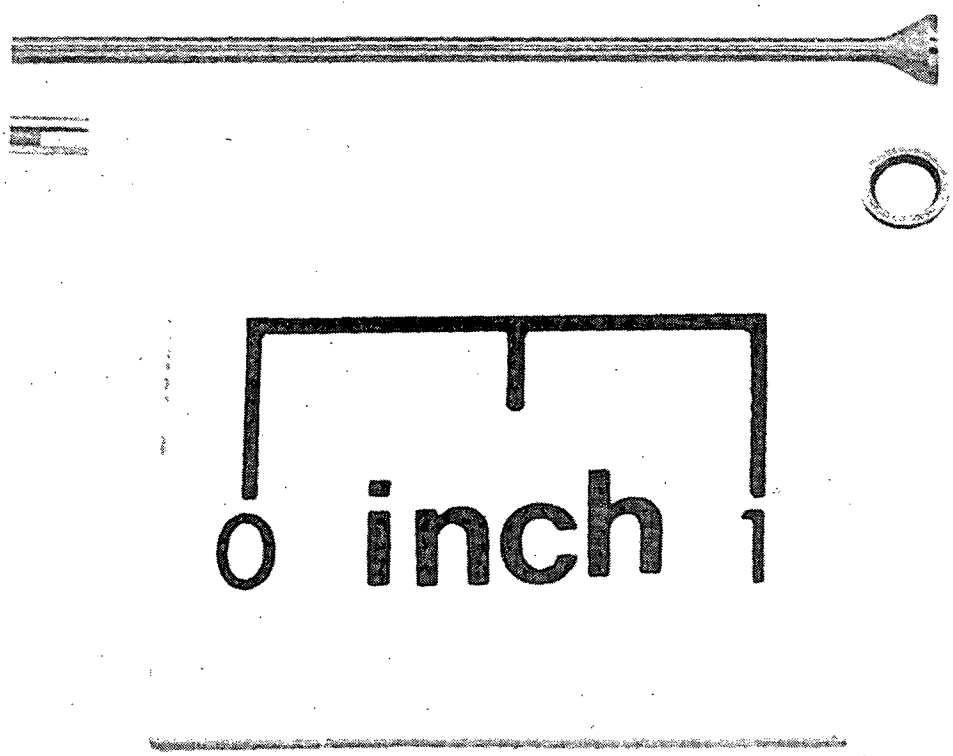

NEG. 9939-11

FIGURE 6.

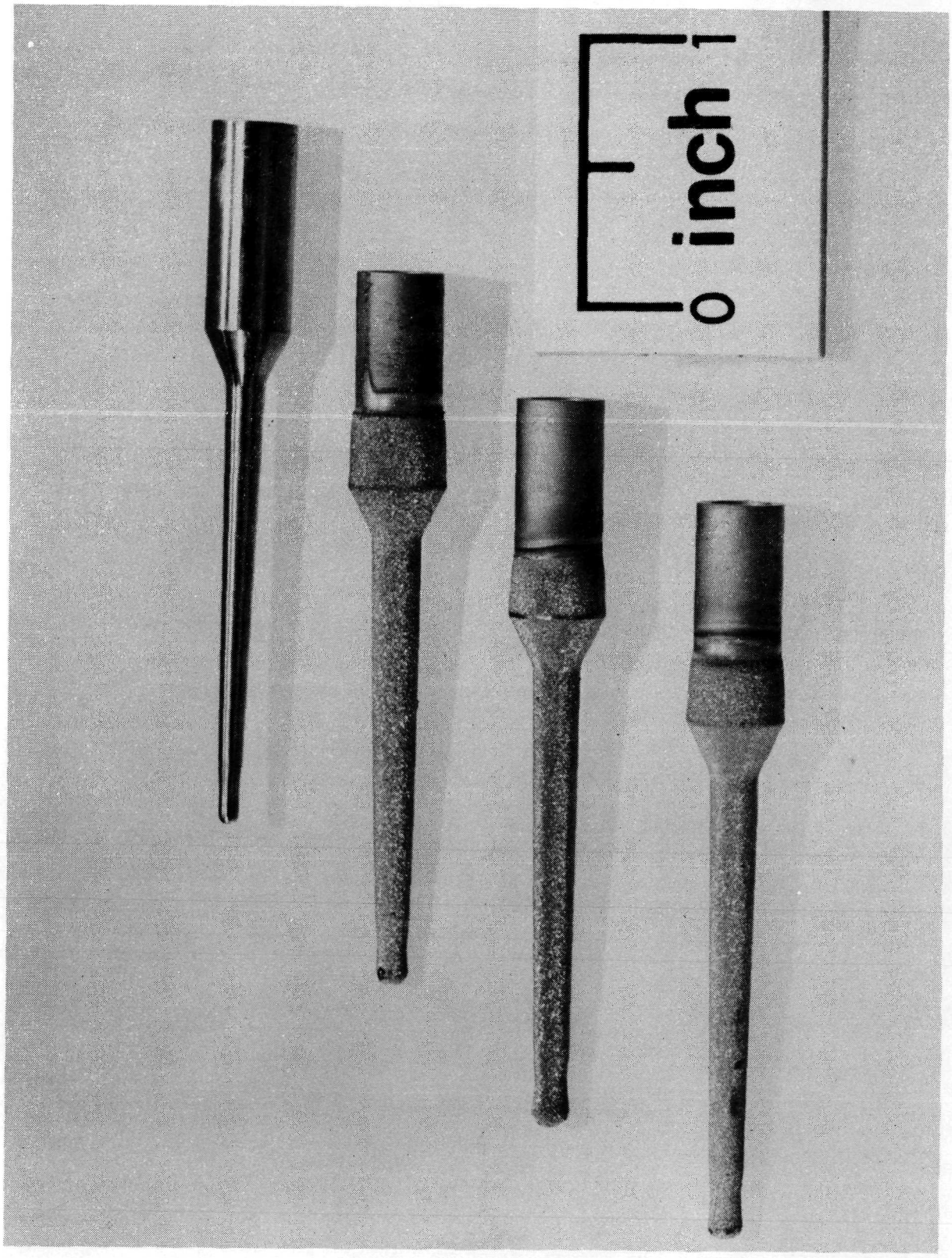

FIGURE 7. MANDREL AND VAPOR DEPOSITED PARTS FOR P/N 232634 HEATER TUBE

RUGGEDIZED RESISTOJET MODEL R-110
232633 HEATER TUBE

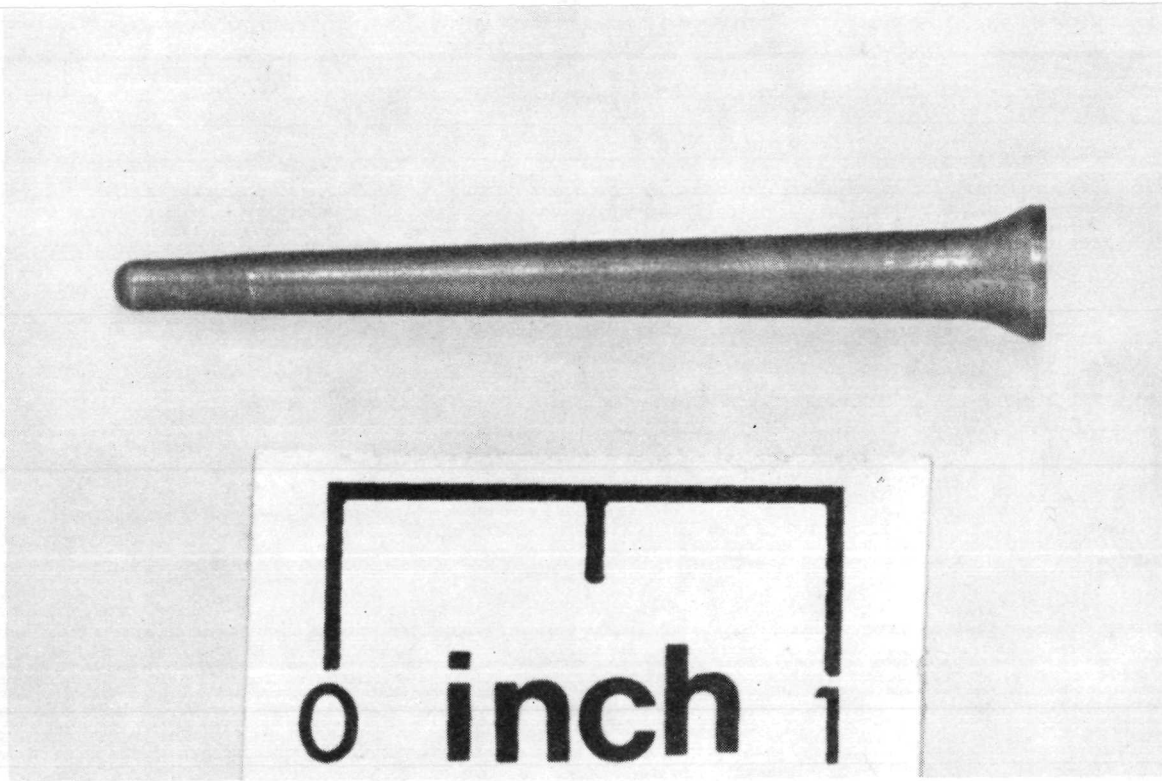

NEG. 9939-7

FIGURE 8.

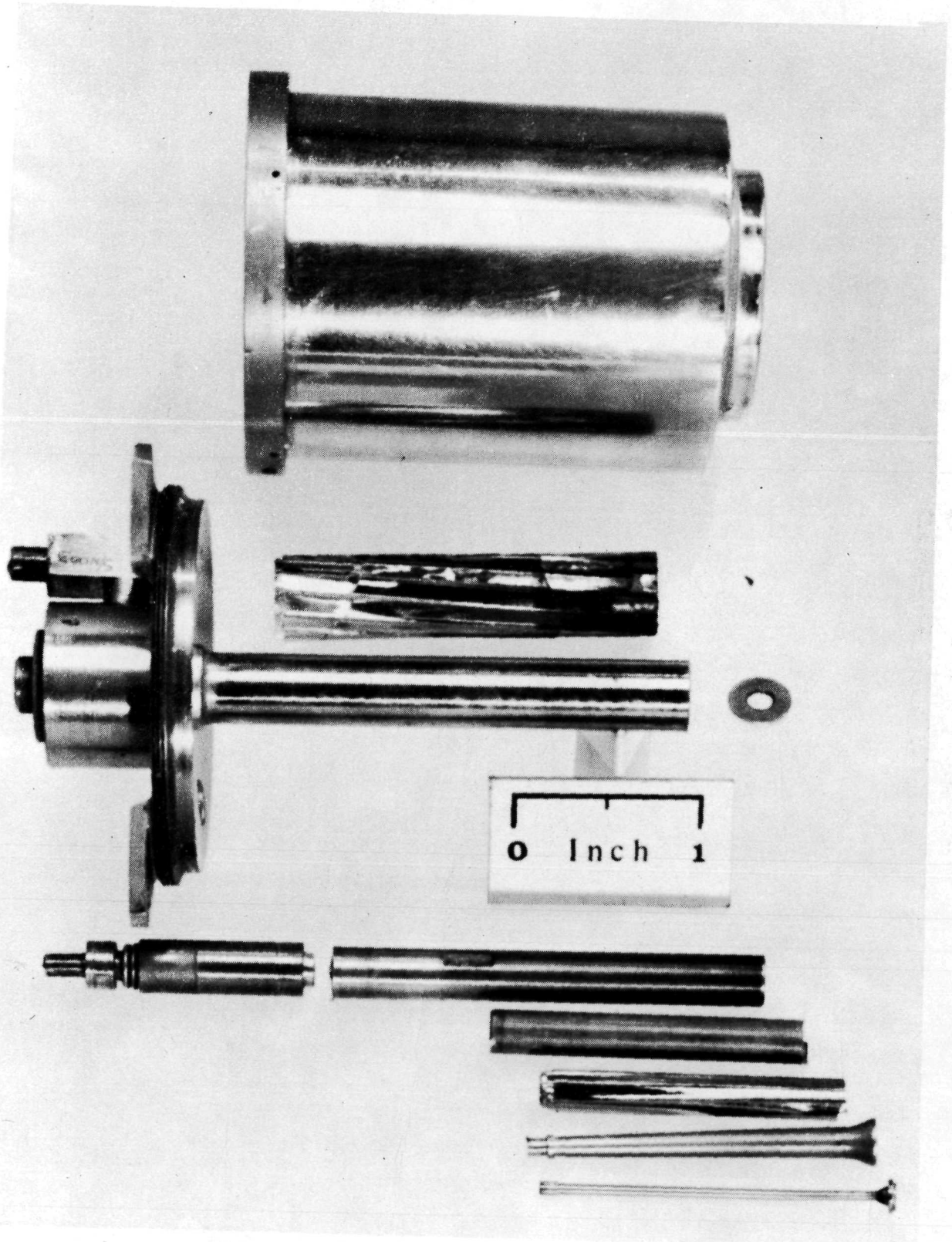

FIGURE 9. EXPLODED ASSEMBLY OF S/N 003 RUGGEDIZED RESISTOJET

RUGGEDIZED RESISTOJET MODEL R-110
232610 HOUSING SUBASSEMBLY

NEG. 9939-4

FIGURE 10.

RUGGEDIZED RESISTOJET MODEL R-110
232612 STEM SUBASSEMBLY

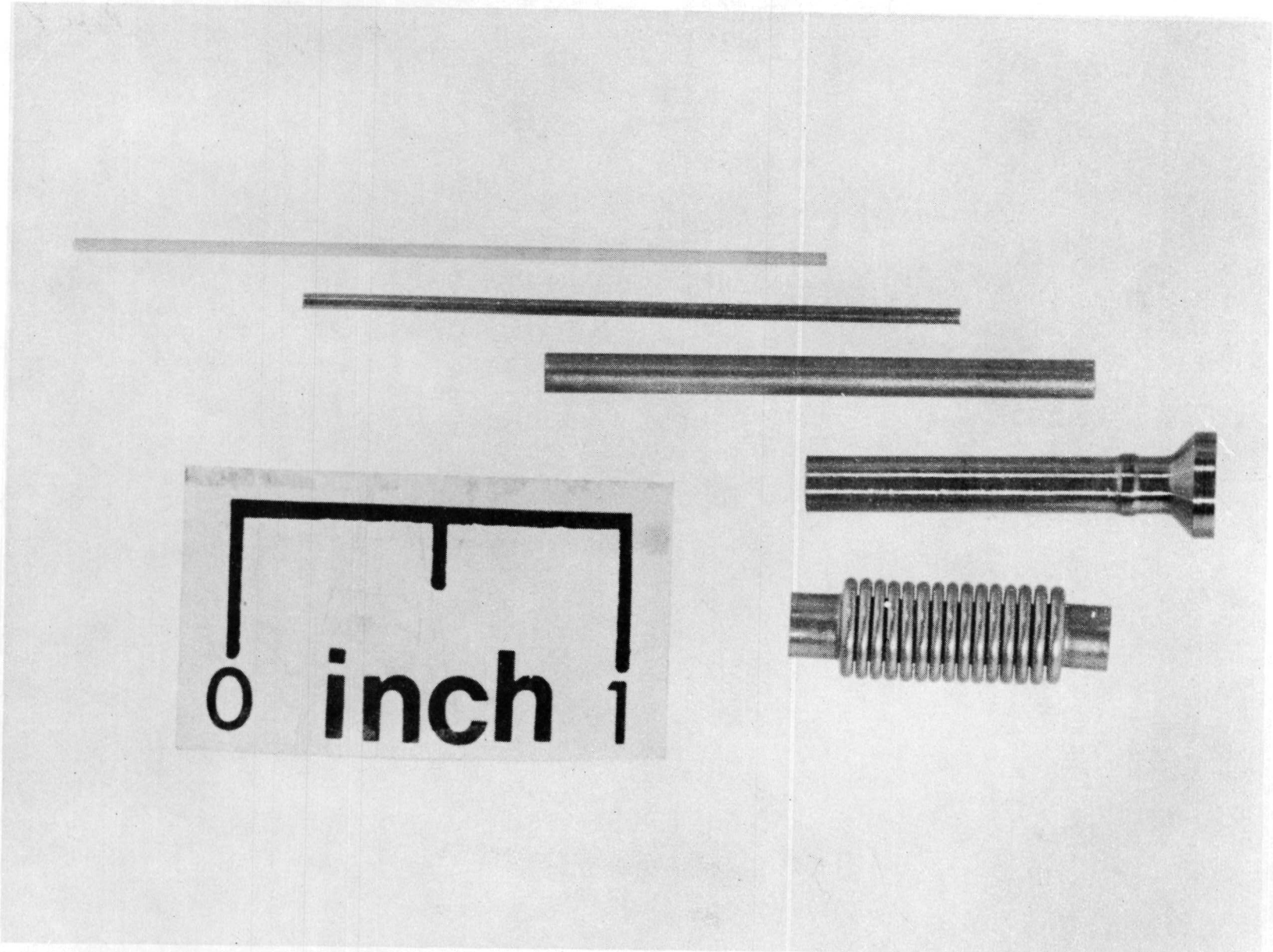

FIGURE 11.

NEG. 9939-8

A72-7-290-4

braze surface with a 0.001 to 0.0015 inch thick moly-manganese and nickel overcoat. The Nickel 200 material and the metallized surface of the ceramic were then machined to obtain a maximum 0.002 diametral clearance fit for brazing. The leak tight joint was obtained using Croniro braze alloy (72% Au, 22% Ni and 6% Cr) with a melting temperature of 1280°K in a vacuum furnace. In order to monitor voltage drop and thus power absorbed by the inner heating element, a rhenium wire was attached to the forward end of the joint between the inner and second heating element tubes as shown in Figure 12, a view of the innerbody assembly. A voltage measurement was then made using the fine wire. This provided a means for better determining the power utilization within the thruster. A photograph of the three thrusters fabricated during the program is shown in Figure 13.

Thruster Valve

One further addition the program over the previous development program included the development of a suitable latching solenoid valve for control of thruster gas flow and incorporation of the valve into the resistojet assembly structure. Design and development of the valve used for the program is discussed in Volume II of this report. A photograph of the valve is shown in Figure 14. Final assembly of the thruster required design and incorporation of a mounting bracket to hold both the thruster and the gas control valve. A photograph of the forward end of the completed assembly including the mount bracket and valve is shown in Figure 15. For comparison purposes, a photograph of one of the ruggedized thrusters with valve is shown with one of the original life test development units in Figure 16. It is interesting to note that the entire ruggedized thruster assembly including its mount bracket and valve is considerably shorter and more compact than the original development unit. The program results justify the efforts involved in redesign; a more compact, stronger structure evolved which is thermally superior to previous designs.

RUGGEDIZED RESISTOJET MODEL R-110
P/N 232609 INNERBODY SUBASSEMBLY

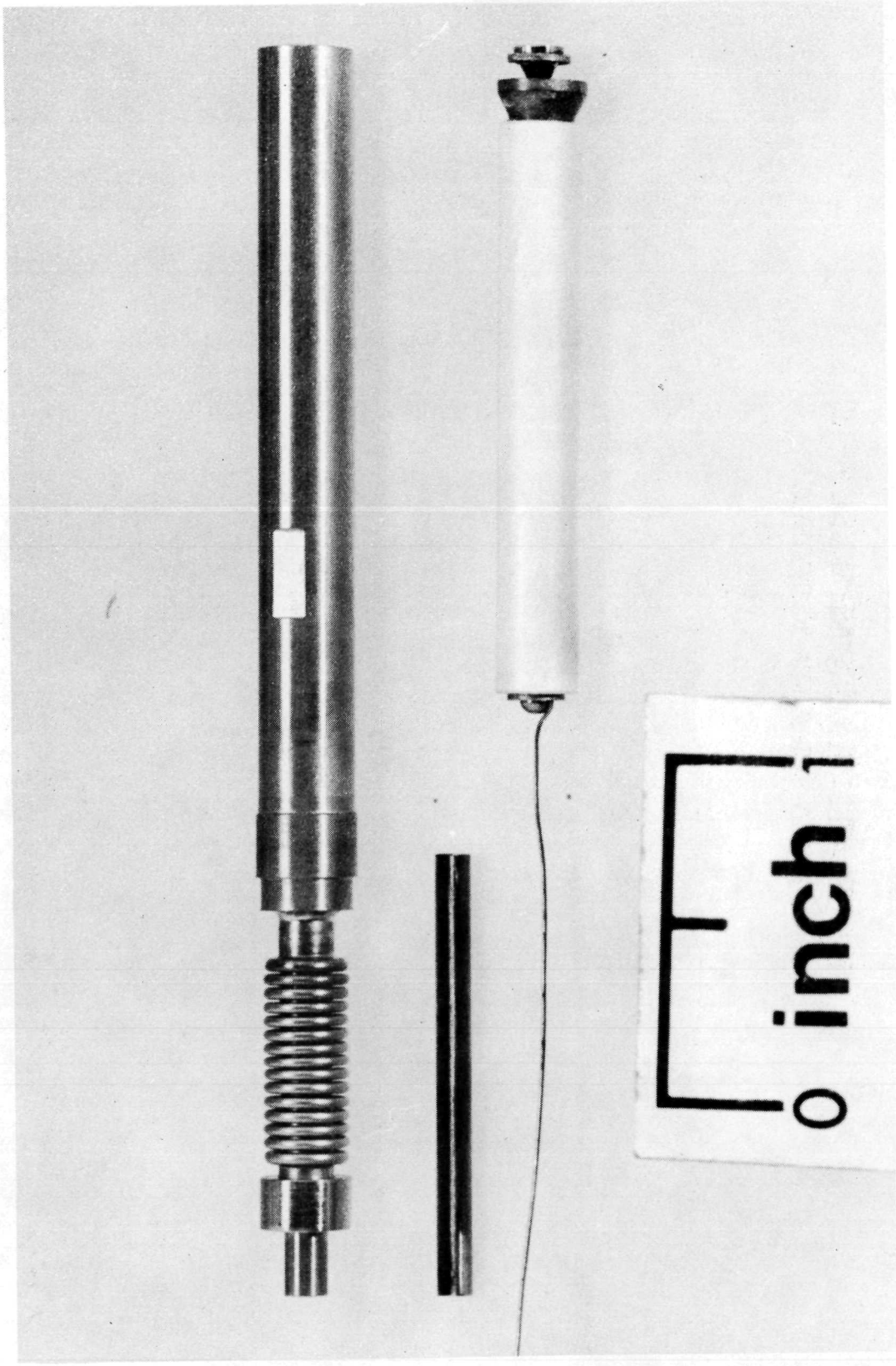

FIGURE 12.

RUGGEDIZED RESISTOJET MODEL R-110
232600 THRUSTER ASSEMBLIES

EG. 9939-28

FIGURE 13.

BISTABLE VALVE
P/N X28050

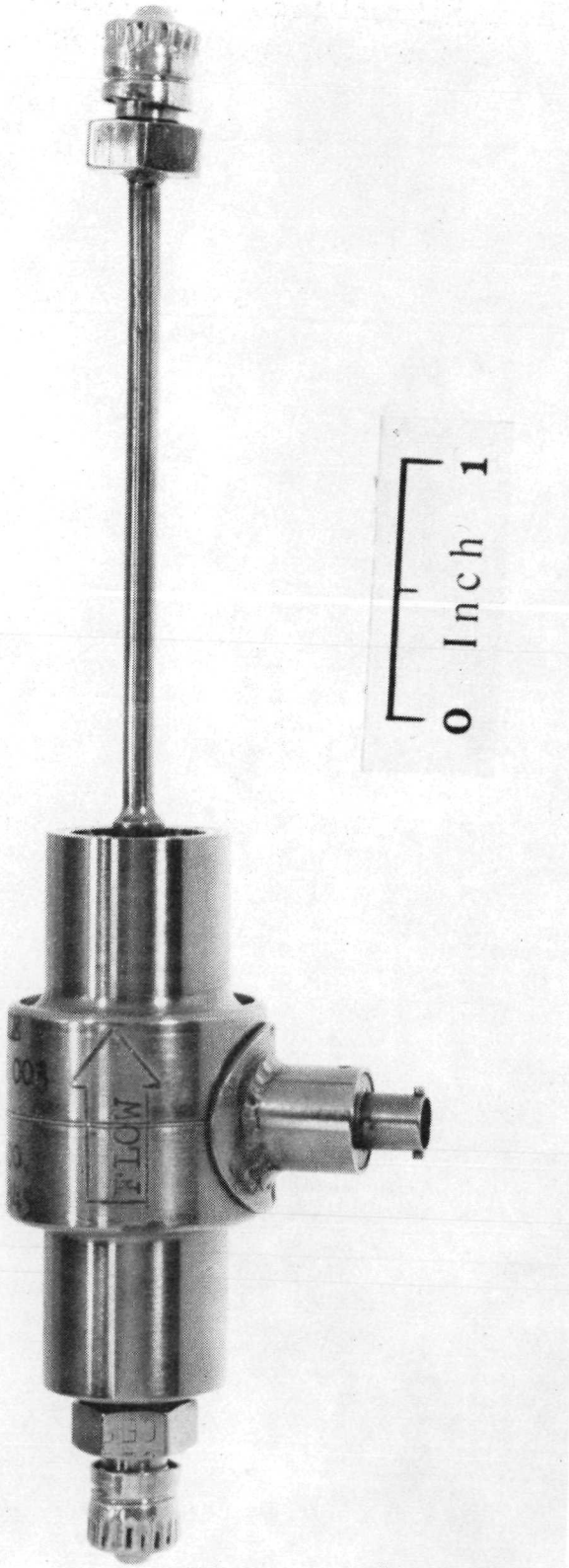

NEG. 71-151-1

FIGURE 14.

RUGGEDIZED RESISTOJET MODEL R-110
P/N 28200 RESISTOJET ASSEMBLY

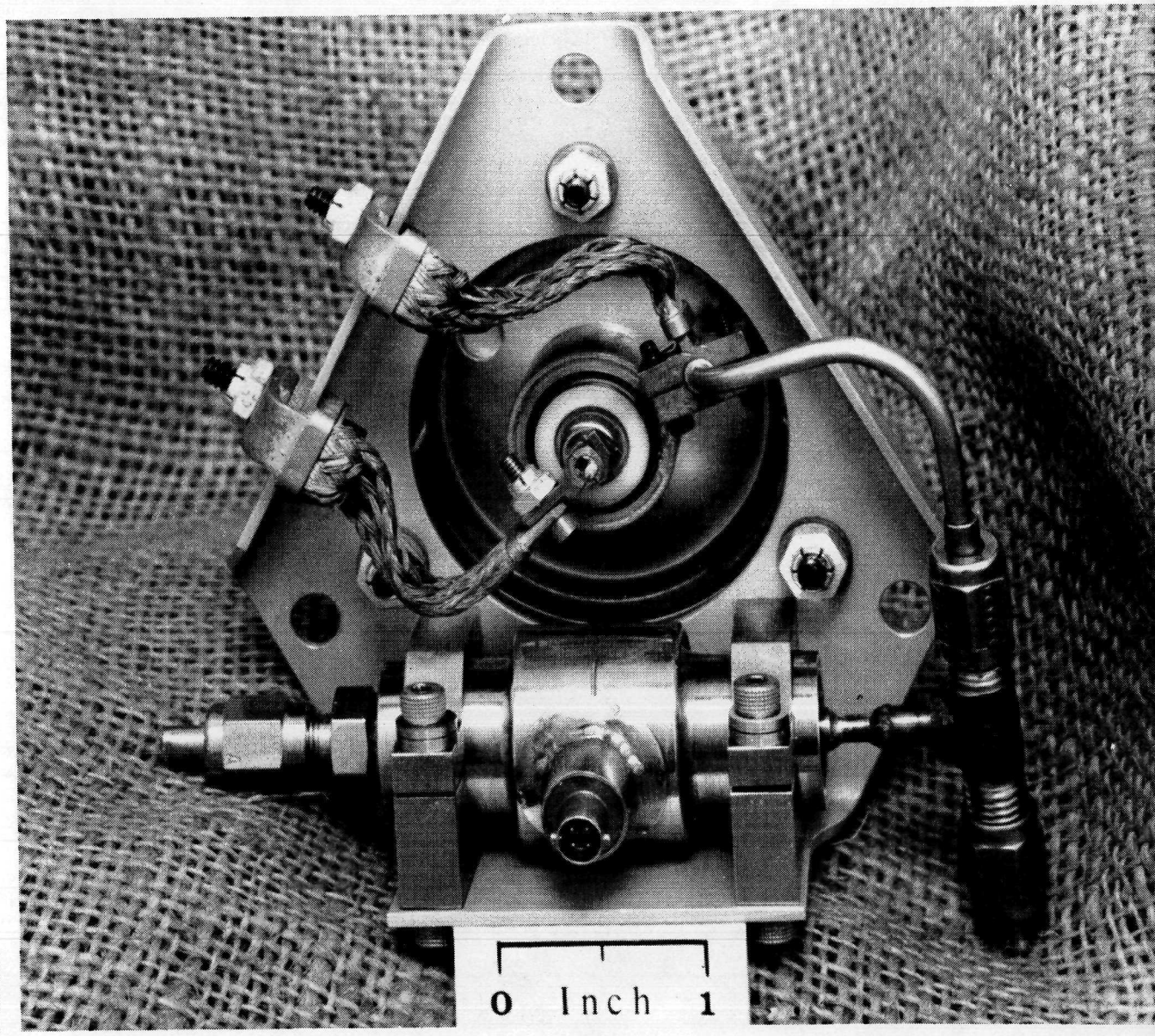

NEG. 9939-30

FIGURE 15.

RUGGEDIZED RESISTOJET THRUSTER WITH LIFE TEST THRUSTER

FIGURE 16.

THRUSTER ENVIRONMENTAL TESTS

Test Summary

Dynamic environmental tests including shock, acceleration, and random and sinusoidal vaibration were conducted on two Model R-110 resistojet thruster assemblies of which the thruster latch valves were an integral part. These tests were conducted at the Durkee Environmental Laboratories of Torrance, California. In addition to the contract work statement requirements, additional tests and data acquisition were also included in the test program to better define natural frequencies and amplification factors for the critical components of the thrusters.

The additional tests performed included the following:

1. Sinusoidal sweeps on the individual thruster assemblies at the beginning and end of the program.

2. S/N 003 resistojet thruster assembly was subjected to a substantially higher random vibration spectrum to provide confidence in the design margins of the thruster as well as provide a better definition of the natural frequencies and amplification factors of the thruster assembly.

3. Detailed instrumentation including a micro minerature accelerometer mounted on the heater tube stem was recorded during the vibration tests. Figure 17 defines the accelerometer locations for the vibration tests.

Except for the failure of a non-flight type weld on the inlet supply line of thruster S/N 001, both thrusters completed all the specification dynamic environment tests in excellent condition as evidenced by detailed visual examination and resistance and leakage tests. Following completion of the specification required tests, the S/N 003 resistojet thruster assembly was subjected to a substantially higher random vibration spectrum (37 g_{rms}) to evaluate the design margins of the assembly. The electron beam weld between the nozzle and the outer pressure case failed during this out of specification vibration condition. Post test inspections of both latching solenoid valves, including the one which was subjected to the 37 g_{rms} spectrum, revealed that both were in excellent condition.

Tests Performed

Detailed descriptions of the work statement required tests conducted are presented in the following paragraphs:

VIBRATION TEST ACCELEROMETER LOCATIONS

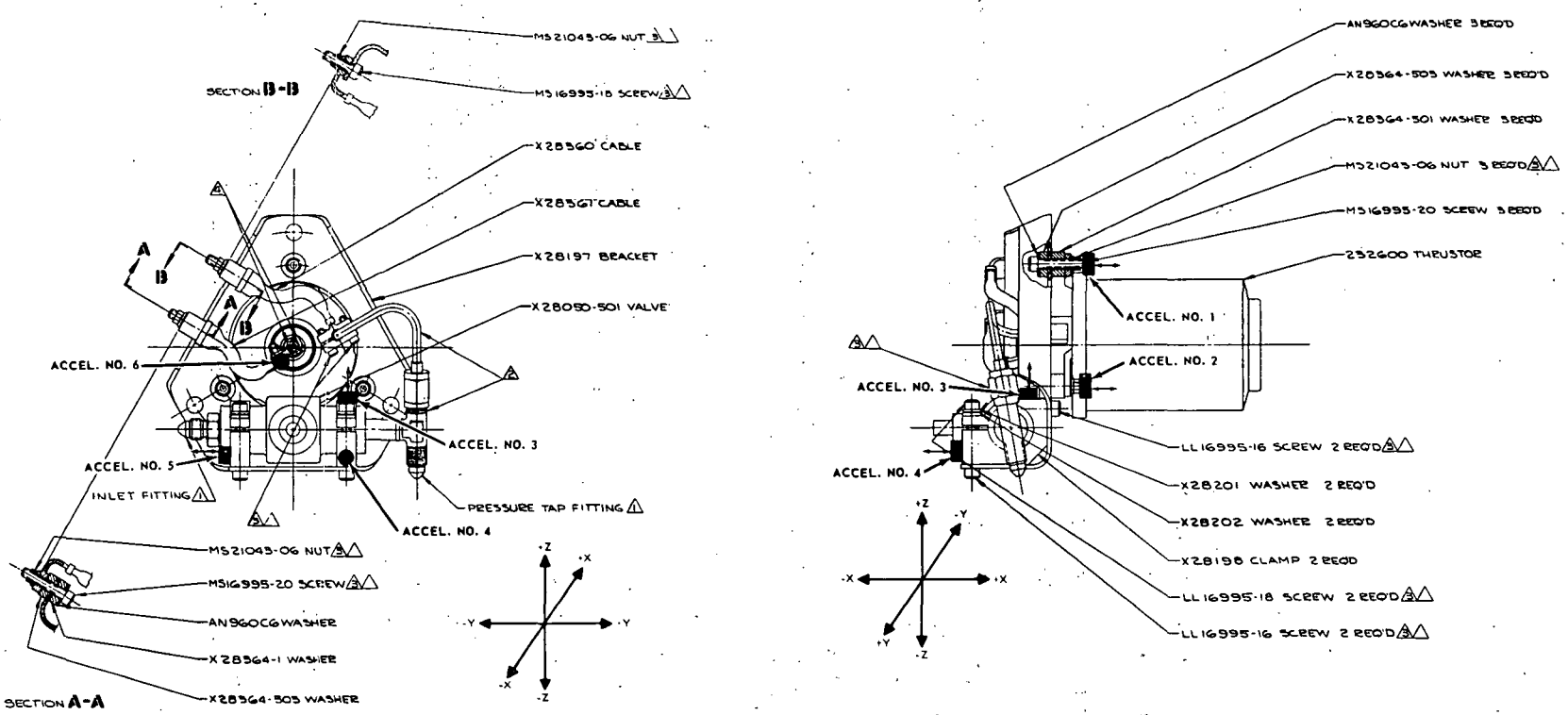

FIGURE 17.

Sinusoidal sweeps. Each resistojet assembly was individually subjected to the following sine sweep test to define the natural frequencies and amplification factors for the critical components. Tests were conducted in each of three mutually perpendicular axes at a sweep rate of one octave/minute. A photograph of a typical vibration test setup is shown in Figure 18.

20	to	60 cps, 0.13 g peak
60	to	235 cps, 0.00071 inch (double amplitude)
235	to	2000 cps, 2.0 g peak

Flight environment - sinusoidal vibration. - Both resistojet assemblies were subject to the following vibrations in each of three mutually perpendicular axes at a sweep rate of 3 octaves/minute.

1.5 to 8.5 cycles/sec, 0.12 in. double amplitude
8.5 to 30 cycles/sec, 0.48 g peak.

Ground handling environments - vibration test. - Both assemblies were subjected to the following vibration in each of three mutually perpendicular axes at a sweep rate of 1 octave/minute.

5.0	to	27.5 cps ± 1.56 g
27.5	to	53 cps - 0.043 double amplitude
52.0	to	500 cps ± 6.0 g

Shock test - The two ruggedized resistojet assemblies were mounted on a shock test fixture and subjected to one shock of 30 $^{+5}_{-0}$g over a duration of 11 ± milliseconds, with terminal peak sawtooth pulse, in two diametrical opposite directions for each of the three mutually perpendicular axes. A photograph of the shock test setup is shown in Figure 19.

Acceleration test. - The two ruggedized resistojet assemblies were mounted on the arm of a centrifuge. Acceleration of 8 g for 120 seconds was applied in each direction for three mutually perpendicular axes. A photograph of the thrusters mounted on the centrifuge is shown in Figure 20.

Flight environment - random vibration. -

The two ruggedized resistojet assemblies were subjected to the following vibrations in each of three mutually perpendicular axes.

TYPICAL VIBRATION TEST SETUP

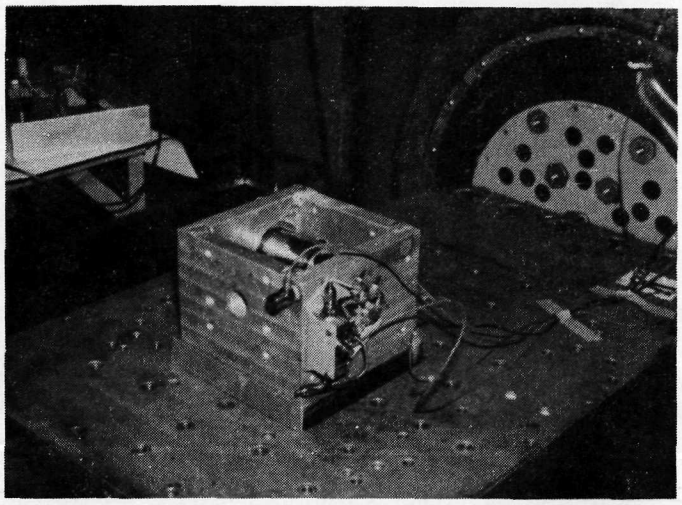

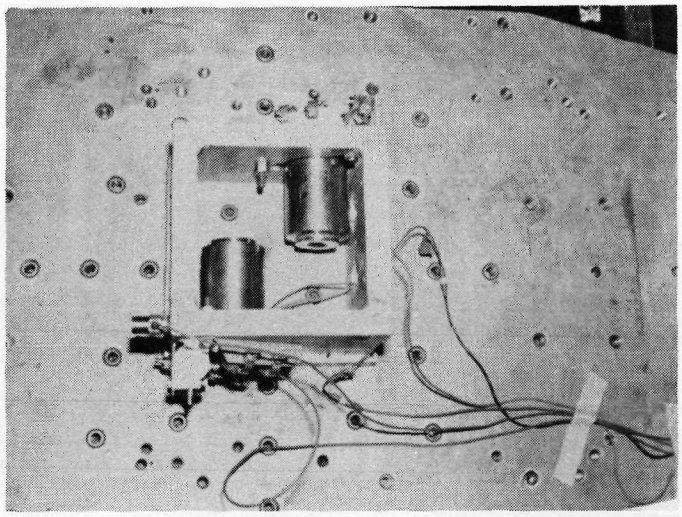

FIGURE 18.

TYPICAL SHOCK TEST SETUP AND SHOCK INPUT SPECTRUM

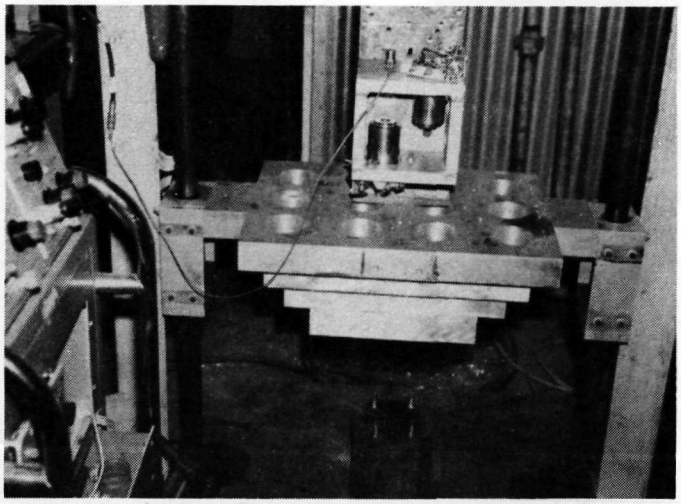

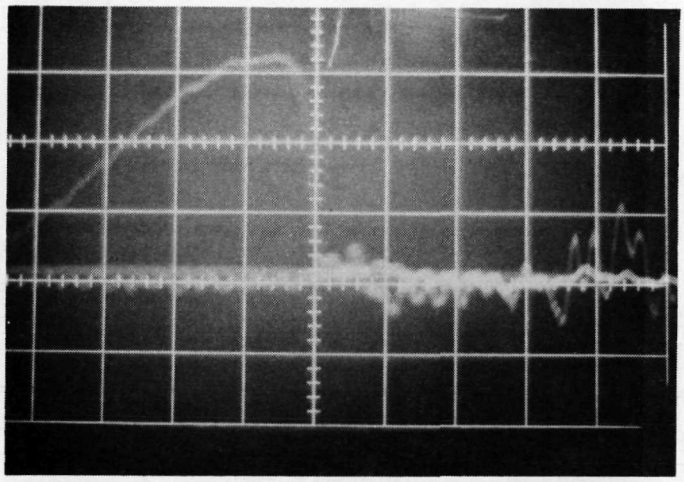

FIGURE 19.

TYPICAL ACCELERATION TEST SETUP

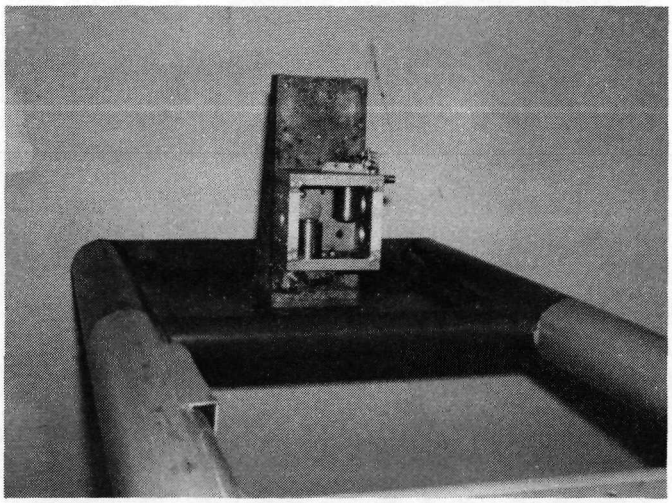

FIGURE 20.

Lower Level - One Minute Per Axis

20 to 100 cps, 0.5 g^2/cps PSD (Power Spectral Density)
100 to 200 cps, decreasing PSD @ 6 db/octave
200 to 400 cps, 0.13 g^2/cps PSD
400 to 470 cps, decreasing PSD @ 9 db/octave
470 to 1500 cps, 0.08^2/cps PSD
1500 to 2000 cps, decreasing PSD @ 9 db/octave
2000 cps, 0.032 g^2 PSD

Higher Level - Two Minutes Per Axis

20 to 100 cps, .018 g^2/cps PSD
100 to 200 cps, decreasing PSD @ 6 db/octave
200 to 400 cps, 0.047 g^2/cps PSD
400 to 470 cps, decreasing PSD @ 9 db/octave
470 to 1500 cps, 0.029 g^2/cps PSD
1500 to 2000 cps, decreasing PSD @ 90 db/octave
2000 cps, 0.012 g^2/cps PSD

During the higher level random vibration, the inlet supply line between the valve and the instrumentation fitting failed at the connecting weld joint as shown in Figure 21. This failure was not considered significant since this element of the thruster assembly is non-representative of a flight-type design. On subsequent designs, the following typical changes would be implemented to eliminate the experienced failure mode.

(1) Relatively heavy instrumentation fittings would be eliminated or at least not cantilevered from a thin support tube.

(2) Appropriate tie-down of the feed lines and connecting fitting would be made to the basic structural support bracket to eliminate critical resonant frequencies and excessive movement of such parts.

All other post-test checks of the thrusters, including resistance and leakage checks, showed both thrusters to be in excellent condition except for the above noted supply line discrepancy.

Off-specification high level random vibration test.- S/N 003 ruggedized resistojet assembly was subjected to the following off-specification high level random vibration test to evaluate the design margins of the thruster as well as to provide a better definition of the natural frequencies and amplification factors of the thruster assembly.

RUGGEDIZED RESISTOJET THRUSTER S/N 003 AFTER DYNAMIC ENVIRONMENT TESTS

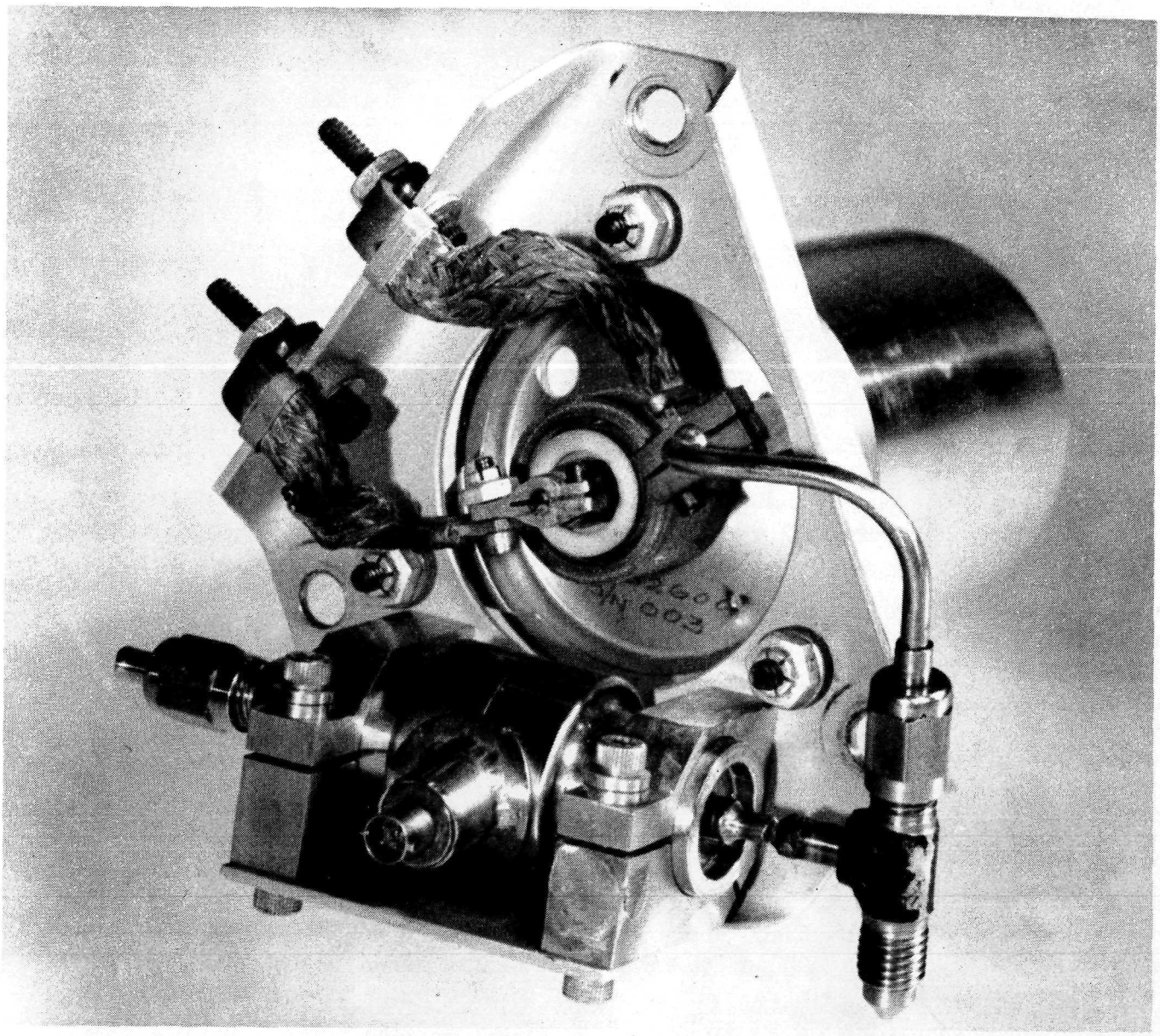

NEG. 9939-35

FIGURE 21.

20 to 100 cps, increasing PSD to 1 g^2/cps @ 6 db/octave
100 to 1000 cps, 1 g^2/cps PSD
1000 to 2000 cps, decreasing PSD @ 10 db/octave

A comparison of this vibration spectrum is shown in Figure 22 along with the two random vibration spectrums specified by the work statement. The S/N 003 resistojet assembly was subjected to the following tests at these off-specification vibration levels before terminating the test:

X axis - 2 minutes
Z axis - 2 minutes

Following the tests in the Z axis, it was noted that the Electron Beam weld between the nozzle and the outer case had failed. A close-up photograph of the discrepancy is shown in Figure 23. Results of the metallographic examination to determine the cause of failure revealed that inadequate penetration of this critical weld had occurred during the fabrication process. Detailed discussion of this examination is presented in the following section (Metallographic Analysis).

Post-test sinusoidal sweeps - S/N 001 resistojet thruster assembly was subjected to the following sine-sweep test to determine if any of the critical natural frequencies and associated amplification factors had shifted from those documented during the pre-test sinusoidal sweeps. Tests were conducted in each of three mutually perpendicular axes at a sweep rate of one octave/minute.

20 to 60 cps, 0.13 g peak
60 to 235 cps, 0.00071 inch (double amplitude)
235 to 2000 cps, 2.0 g peak

No significant shifts in the dynamic response characteristics from the pre-test sinusoidal tests were noted on the S/N 001 resistojet thruster assembly.

Post-Test Checks and Inspection

Periodic resistance and leakage tests were conducted on both S/N 001 and S/N 003 resistojet assemblies during the test program. As previously noted, both resistojet assemblies were in excellent condition following completion of all dynamic environment tests required by the work statement except for the failure of the non-flight type weld on the inlet supply line tubing, i.e., no significant changes in thruster resistance and no apparent valve leakage.

RAMDOM VIBRATION SPECTRUM COMPARISON

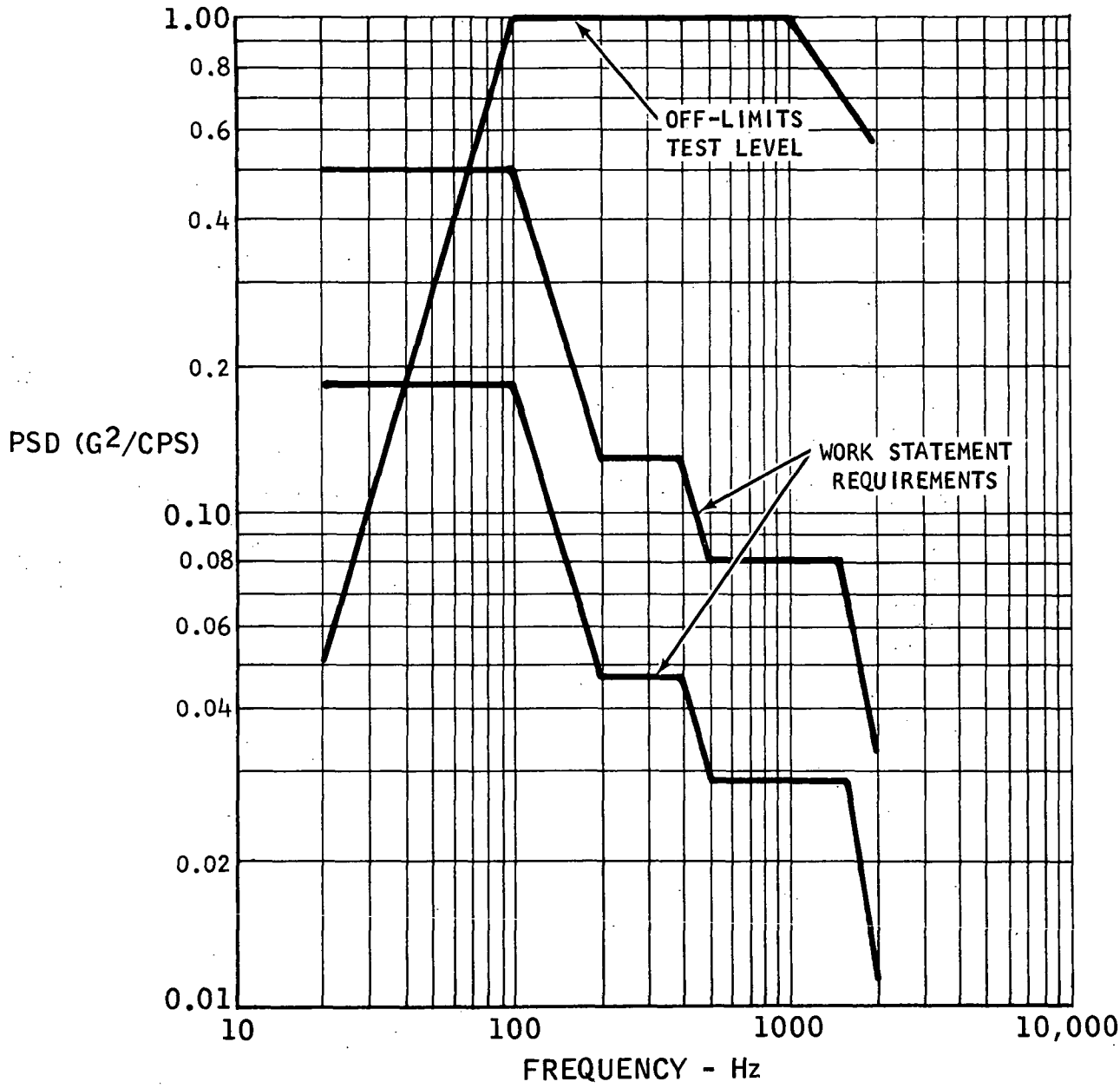

FIGURE 22.

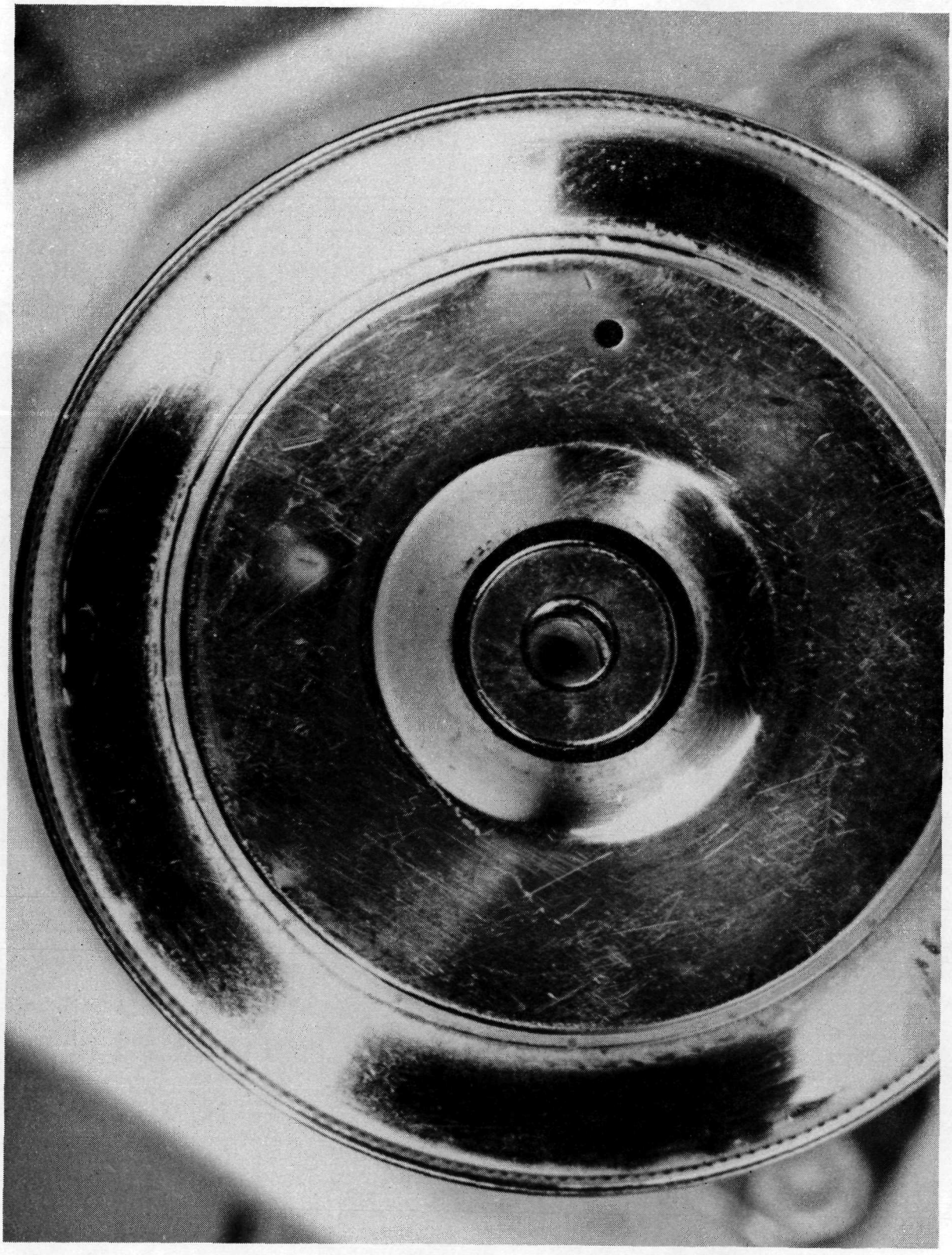

NEG. 9939-36

FIGURE 23. NOZZLE WELD FAILURE OF S/N 003 THRUSTER FOLLOWING THE OFF-LIMITS VIBRATION TEST

After return of the thruster assemblies to Marquardt, the latching solenoid valves were subjected to detailed component bench tests. Both valves, including the one on S/N 003 resistojet assembly which had been subjected to out of specification high level random vibration tests, proved to be in excellent condition. Zero leakage was exhibited at test pressures of both 20 and 100 psia and the pull-in current and drop-out current characteristics repeated consistently with their pre-test values.

Analysis of the vibration data showed good agreement between the predicted and actual natural frequencies of the critical components. However, the amplification factors for the heater tube was substantially less than previously used in the structural analysis (Reference 3). The structural analysis which used a conservative amplification factor of twenty to twenty-five because of the many variables and unknowns that were required to be assumed in the structural model is approximately five times greater than the actual dynamic response characteristics exhibited by these resistojet assemblies.

Refinement of the amplification factors provided a very important input into the design requirements for the biowaste thrusters being developed on NASA Contract NAS 1-9474.

Metallographic Analysis of S/N 003 Thruster Electron Beam Weld Failure

S/N 003 thruster incurred damage to the nozzle to end-case electron beam weld (See Figure 23) during the off-limits vibration test. Detailed metallographic examinations were made to determine the quality of this weld (E. B. #6 of Figure 24) as well as the other critical welds of this thruster (E. B. #2 and #4 of Figure 24).

Figure 25 shows macrophotos of both sides of the P/N 232615 disc. The exit side of the disc, which is the side from which the electron beam weld was initiated, indicates an excellent weld. However, the other side of the disc shows little or no penetration occurred through the disc to the backup ring (P/N 232638). The disc was subsequently cross-sectioned for further detailed metallographic examination. Figures 26 and 27 show respectively the exit side and interior side of the cross-sectioned disc. The exit side definitely shows a weld fillet had occurred between the exit end of the disc and the exit end of the inner tube, P/N 232635. The degree of penetration of the weld cannot be determined since the microstructure of the entire disc had been recrystallized from previous testing as shown by the etched microphotographs on the bottom of Figures 26 and 27. However, it appears that the weld did not penetrate all the way through to the interior side of the disc since Figure 27 shows the apparent original chamfer of the edge and no evidence of a weld fillet. The conclusion based upon the above examination is that the electron beam weld of the nozzle to exit disc (E. B. #6 of Figure 24) was definitely of non-optimum quality.

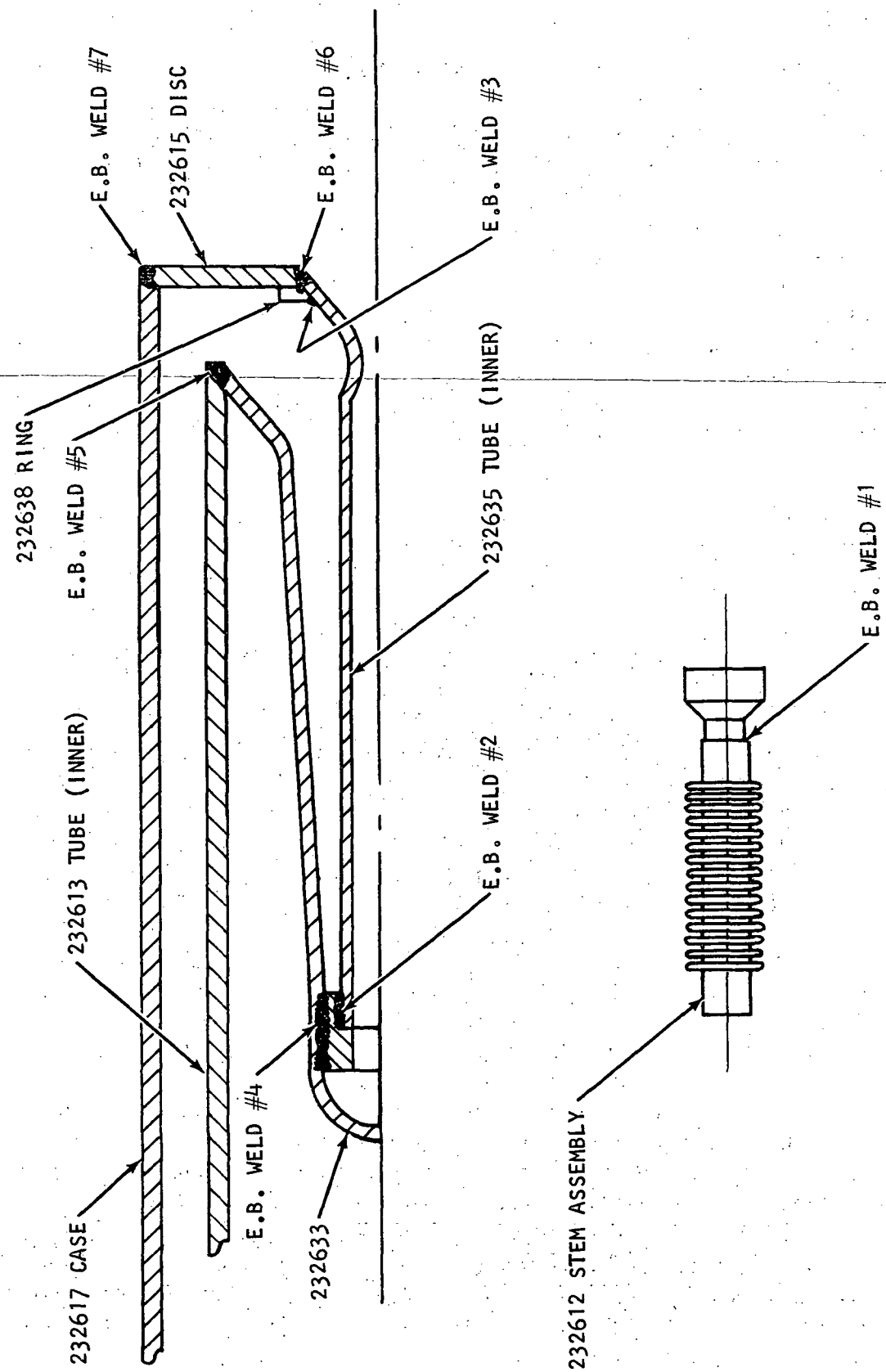
RUGGEDIZED RESISTOJET SCHEMATIC ELECTRON BEAM WELD SEQUENCE
E.B. WELD #7
232615 DISC
E.B. WELD #6
E.B. WELD #3
232638 RING
E.B. WELD #5
232635 TUBE (INNER)
232613 TUBE (INNER)
E.B. WELD #2
E.B. WELD #4
232633
232617 CASE
E.B. WELD #1
232612 STEM ASSEMBLY

FIGURE 24.

P/N 232615 DISC FROM S/N 003 RUGGEDIZED THRUSTER

X 20

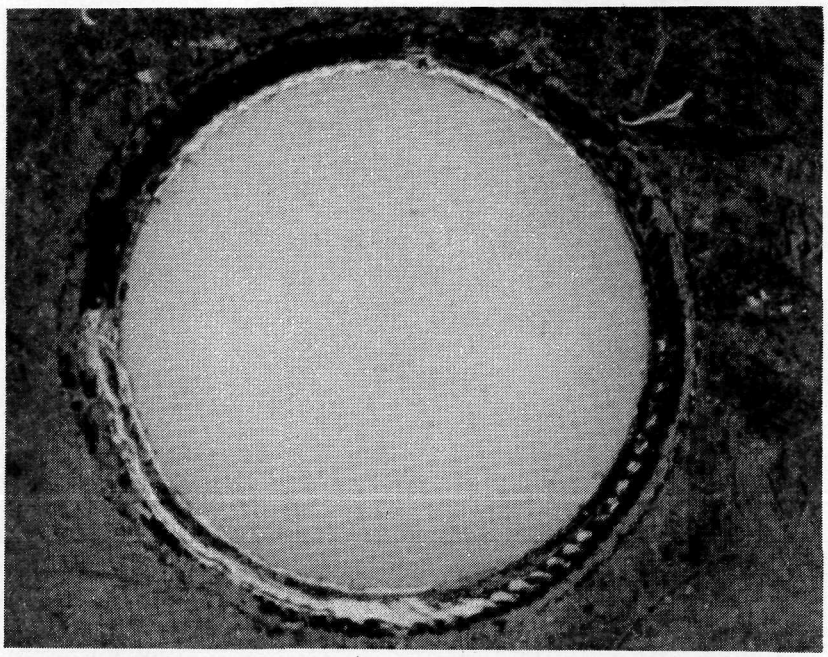

EXIT SIDE OF DISC

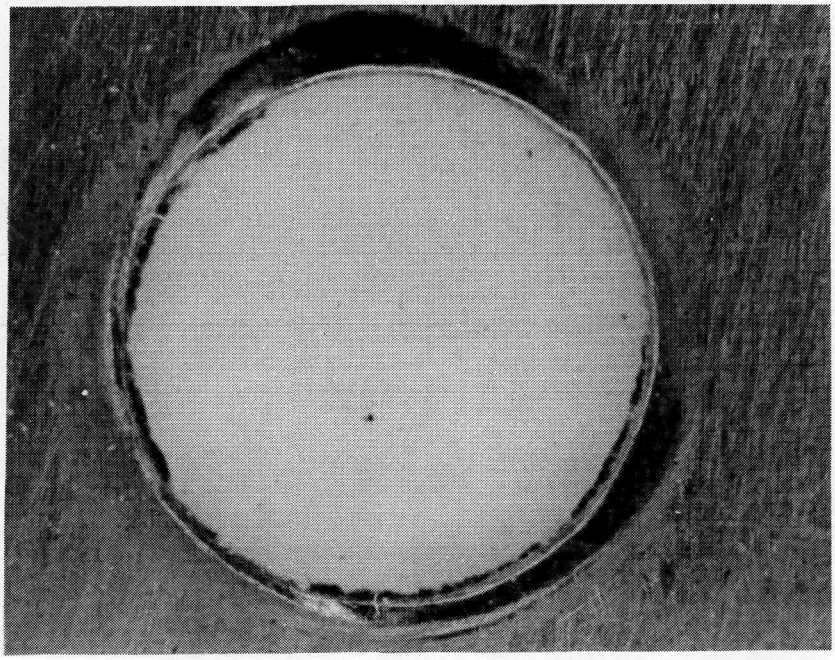

INTERIOR SIDE OF DISC

FIGURE 25.

CROSS SECTION OF P/N 232615 DISC

EXIT SIDE - X 500

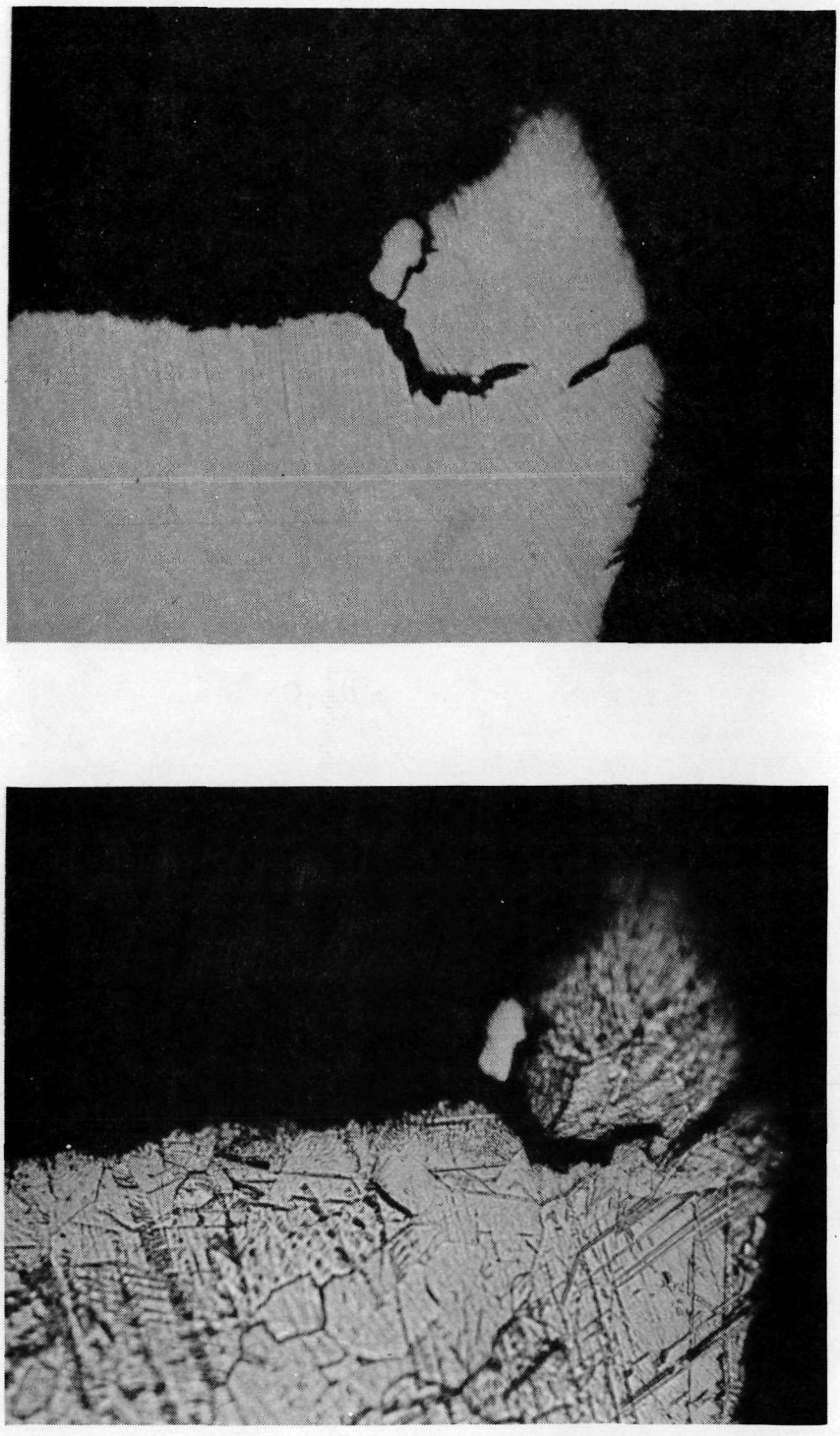

FIGURE 26.

CROSS SECTION OF P/N 232615 DISC

INTERIOR SIDE - X 500

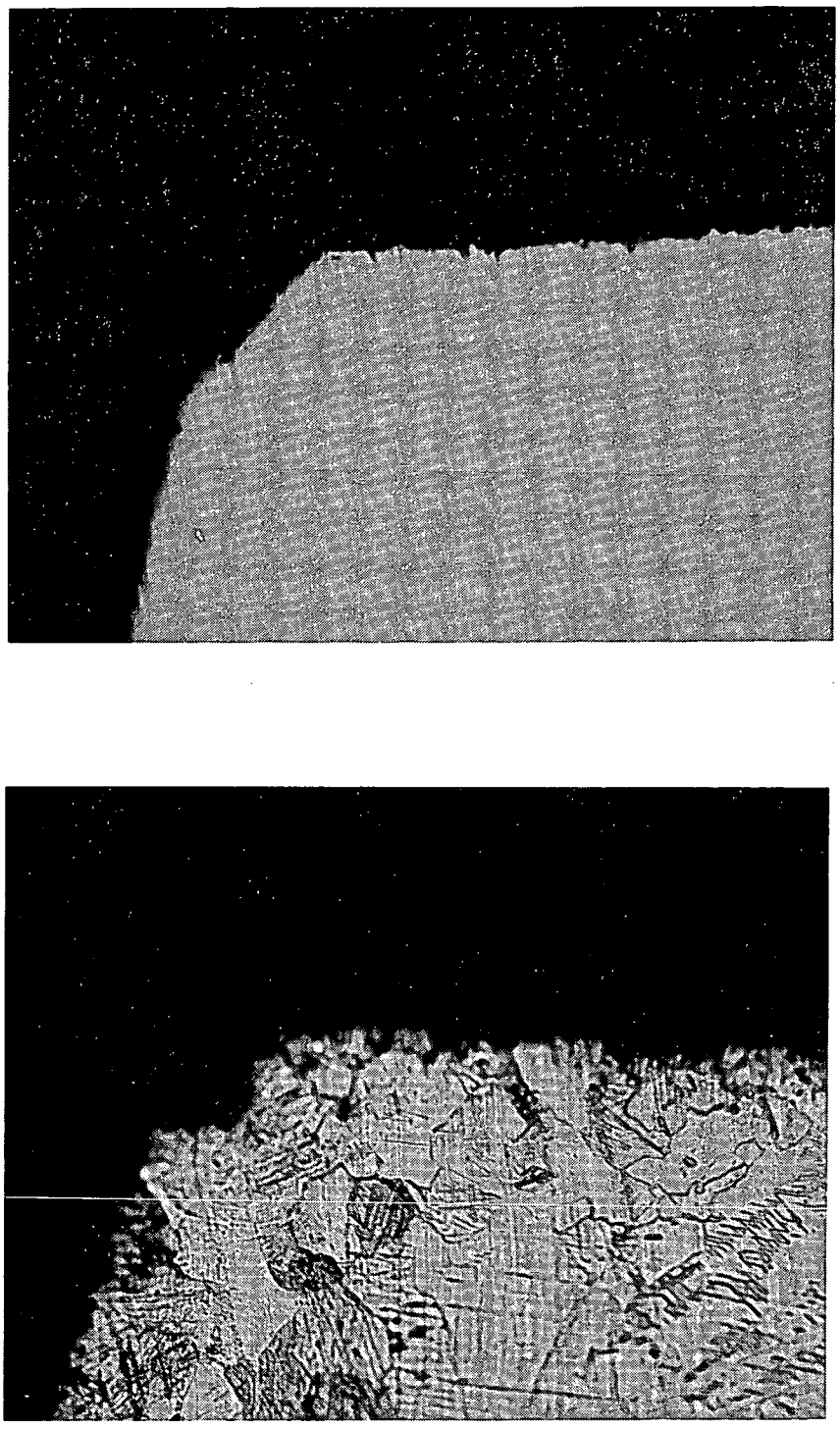

FIGURE 27.

Similar metallographic examination of the electron beam welds of the struts to the heater tubes (E.B. welds #2 and #4 of Figure 24) were also of non-optimum quality. The top photo of Figure 28 shows a cross-section of this weld area. During disassembly, one strut had retained itself to the second heater tube (P/N 232633). The two remaining struts show that maximum penetration had not occurred between the struts and the inner tube (P/N 232635).

The bottom photo of Figure 28 shows the micro-structure of one of these struts. On this particular strut at the cross-sectioned area, a crack is evident through the weld between the inner heater tube and strut. The top of the strut shows some evidence of work-hardening, but very little evidence of penetration of the weld between the strut and the second heater tube.

Results of the metallographic examination of S/N 003 indicate that the failure which occurred during the high level vibration test was not typical of a thruster structure in which the welds were complete. Probability of this kind of failure would be low in a production program involving more hardware where weld schedules and weld quality would be better controlled.

RUGGEDIZED RESISTOJET MODEL R-110
232636 INNER TUBE MANDREL AND VAPOR DEPOSITED PART

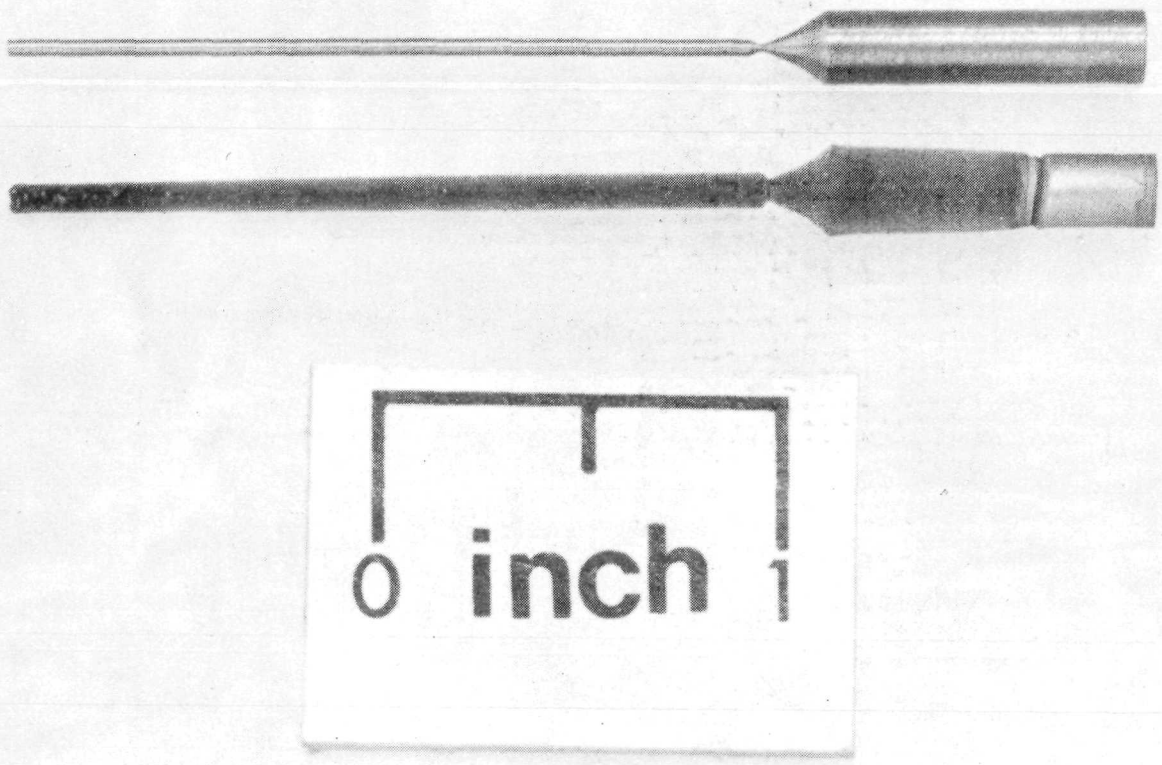

NEG. 9939-4A

FIGURE 5.

RUGGEDIZED RESISTOJET MODEL R-110
232632 TUBE SUBASSEMBLY-INNER

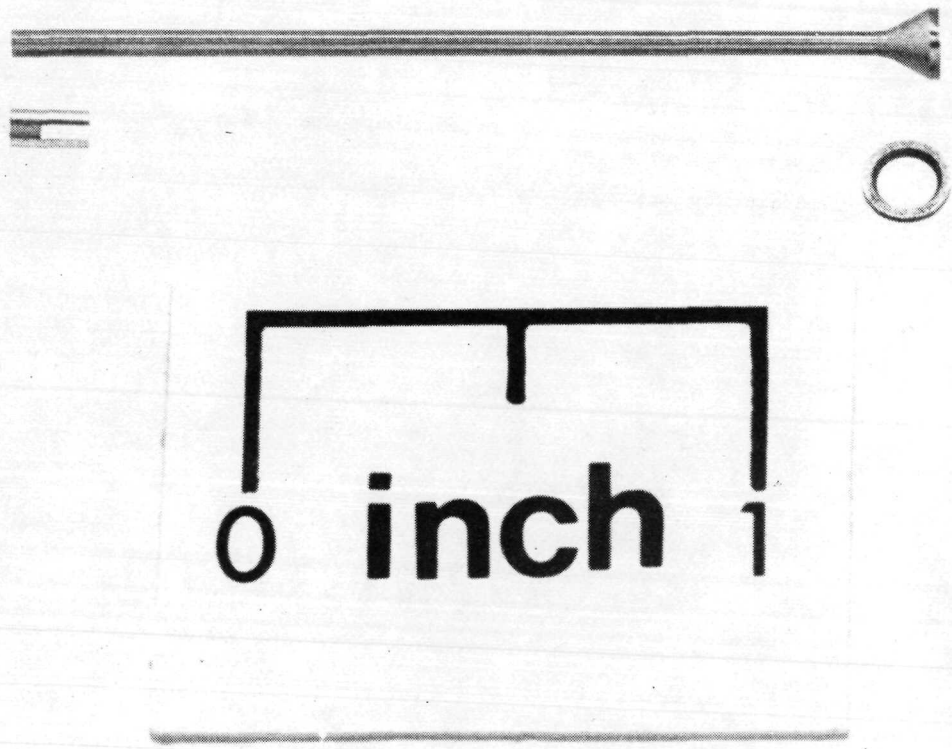

NEG. 9939-11

FIGURE 6.

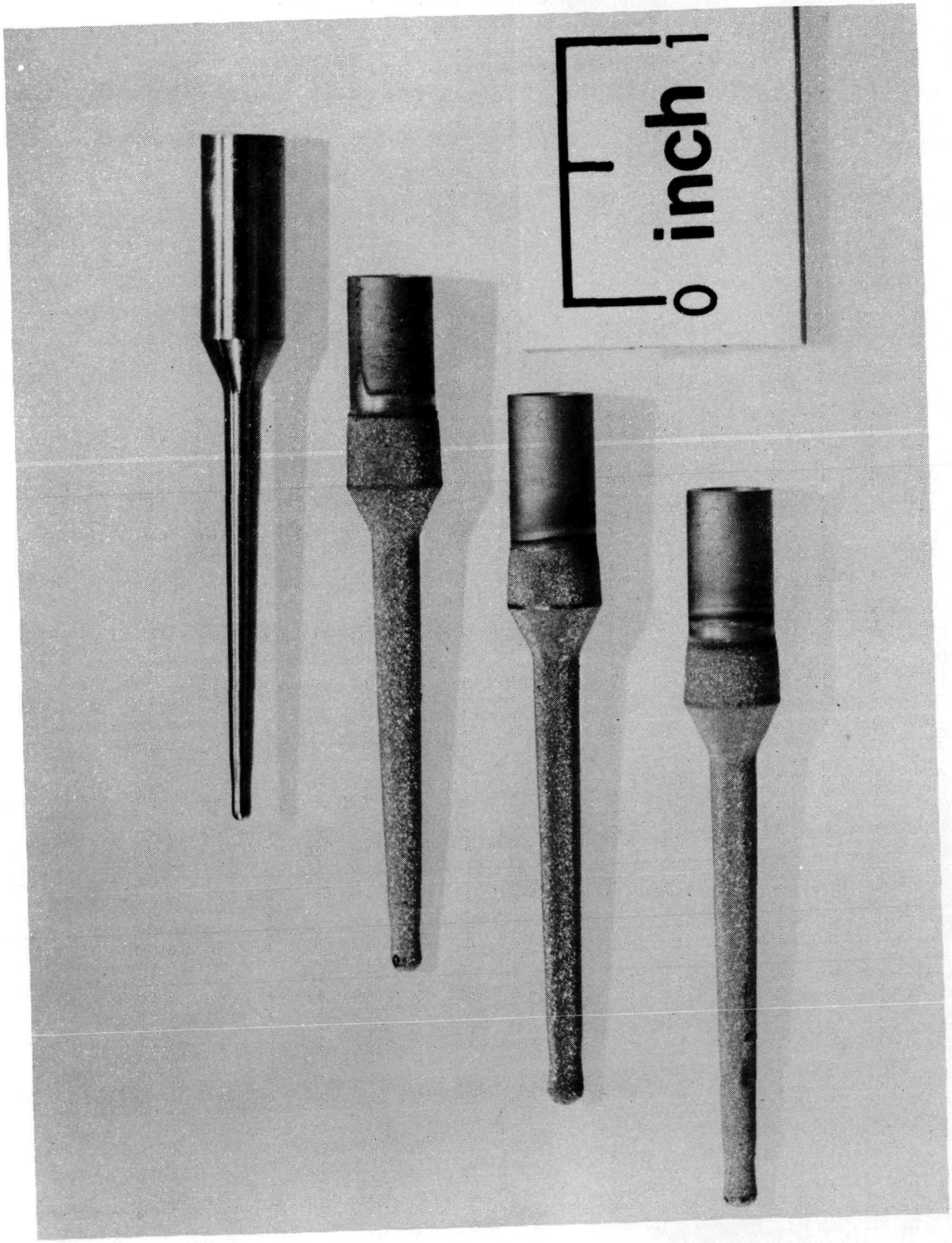

FIGURE 7. MANDREL AND VAPOR DEPOSITED PARTS FOR P/N 232634 HEATER TUBE

RUGGEDIZED RESISTOJET MODEL R-110
232633 HEATER TUBE

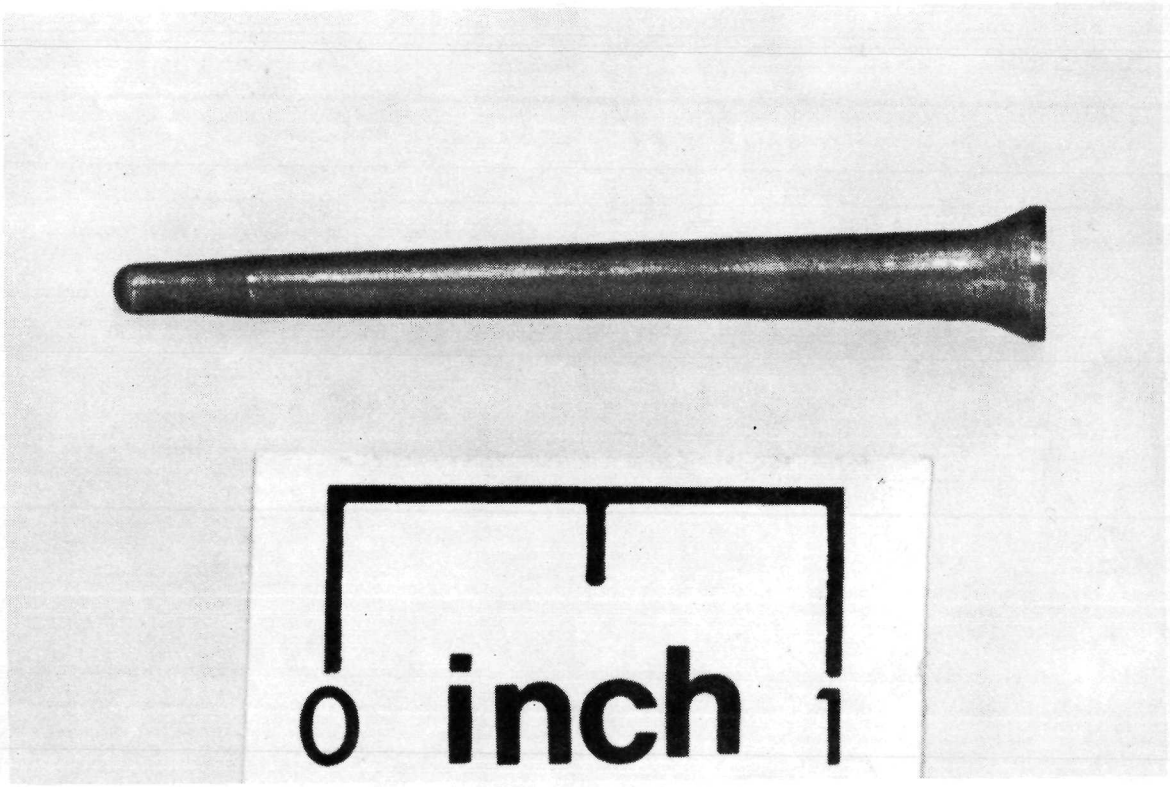

FIGURE 8.

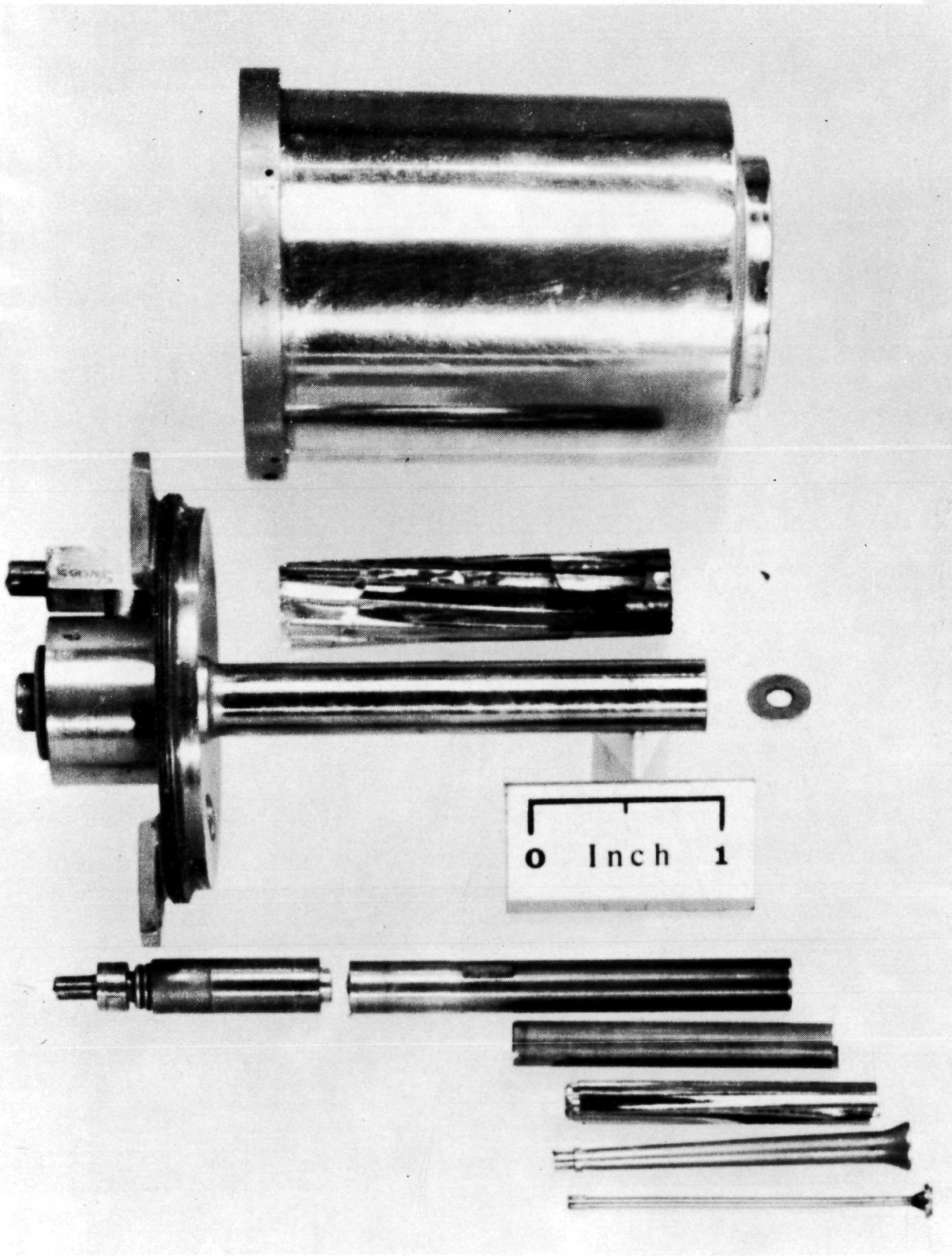

FIGURE 9. EXPLODED ASSEMBLY OF S/N 003 RUGGEDIZED RESISTOJET

RUGGEDIZED RESISTOJET MODEL R-110
232610 HOUSING SUBASSEMBLY

NEG. 9939-4

FIGURE 10.

A72-7-290-4

RUGGEDIZED RESISTOJET MODEL R-110
232612 STEM SUBASSEMBLY

NEG. 9939-8

FIGURE 11.

braze surface with a 0.001 to 0.0015 inch thick moly-manganese and nickel overcoat. The Nickel 200 material and the metallized surface of the ceramic were then machined to obtain a maximum 0.002 diametral clearance fit for brazing. The leak tight joint was obtained using Croniro braze alloy (72% Au, 22% Ni and 6% Cr) with a melting temperature of 1280°K in a vacuum furnace. In order to monitor voltage drop and thus power absorbed by the inner heating element, a rhenium wire was attached to the forward end of the joint between the inner and second heating element tubes as shown in Figure 12, a view of the innerbody assembly. A voltage measurement was then made using the fine wire. This provided a means for better determining the power utilization within the thruster. A photograph of the three thrusters fabricated during the program is shown in Figure 13.

Thruster Valve

One further addition the program over the previous development program included the development of a suitable latching solenoid valve for control of thruster gas flow and incorporation of the valve into the resistojet assembly structure. Design and development of the valve used for the program is discussed in Volume II of this report. A photograph of the valve is shown in Figure 14. Final assembly of the thruster required design and incorporation of a mounting bracket to hold both the thruster and the gas control valve. A photograph of the forward end of the completed assembly including the mount bracket and valve is shown in Figure 15. For comparison purposes, a photograph of one of the ruggedized thrusters with valve is shown with one of the original life test development units in Figure 16. It is interesting to note that the entire ruggedized thruster assembly including its mount bracket and valve is considerably shorter and more compact than the original development unit. The program results justify the efforts involved in redesign; a more compact, stronger structure evolved which is thermally superior to previous designs.

RUGGEDIZED RESISTOJET MODEL R-110
P/N 232609 INNERBODY SUBASSEMBLY

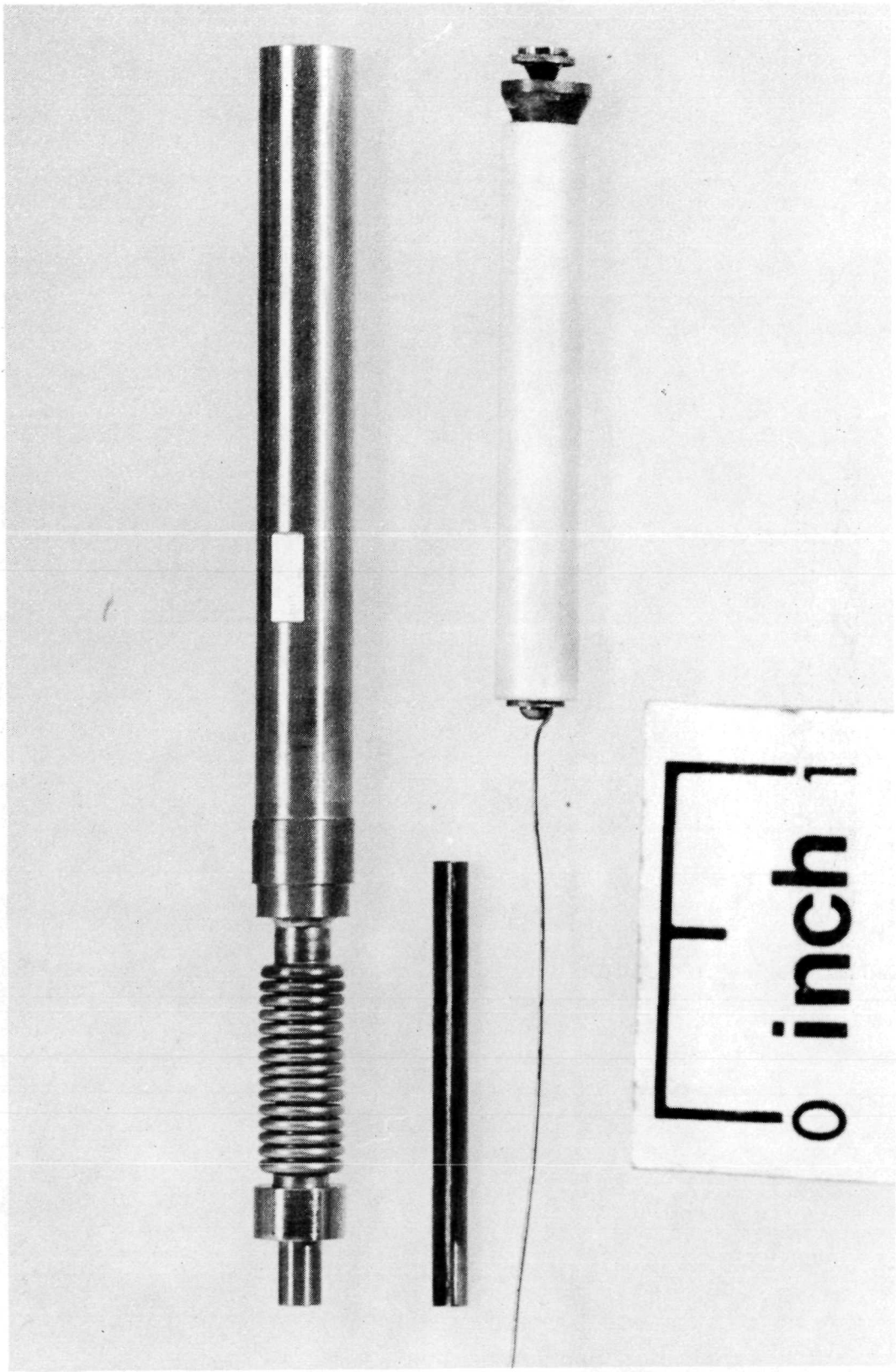

FIGURE 12.

RUGGEDIZED RESISTOJET MODEL R-110
232600 THRUSTER ASSEMBLIES

EG. 9939-28

FIGURE 13.

BISTABLE VALVE
P/N X28050

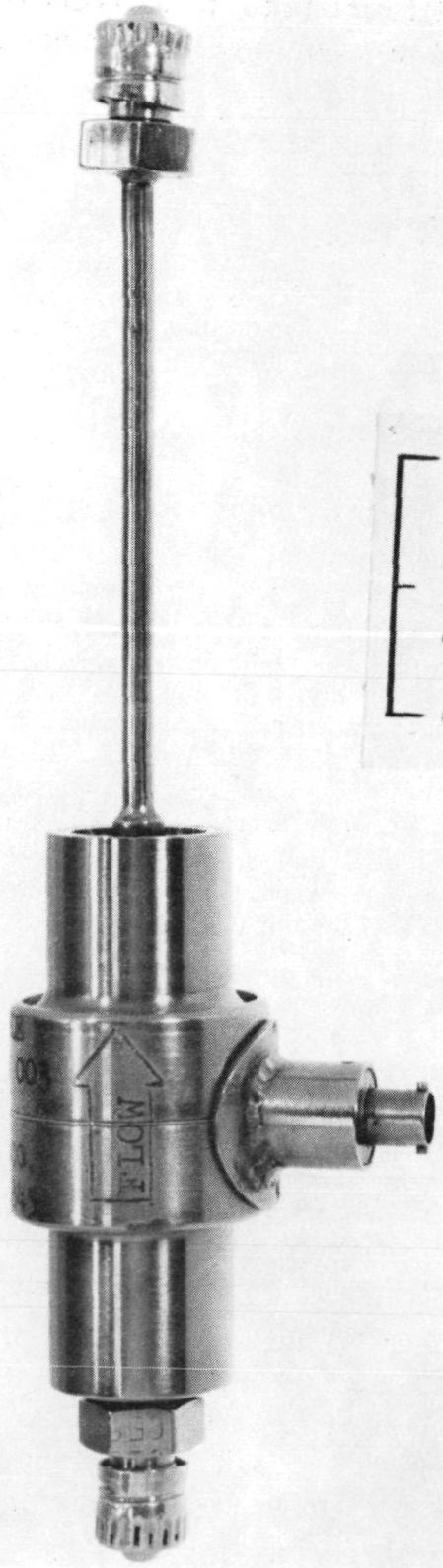

0 Inch 1

NEG. 71-151-1

FIGURE 14.

RUGGEDIZED RESISTOJET MODEL R-110
P/N 28200 RESISTOJET ASSEMBLY

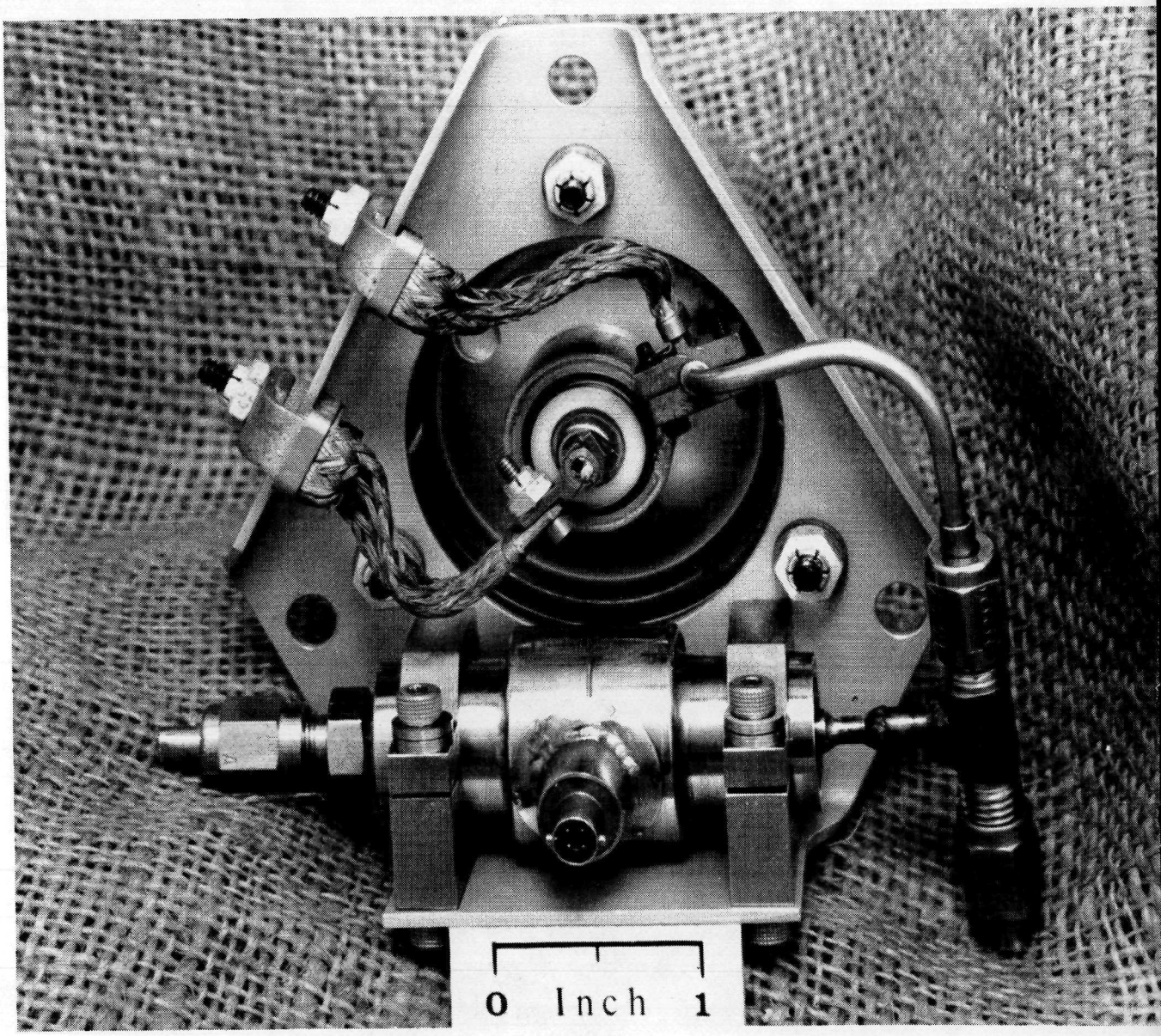

NEG. 9939-30

FIGURE 15.

RUGGEDIZED RESISTOJET THRUSTER WITH LIFE TEST THRUSTER

NEG. 72-203-7

FIGURE 16.

THRUSTER ENVIRONMENTAL TESTS

Test Summary

Dynamic environmental tests including shock, acceleration, and random and sinusoidal vaibration were conducted on two Model R-110 resistojet thruster assemblies of which the thruster latch valves were an integral part. These tests were conducted at the Durkee Environmental Laboratories of Torrance, California. In addition to the contract work statement requirements, additional tests and data acquisition were also included in the test program to better define natural frequencies and amplification factors for the critical components of the thrusters.

The additional tests performed included the following:

1. Sinusoidal sweeps on the individual thruster assemblies at the beginning and end of the program.

2. S/N 003 resistojet thruster assembly was subjected to a substantially higher random vibration spectrum to provide confidence in the design margins of the thruster as well as provide a better definition of the natural frequencies and amplification factors of the thruster assembly.

3. Detailed instrumentation including a micro minerature accelerometer mounted on the heater tube stem was recorded during the vibration tests. Figure 17 defines the accelerometer locations for the vibration tests.

Except for the failure of a non-flight type weld on the inlet supply line of thruster S/N 001, both thrusters completed all the specification dynamic environment tests in excellent condition as evidenced by detailed visual examination and resistance and leakage tests. Following completion of the specification required tests, the S/N 003 resistojet thruster assembly was subjected to a substantially higher random vibration spectrum (37 g_{rms}) to evaluate the design margins of the assembly. The electron beam weld between the nozzle and the outer pressure case failed during this out of specification vibration condition. Post test inspections of both latching solenoid valves, including the one which was subjected to the 37 g_{rms} spectrum, revealed that both were in excellent condition.

Tests Performed

Detailed descriptions of the work statement required tests conducted are presented in the following paragraphs:

VIBRATION TEST ACCELEROMETER LOCATIONS

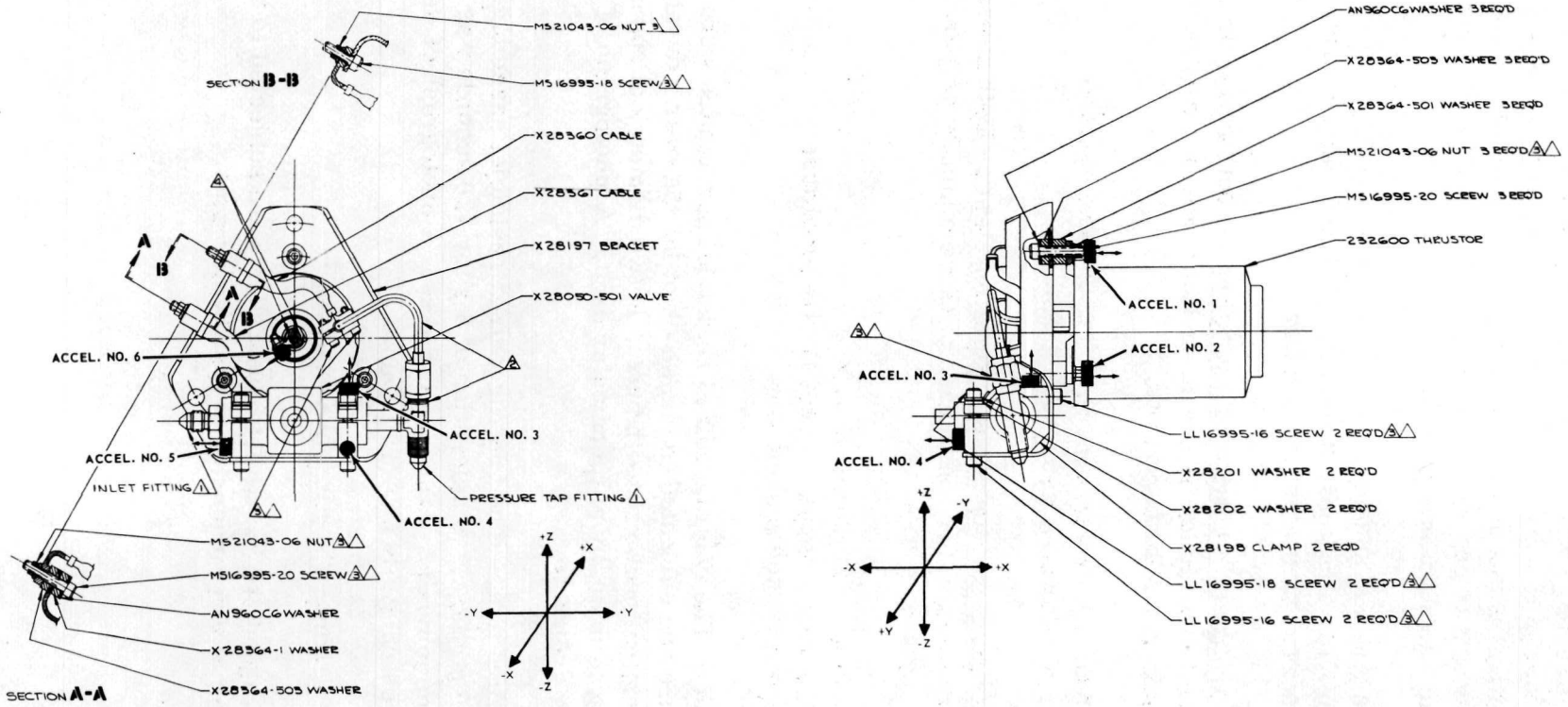

FIGURE 17.

A72-7-290-55

Sinusoidal sweeps. Each resistojet assembly was individually subjected to the following sine sweep test to define the natural frequencies and amplification factors for the critical components. Tests were conducted in each of three mutually perpendicular axes at a sweep rate of one octave/minute. A photograph of a typical vibration test setup is shown in Figure 18.

20	to	60 cps, 0.13 g peak
60	to	235 cps, 0.00071 inch (double amplitude)
235	to	2000 cps, 2.0 g peak

Flight environment - sinusoidal vibration. - Both resistojet assemblies were subject to the following vibrations in each of three mutually perpendicular axes at a sweep rate of 3 octaves/minute.

1.5 to 8.5 cycles/sec, 0.12 in. double amplitude
8.5 to 30 cycles/sec, 0.48 g peak.

Ground handling environments - vibration test. - Both assemblies were subjected to the following vibration in each of three mutually perpendicular axes at a sweep rate of 1 octave/minute.

5.0	to	27.5 cps ± 1.56 g
27.5	to	53 cps - 0.043 double amplitude
52.0	to	500 cps ± 6.0 g

Shock test - The two ruggedized resistojet assemblies were mounted on a shock test fixture and subjected to one shock of 30 $^{+5}_{-0}$g over a duration of 11 ± milliseconds, with terminal peak sawtooth pulse, in two diametrical opposite directions for each of the three mutually perpendicular axes. A photograph of the shock test setup is shown in Figure 19.

Acceleration test. - The two ruggedized resistojet assemblies were mounted on the arm of a centrifuge. Acceleration of 8 g for 120 seconds was applied in each direction for three mutually perpendicular axes. A photograph of the thrusters mounted on the centrifuge is shown in Figure 20.

Flight environment - random vibration. -

The two ruggedized resistojet assemblies were subjected to the following vibrations in each of three mutually perpendicular axes.

TYPICAL VIBRATION TEST SETUP

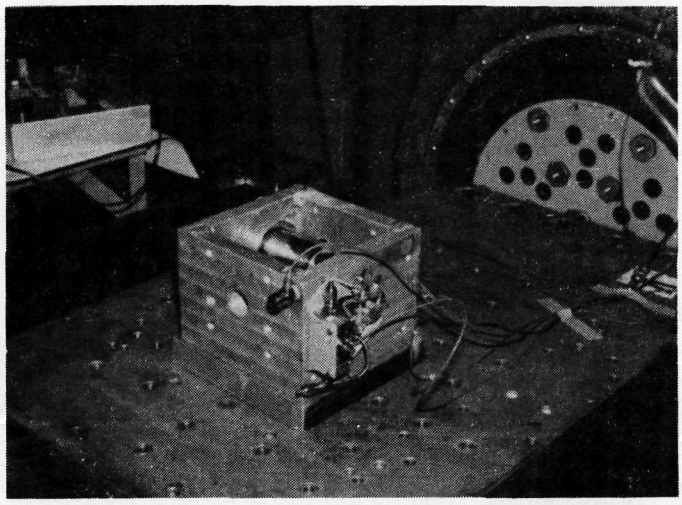

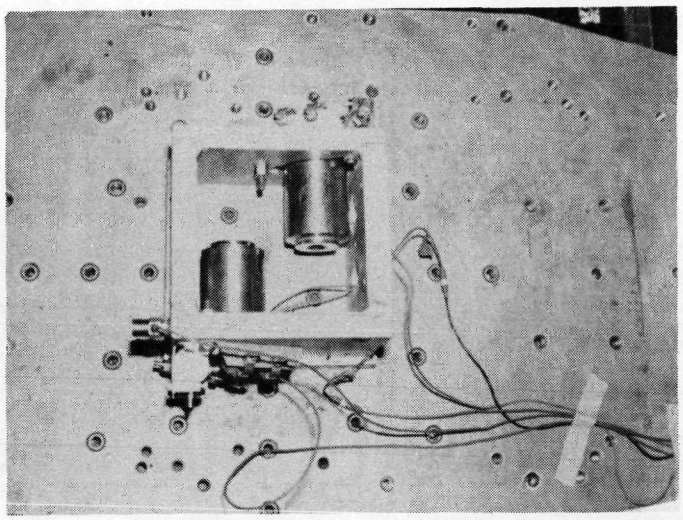

FIGURE 18.

TYPICAL SHOCK TEST SETUP AND SHOCK INPUT SPECTRUM

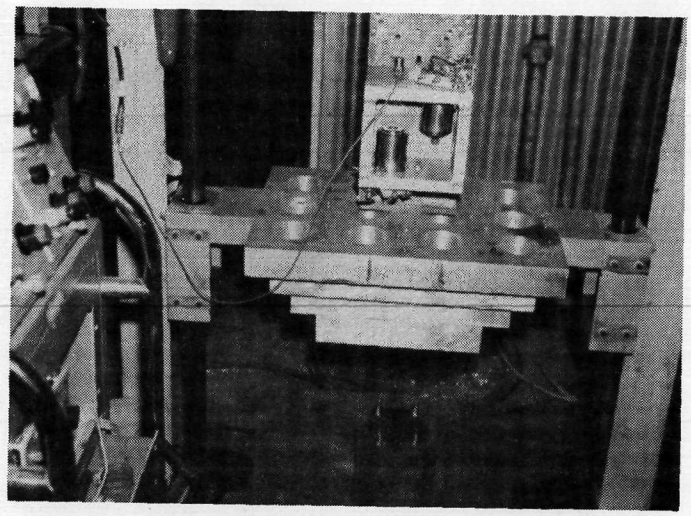

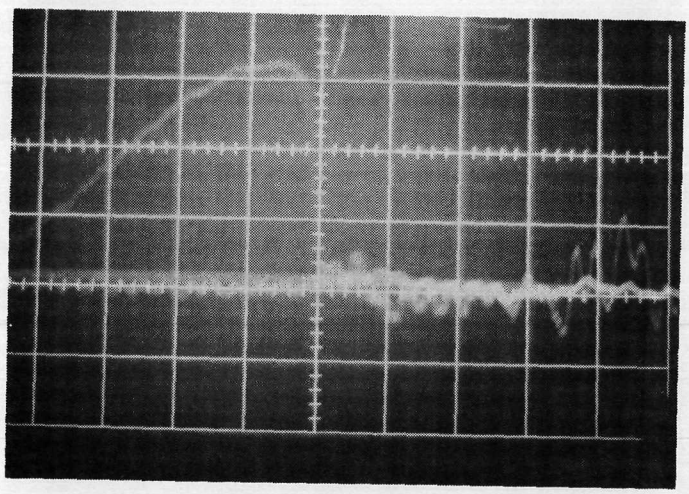

FIGURE 19.

TYPICAL ACCELERATION TEST SETUP

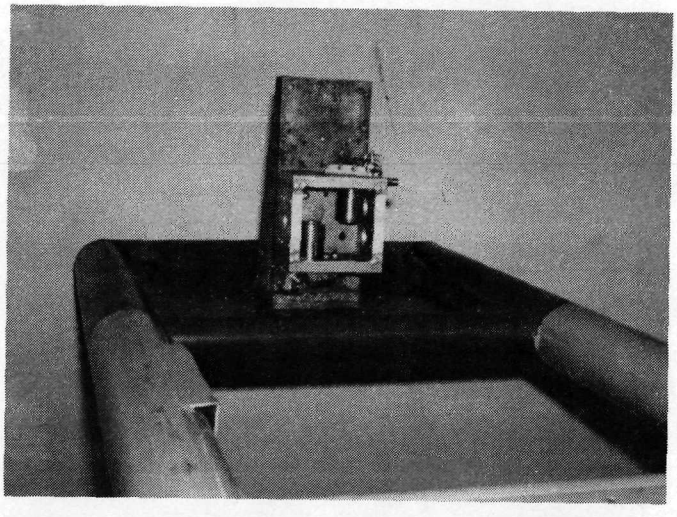

FIGURE 20.

Lower Level - One Minute Per Axis

20 to 100 cps, 0.5 g^2/cps PSD (Power Spectral Density)
100 to 200 cps, decreasing PSD @ 6 db/octave
200 to 400 cps, 0.13 g^2/cps PSD
400 to 470 cps, decreasing PSD @ 9 db/octave
470 to 1500 cps, 0.08^2/cps PSD
1500 to 2000 cps, decreasing PSD @ 9 db/octave
2000 cps, 0.032 g^2 PSD

Higher Level - Two Minutes Per Axis

20 to 100 cps, .018 g^2/cps PSD
100 to 200 cps, decreasing PSD @ 6 db/octave
200 to 400 cps, 0.047 g^2/cps PSD
400 to 470 cps, decreasing PSD @ 9 db/octave
470 to 1500 cps, 0.029 g^2/cps PSD
1500 to 2000 cps, decreasing PSD @ 90 db/octave
2000 cps, 0.012 g^2/cps PSD

During the higher level random vibration, the inlet supply line between the valve and the instrumentation fitting failed at the connecting weld joint as shown in Figure 21. This failure was not considered significant since this element of the thruster assembly is non-representative of a flight-type design. On subsequent designs, the following typical changes would be implemented to eliminate the experienced failure mode.

(1) Relatively heavy instrumentation fittings would be eliminated or at least not cantilevered from a thin support tube.

(2) Appropriate tie-down of the feed lines and connecting fitting would be made to the basic structural support bracket to eliminate critical resonant frequencies and excessive movement of such parts.

All other post-test checks of the thrusters, including resistance and leakage checks, showed both thrusters to be in excellent condition except for the above noted supply line discrepancy.

Off-specification high level random vibration test. - S/N 003 ruggedized resistojet assembly was subjected to the following off-specification high level random vibration test to evaluate the design margins of the thruster as well as to provide a better definition of the natural frequencies and amplification factors of the thruster assembly.

RUGGEDIZED RESISTOJET THRUSTER S/N 003 AFTER DYNAMIC ENVIRONMENT TESTS

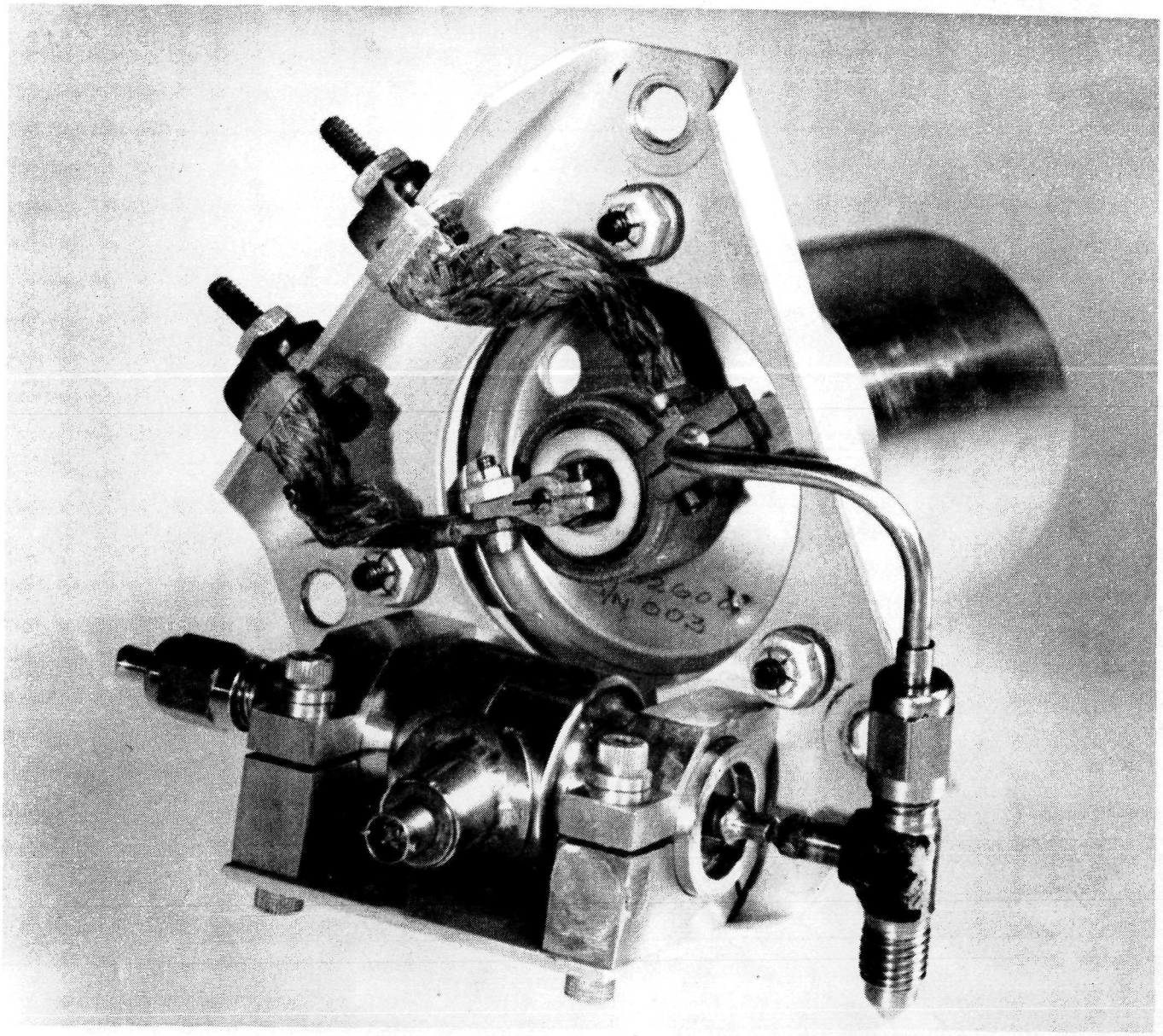

NEG. 9939-35

FIGURE 21.

20 to 100 cps, increasing PSD to 1 g^2/cps @ 6 db/octave
100 to 1000 cps, 1 g^2/cps PSD
1000 to 2000 cps, decreasing PSD @ 10 db/octave

A comparison of this vibration spectrum is shown in Figure 22 along with the two random vibration spectrums specified by the work statement. The S/N 003 resistojet assembly was subjected to the following tests at these off-specification vibration levels before terminating the test:

X axis - 2 minutes
Z axis - 2 minutes

Following the tests in the Z axis, it was noted that the Electron Beam weld between the nozzle and the outer-case had failed. A close-up photograph of the discrepancy is shown in Figure 23. Results of the metallographic examination to determine the cause of failure revealed that inadequate penetration of this critical weld had occurred during the fabrication process. Detailed discussion of this examination is presented in the following section (Metallographic Analysis).

Post-test sinusoidal sweeps - S/N 001 resistojet thruster assembly was subjected to the following sine-sweep test to determine if any of the critical natural frequencies and associated amplification factors had shifted from those documented during the pre-test sinusoidal sweeps. Tests were conducted in each of three mutually perpendicular axes at a sweep rate of one octave/minute.

20 to 60 cps, 0.13 g peak
60 to 235 cps, 0.00071 inch (double amplitude)
235 to 2000 cps, 2.0 g peak

No significant shifts in the dynamic response characteristics from the pre-test sinusoidal tests were noted on the S/N 001 resistojet thruster assembly.

Post-Test Checks and Inspection

Periodic resistance and leakage tests were conducted on both S/N 001 and S/N 003 resistojet assemblies during the test program. As previously noted, both resistojet assemblies were in excellent condition following completion of all dynamic environment tests required by the work statement except for the failure of the non-flight type weld on the inlet supply line tubing, i.e., no significant changes in thruster resistance and no apparent valve leakage.

RAMDOM VIBRATION SPECTRUM COMPARISON

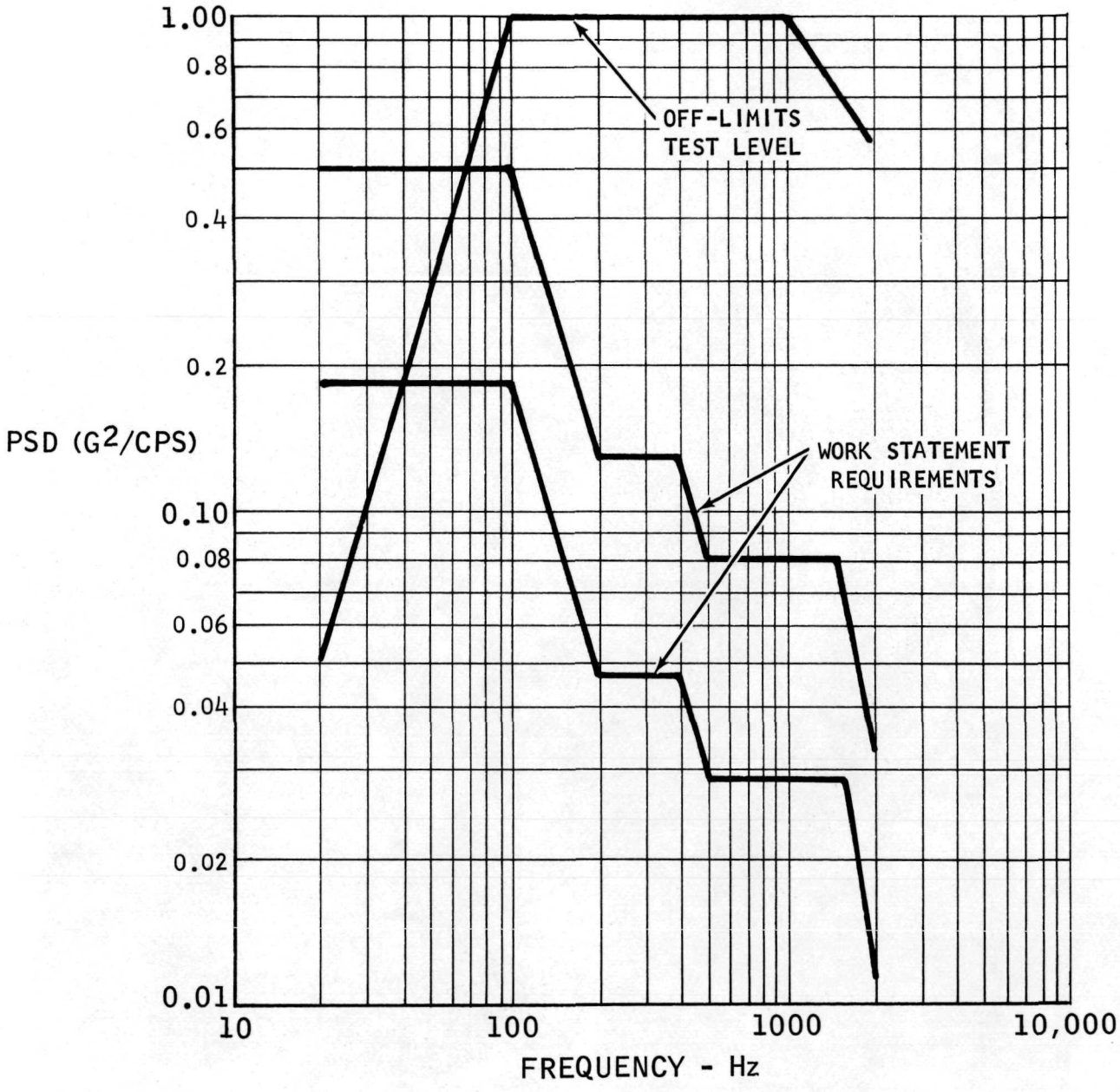

FIGURE 22.

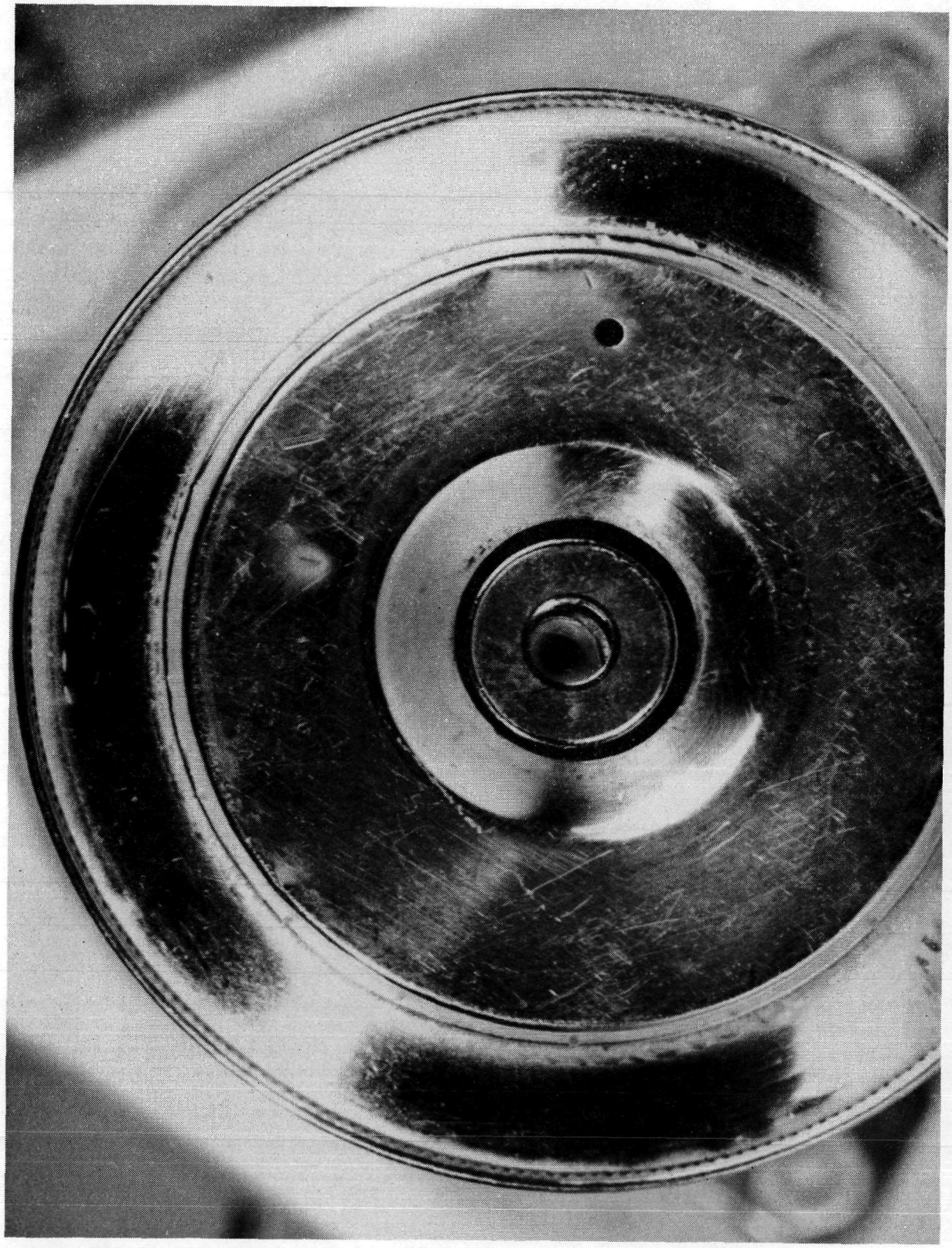

NEG. 9939-35

FIGURE 23. NOZZLE WELD FAILURE OF S/N 003 THRUSTER FOLLOWING THE OFF-LIMITS VIBRATION TEST

After return of the thruster assemblies to Marquardt, the latching solenoid valves were subjected to detailed component bench tests. Both valves, including the one on S/N 003 resistojet assembly which had been subjected to out of specification high level random vibration tests, proved to be in excellent condition. Zero leakage was exhibited at test pressures of both 20 and 100 psia and the pull-in current and drop-out current characteristics repeated consistently with their pre-test values.

Analysis of the vibration data showed good agreement between the predicted and actual natural frequencies of the critical components. However, the amplification factors for the heater tube was substantially less than previously used in the structural analysis (Reference 3). The structural analysis which used a conservative amplification factor of twenty to twenty-five because of the many variables and unknowns that were required to be assumed in the structural model is approximately five times greater than the actual dynamic response characteristics exhibited by these resistojet assemblies.

Refinement of the amplification factors provided a very important input into the design requirements for the biowaste thrusters being developed on NASA Contract NAS 1-9474.

Metallographic Analysis of S/N 003 Thruster Electron Beam Weld Failure

S/N 003 thruster incurred damage to the nozzle to end-case electron beam weld (See Figure 23) during the off-limits vibration test. Detailed metallographic examinations were made to determine the quality of this weld (E. B. #6 of Figure 24) as well as the other critical welds of this thruster (E. B. #2 and #4 of Figure 24).

Figure 25 shows macrophotos of both sides of the P/N 232615 disc. The exit side of the disc, which is the side from which the electron beam weld was initiated, indicates an excellent weld. However, the other side of the disc shows little or no penetration occurred through the disc to the backup ring (P/N 232638). The disc was subsequently cross-sectioned for further detailed metallographic examination. Figures 26 and 27 show respectively the exit side and interior side of the cross-sectioned disc. The exit side definitely shows a weld fillet had occurred between the exit end of the disc and the exit end of the inner tube, P/N 232635. The degree of penetration of the weld cannot be determined since the microstructure of the entire disc had been recrystallized from previous testing as shown by the etched microphotographs on the bottom of Figures 26 and 27. However, it appears that the weld did not penetrate all the way through to the interior side of the disc since Figure 27 shows the apparent original chamfer of the edge and no evidence of a weld fillet. The conclusion based upon the above examination is that the electron beam weld of the nozzle to exit disc (E. B. #6 of Figure 24) was definitely of non-optimum quality.

RUGGEDIZED RESISTOJET SCHEMATIC ELECTRON BEAM WELD SEQUENCE

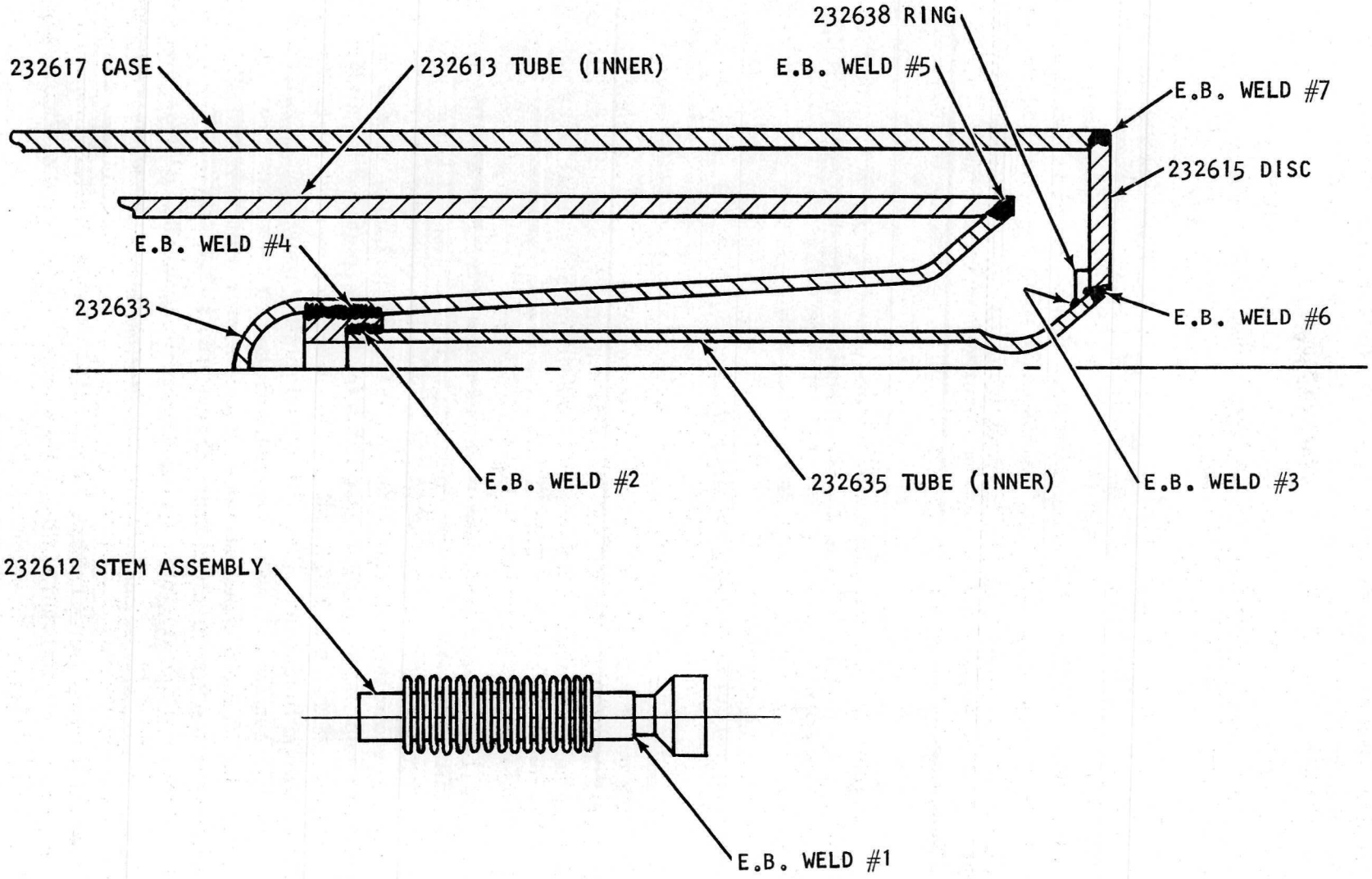

FIGURE 24.

A72-7-290-34

P/N 232615 DISC FROM S/N 003 RUGGEDIZED THRUSTER

X 20

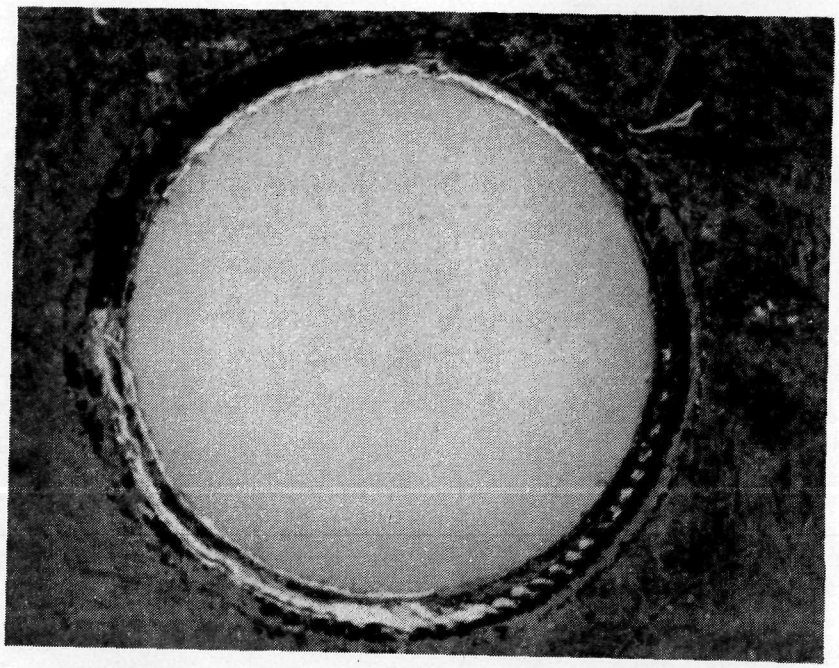

EXIT SIDE OF DISC

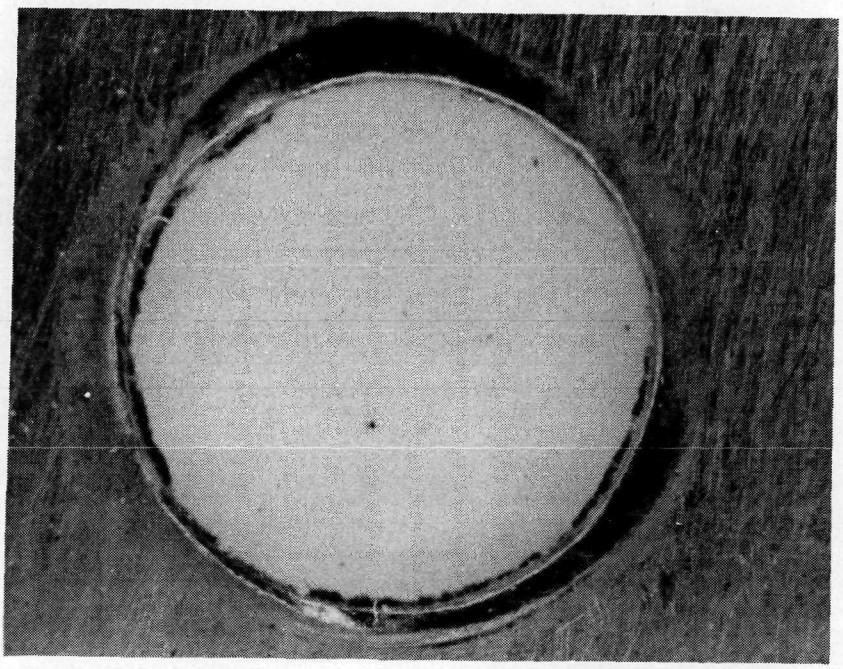

INTERIOR SIDE OF DISC

FIGURE 25.

CROSS SECTION OF P/N 232615 DISC

EXIT SIDE - X 500

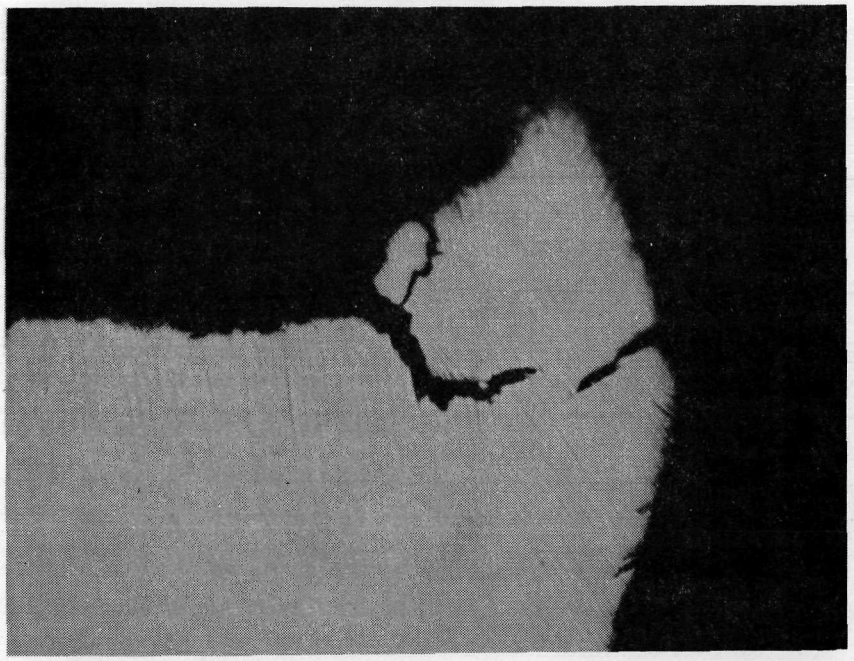

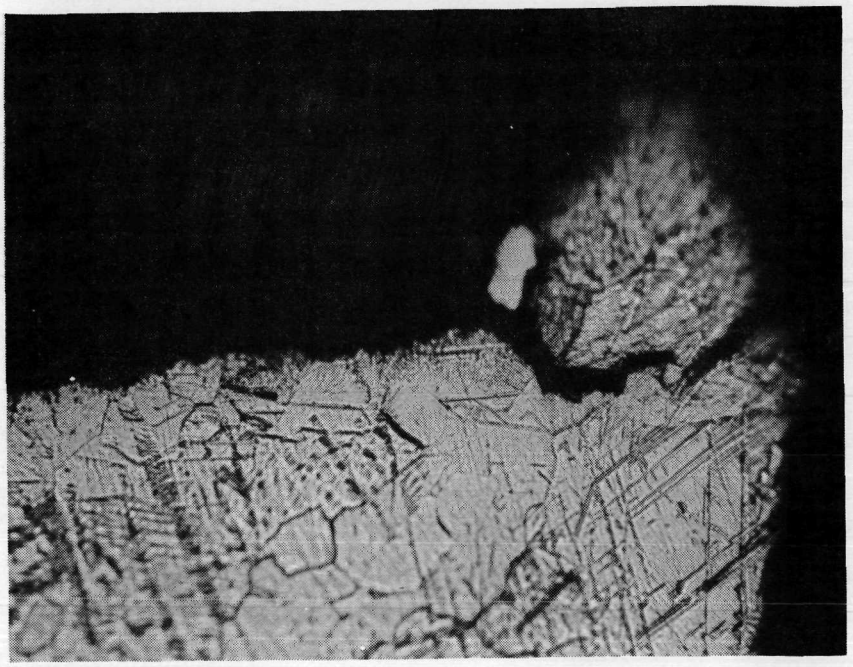

FIGURE 26.

CROSS SECTION OF P/N 232615 DISC

INTERIOR SIDE - X 500

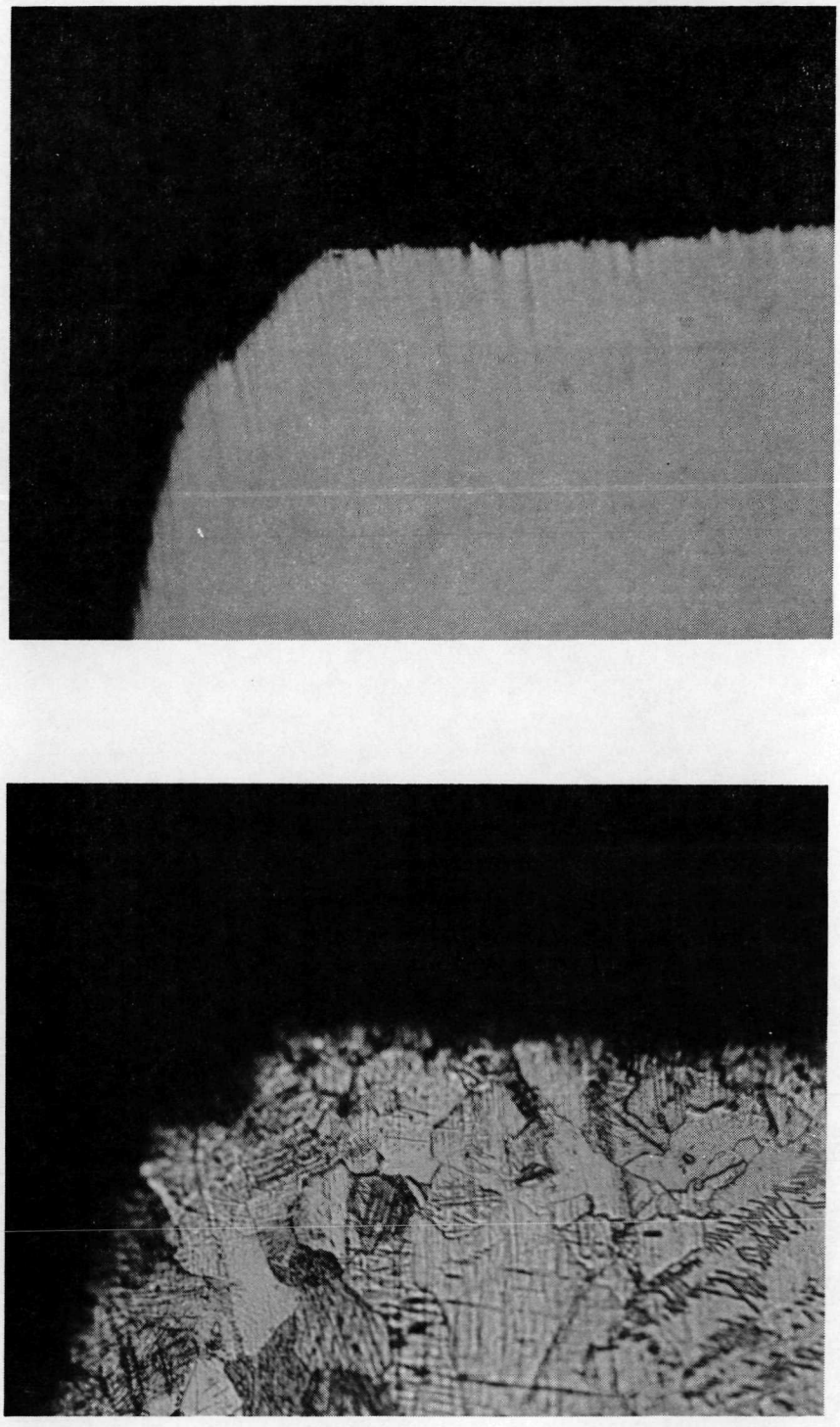

FIGURE 27.

Similar metallographic examination of the electron beam welds of the struts to the heater tubes (E. B. welds #2 and #4 of Figure 24) were also of non-optimum quality. The top photo of Figure 28 shows a cross-section of this weld area. During disassembly, one strut had retained itself to the second heater tube (P/N 232633). The two remaining struts show that maximum penetration had not occurred between the struts and the inner tube (P/N 232635).

The bottom photo of Figure 28 shows the micro-structure of one of these struts. On this particular strut at the cross-sectioned area, a crack is evident through the weld between the inner heater tube and strut. The top of the strut shows some evidence of work-hardening, but very little evidence of penetration of the weld between the strut and the second heater tube.

Results of the metallographic examination of S/N 003 indicate that the failure which occurred during the high level vibration test was not typical of a thruster structure in which the welds were complete. Probability of this kind of failure would be low in a production program involving more hardware where weld schedules and weld quality would be better controlled.

CROSS SECTION OF STRUT TO INNER TUBE WELD

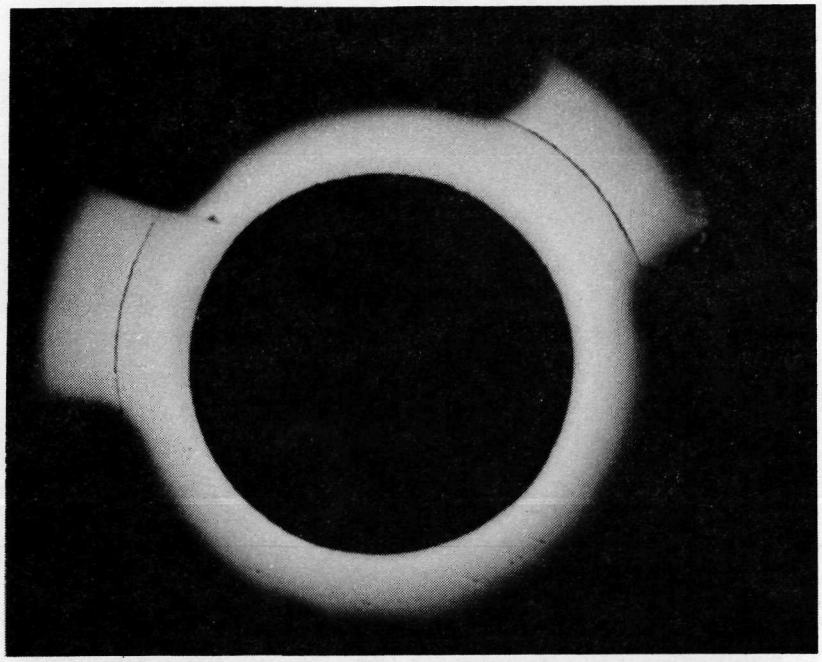

X 50

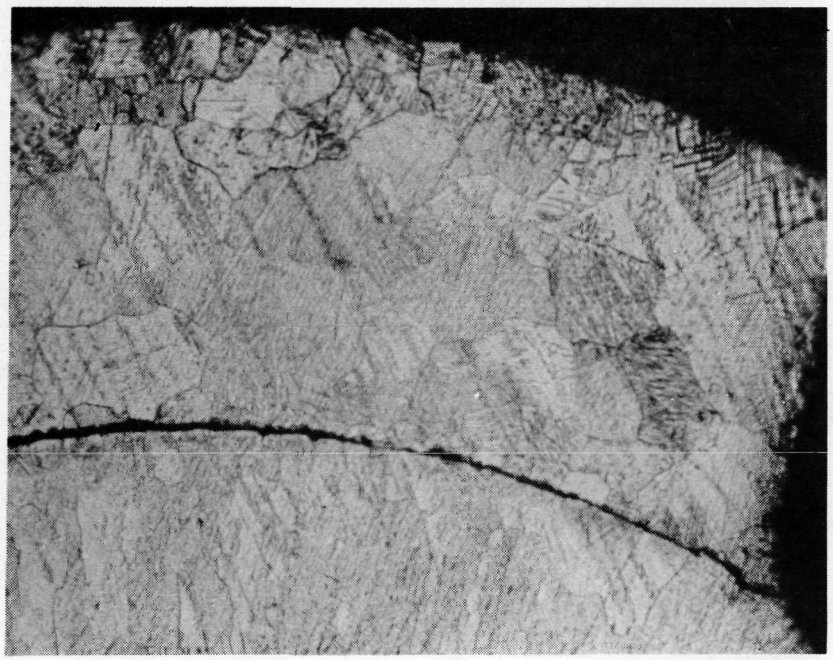

X 200

FIGURE 28.

LIFE TEST FACILITY

Pumping Station

Thruster operational testing was conducted in Marquardt's Electrical Propulsion Laboratory, high vacuum test cell. The cell is capable of providing cell pressures of less than 1.0 micron while operating the ruggedized thrusters at 10 millipounds thrust.

The cell includes a rollaway stainless steel test chamber 48 inches in diameter and 51 inches long. A view of the test chamber rolled up to the pumping system interface is shown in Figure 29. The thrust dynamometer is cantilivered from the stationary forward section and is readily accessible when the chamber is rolled back. A schematic or the pumping system is shown in Figure 30 and a photo of the pumps is shown in Figure 31. The test cell portion is isolated from the remainder of the pumping station by a 54 inch butterfly valve to provide access to the test hardware without having to shut the pumping system down. High vacuum pumping is provided by two fractionating oil diffusion pumps backed by a 300 cfm Stokes mechanical pump coupled with a 3680 cfm Rootes type blower. The system is versatile in that the mechanical pump can be run alone or in combination with the blower or the mechanical station can be coupled to the 48 inch diffusion pumps for higher vacuum capability. Most of the life test was run using the mechanical pump system only, with the diffusion pumps utilized only during periodic performance calibrations where extremely high vacuum was critical. The mechanical pumps provided about 23 microns when the NH_3 thruster was running and 70 to 80 microns pressure when the hydrogen thruster was operating. With the diffusion pumps operating as well, environmental pressures of less than one micron could be maintained at nominal life test conditions.

Thruster Electrical Control System

A schematic of the direct thruster power control and valve command control system is shown in Figure 32. Thruster power control was supplied by two independent high current D.C. power supplies. Thruster valve control was provided through a single 24 volt D.C. power supply with valve coil power sequencing provided by a set of preset timer switches. The timer switch bank controlled the thruster power switch relays as well as the thruster propellant valve operation. The switch bank consisted of a series of parallel microswitches all driven from preset cam lobes on a motor driven shaft. Sequencing for each thruster was set so that the power was applied after the thruster reached full operating pressure on startup. Power removal on shutdown of the thrusters preceded closing of the propellant valves by a few seconds as well. This sequencing was required to assure that the thruster was not overheated by operating with insufficient cooling propellant flow.

NEG. 9849-2

FIGURE 29. ELECTRICAL PROPULSION LABORATORY VACUUM TEST CHAMBER

HIGH VACUUM ELECTROTHERMAL PROPULSION LABORATORY
CELL PUMPING SYSTEM

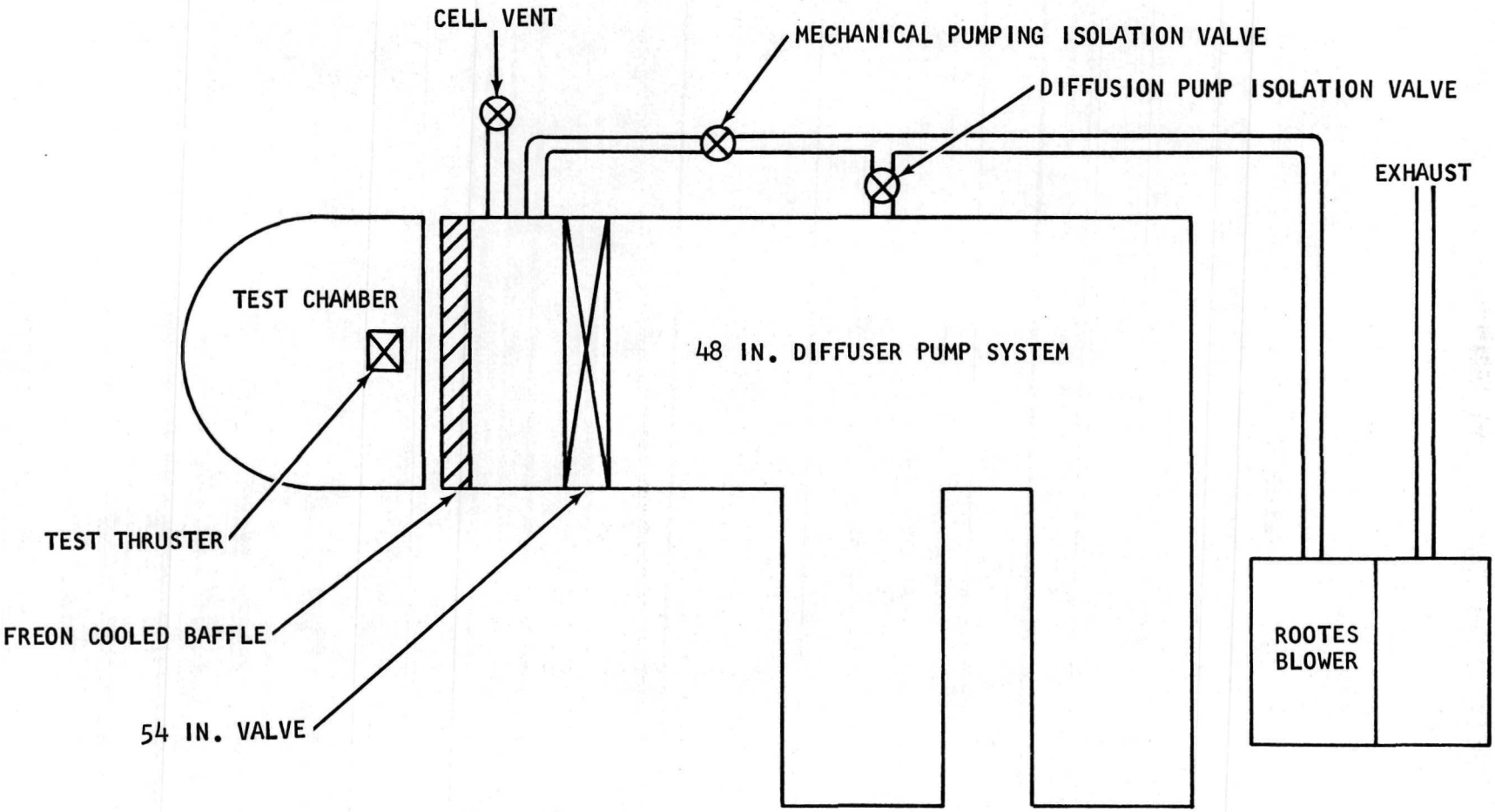

FIGURE 30.

A72-7-290

ELECTRIC PROPULSION LABORATORY HIGH VACUUM PUMPING STATION

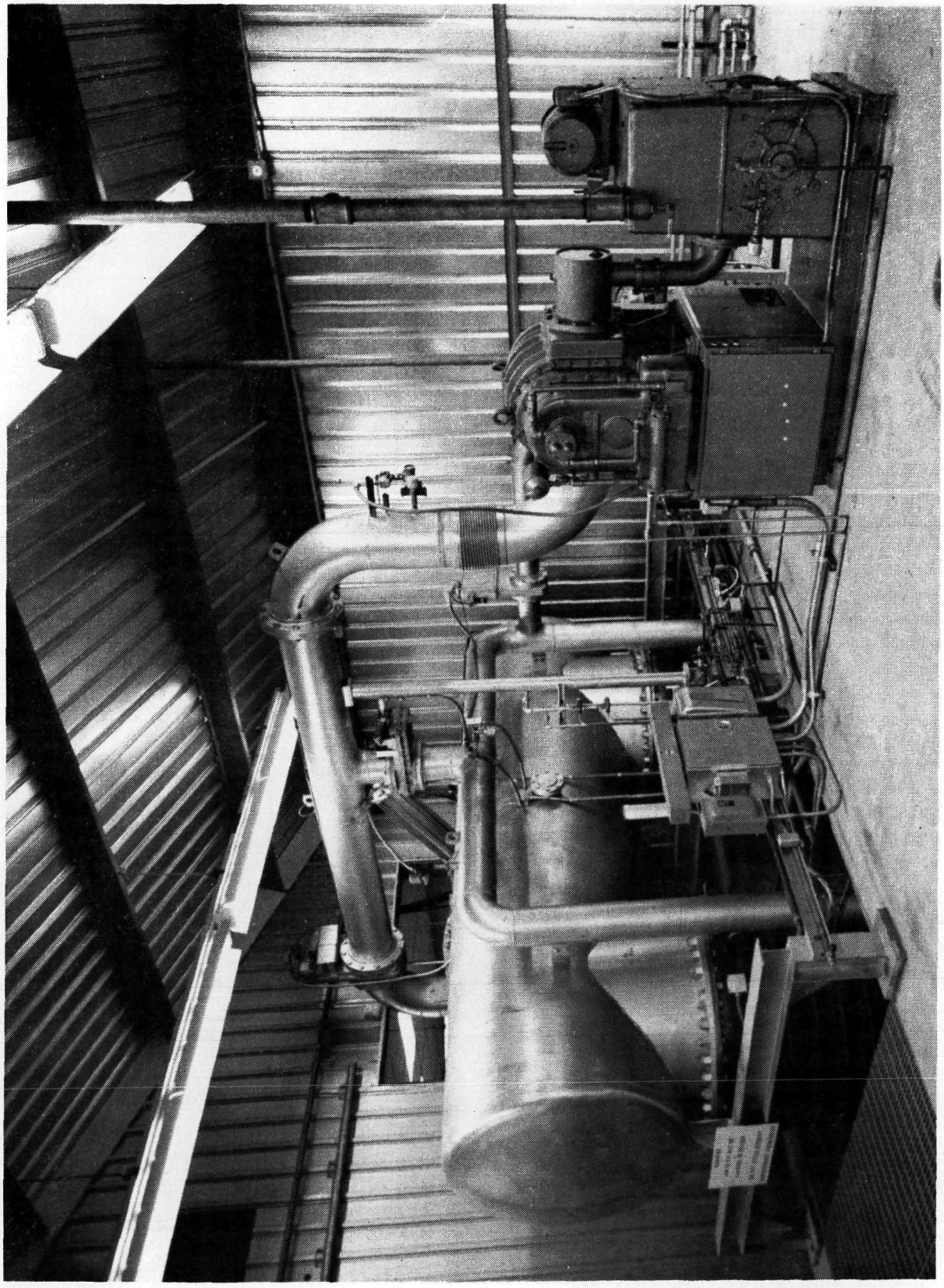

FIGURE 31.

HIGH VACUUM ELECTROTHERMAL PROPULSION LABORATORY
ELECTRICAL CONTROL SCHEMATIC

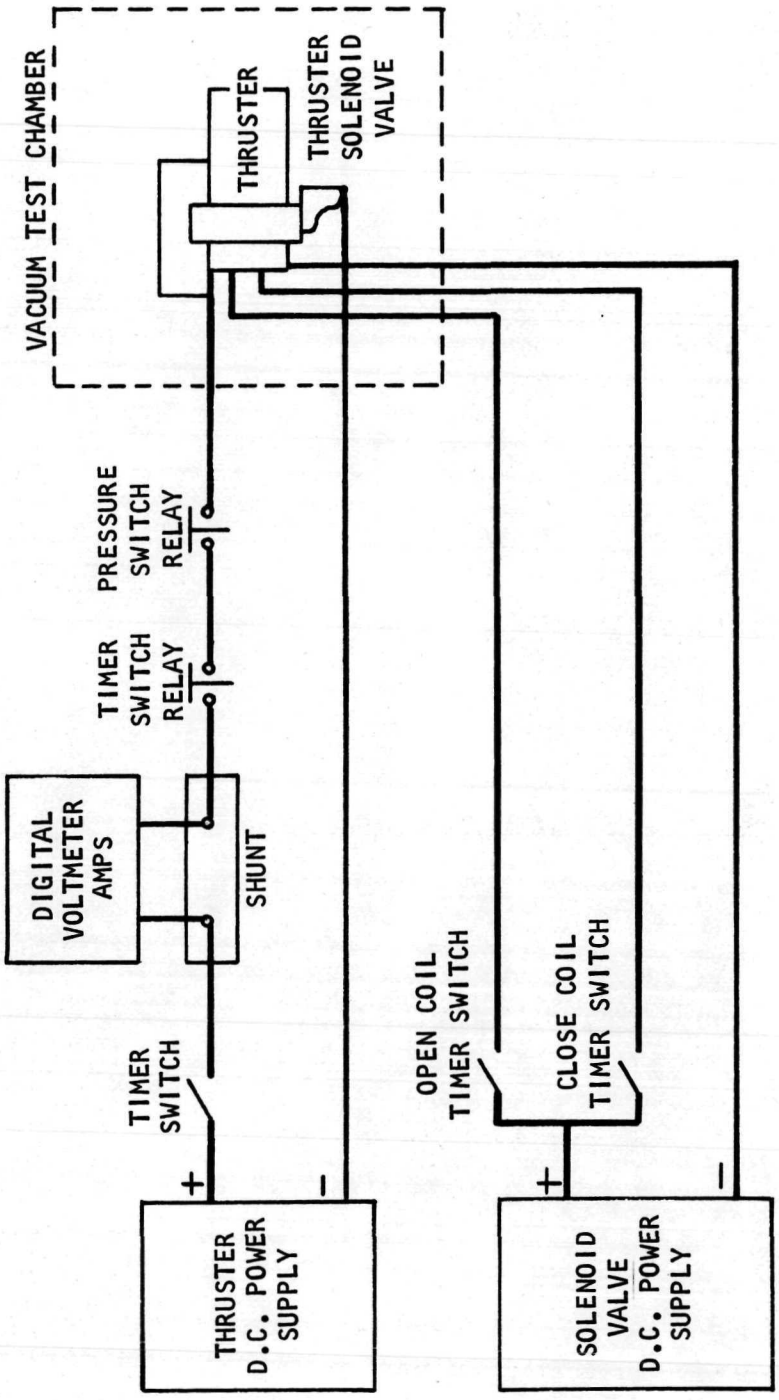

FIGURE 32.

In addition to the direct power control system shown in Figure 32, several other safety devices were included in the facility system to preclude damage to either the test facility or to the thruster as a result of failure of any component. Vacuum pressure switch interlocking in series with the main thruster power control relays was provided to shut off propellant power and flow in the event cell ambient pressure exceeded 500 microns. An electrical interlock switch was provided in series with the timer and pressure switch main relays to provide for safe shutdown of the facility in the event of a facility electrical power failure. Diffusion and mechanical pump systems were protected by cooling line pressure switches to avoid overheating in the event of cooling power pump failure. Either extremely high or slightly low propellant supply pressure would result in thruster propellant flow and power shutdown for facility and thruster protection. The protective systems were required because of the continuous nature of the test with only minimal personnel coverage available to monitor facility and thruster operation on an around-the-clock basis.

Propellants

The propellants used in the life test were the highest purity obtainable at reasonable cost. Hydrogen used was "Ultra High Purity" grade and the ammonia used was "Premium" grade.

One bottle of hydrogen was analyzed to determine purity on a sample basis and was found to have less than 1.0 molar ppm impurities. Ammonia purity was 99.99% minimum. Impurities were:

Non-basic gas in vapor phase	25 ppm maximum
Non-basic gas in liquid phase	10 ppm maximum
Water	33 ppm maximum
Oil	2 ppm maximum.

All propellant supplies were on a double manifold, each one capable of being separately operated or isolated for venting to prevent contamination by air when supplies were being changed.

Thruster Installation and Test Control

The two thrusters were mounted on the end of the dynamometer arm vertically above each other so that the operating lever arm of each thruster was identical. This allowed using a common thrust calibration for measurement of thrust from both thrusters. A close up view of the thrusters mounted in the thrust mount adapter is shown in Figure 33. An overall view of the dynamometer arm with thrusters mounted on the stand on the left side is shown in Figure 34. A close up view of both thrusters with all instrumentation, power leads and propellant supply lines required for running the tests is shown in Figure 35.

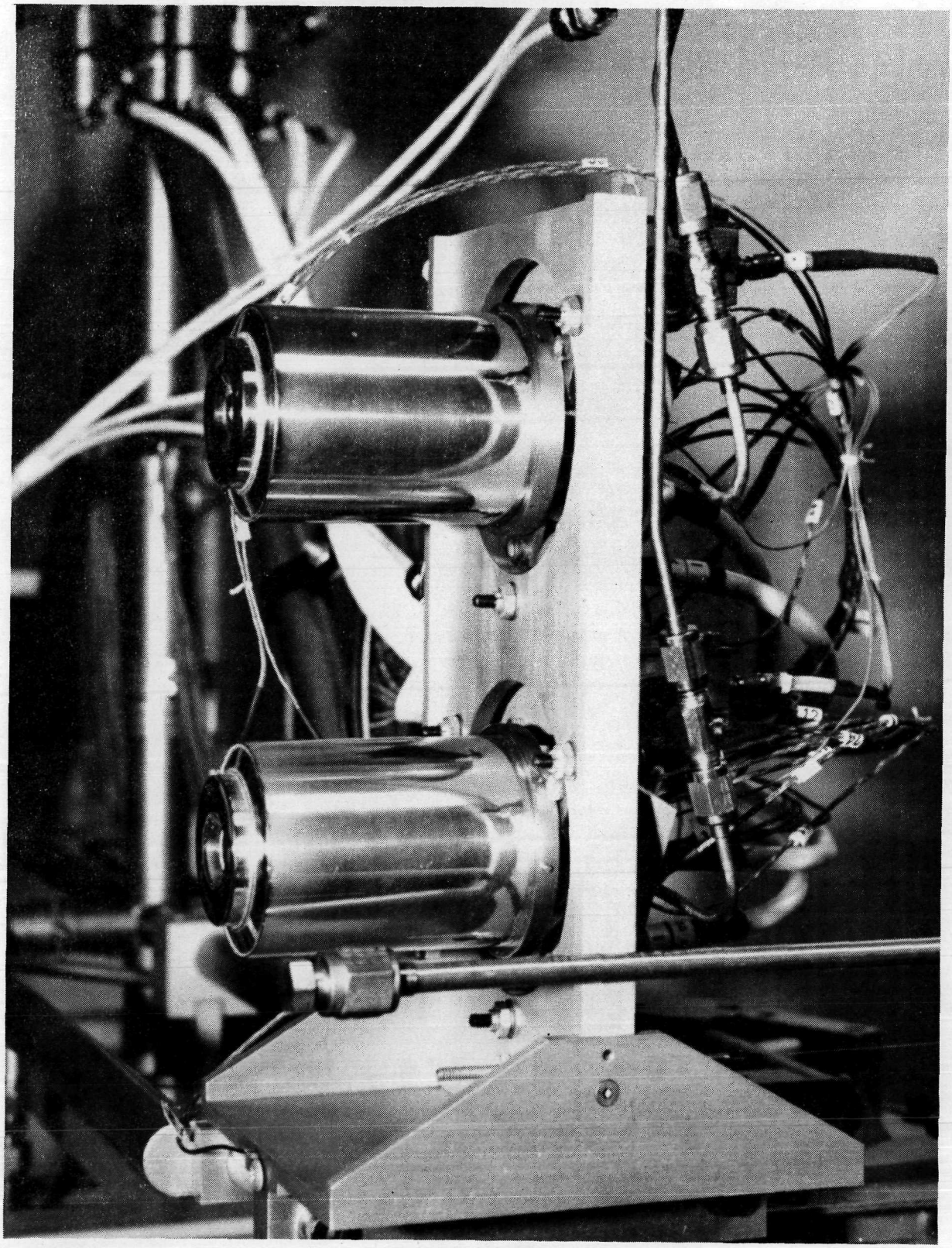

NEG. 72-203-2

FIGURE 33. THRUSTERS IN TEST STAND MOUNT ADAPTER

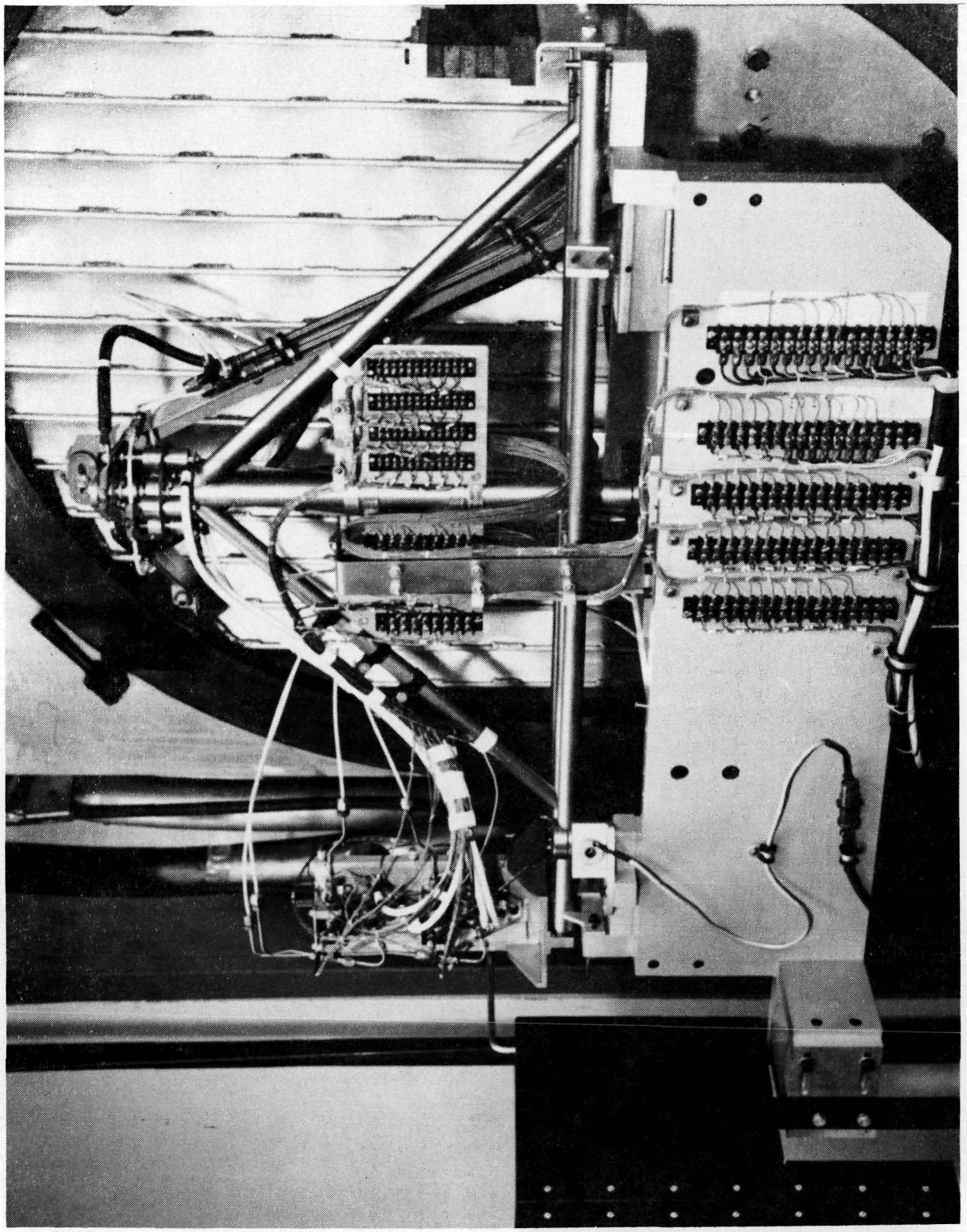

NEG. 72-203-1

FIGURE 34. THRUSTERS MOUNTED ON TEST STAND DYNAMOMETER ARM

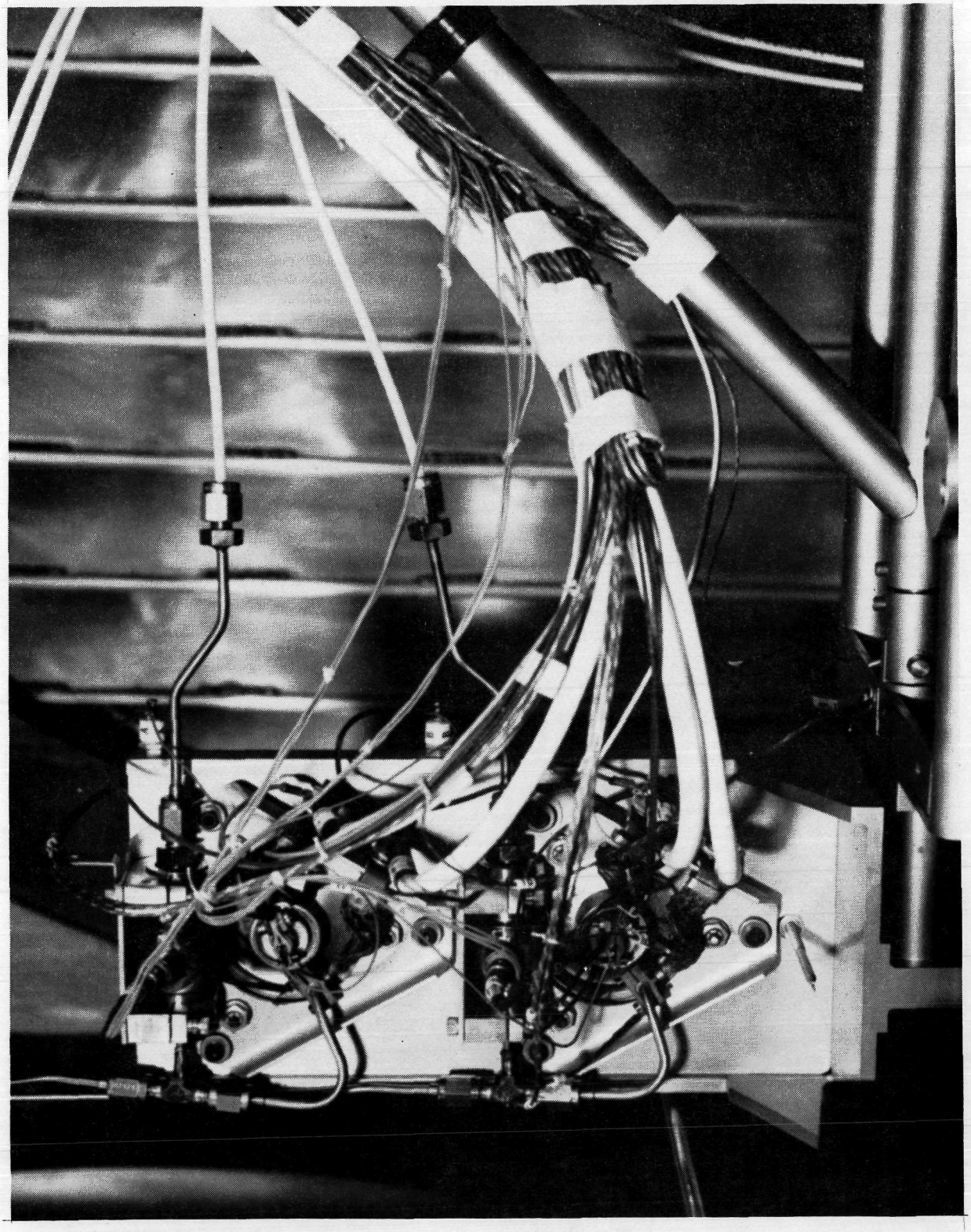

NEG. 72-203-3

56 FIGURE 35. TEST INSTRUMENTATION AND SUPPLY HOOKUP FOR THRUSTERS

Control and operation of both thrusters was provided from two basic consoles which housed the power supplies, flow meters and flow controls and all instrumentation for monitoring thruster power, propellant flow rate and thruster temperatures. A photograph of the control consoles is shown in Figure 36.

Thruster Propellant Systems

Propellant flow (gaseous hydrogen and gaseous NH_3) were provided through separate identical flow path propellant systems. The systems were capable of being interconnected so that either thruster could be operated on either propellant during single thruster operation. This capability was utilized during exploratory portions of the test program where it was desired to determine performance of the same thruster on both propellants without extensive replumbing of the facility. In addition to the normal propellant flow supply capability, an additional propellant path was provided into the test cell to a small orifice used for determining the windage effects on the dynamometer of recirculation of the propellant gasses after being exhausted from the thruster. A schematic of the propellant supply system is shown in Figure 37.

Propellant Flow Measurement

Propellant flow rates were measured by precision rotameters. Two meters were used in series to determine accurate flow rates at both the cold flow and high temperature measurement conditions on the NH_3 flow system. The hydrogen system utilized only a single flowmeter. All flowmeters were calibrated at the use pressure to provide the highest accuracy available. The NH_3 meters were calibrated at 44 psia and the single H_2 meter was calibrated at three pressures, 50, 75 and 100 psia to provide the required accurate ranges of flows. The following formula was used to correct for variations in supply gas temperature and pressure.

$$\dot{m} = \dot{m}_1 \sqrt{\frac{T_c \; P_i}{T_i \; P_c}}$$

Where $\dot{m}$ = mass flow, T = gas temperature,
P = pressure, subscript "i" refers to indicated and "c" to flowmeter calibration values.

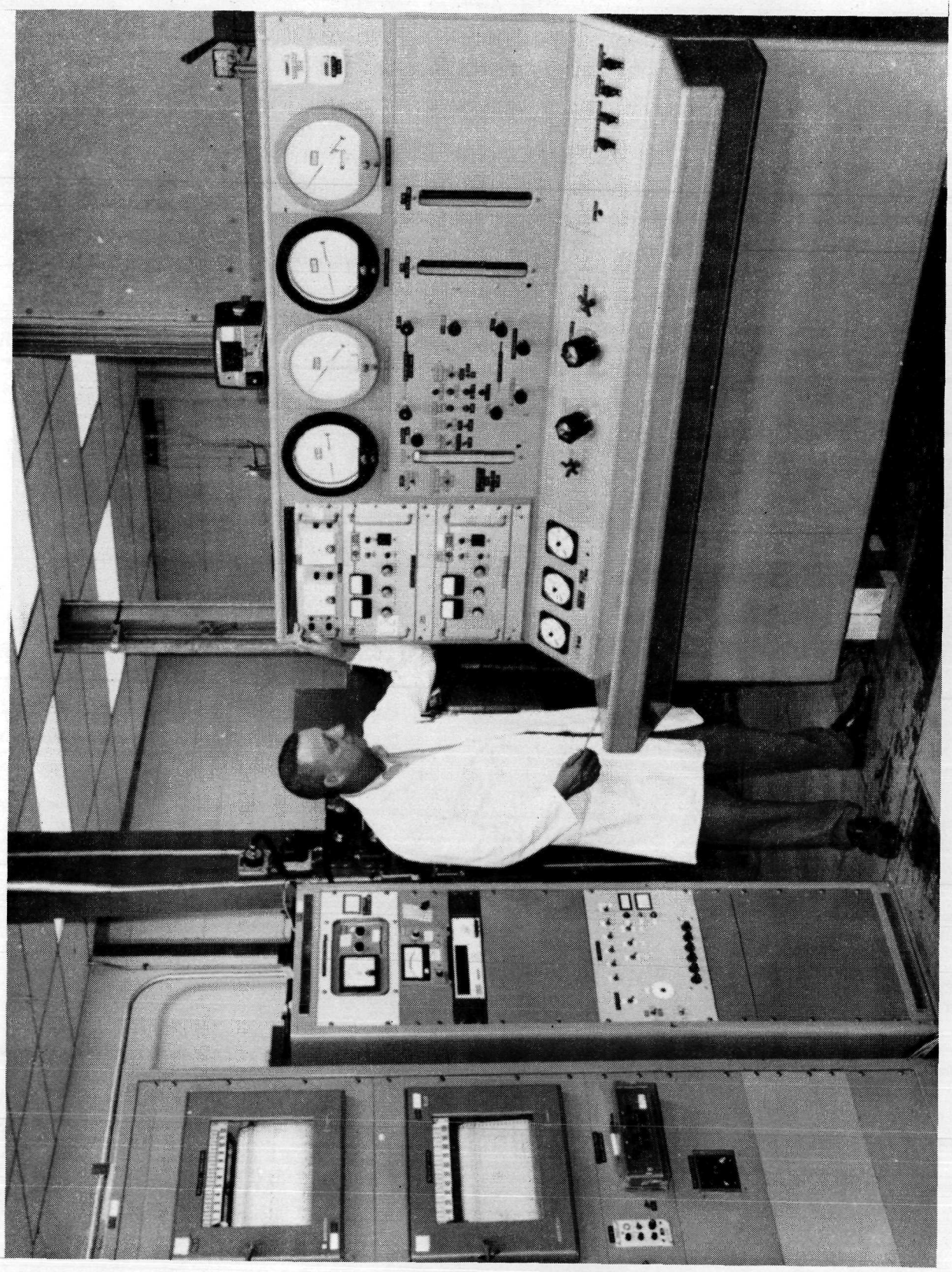

NEG. 72-203-4

58 FIGURE 36. RESISTOJET THRUSTER CONTROL AND INSTRUMENTATION CONSOLE

HIGH VACUUM ELECTROTHERMAL PROPULSION LABORATORY
PROPELLANT SUPPLY SYSTEM

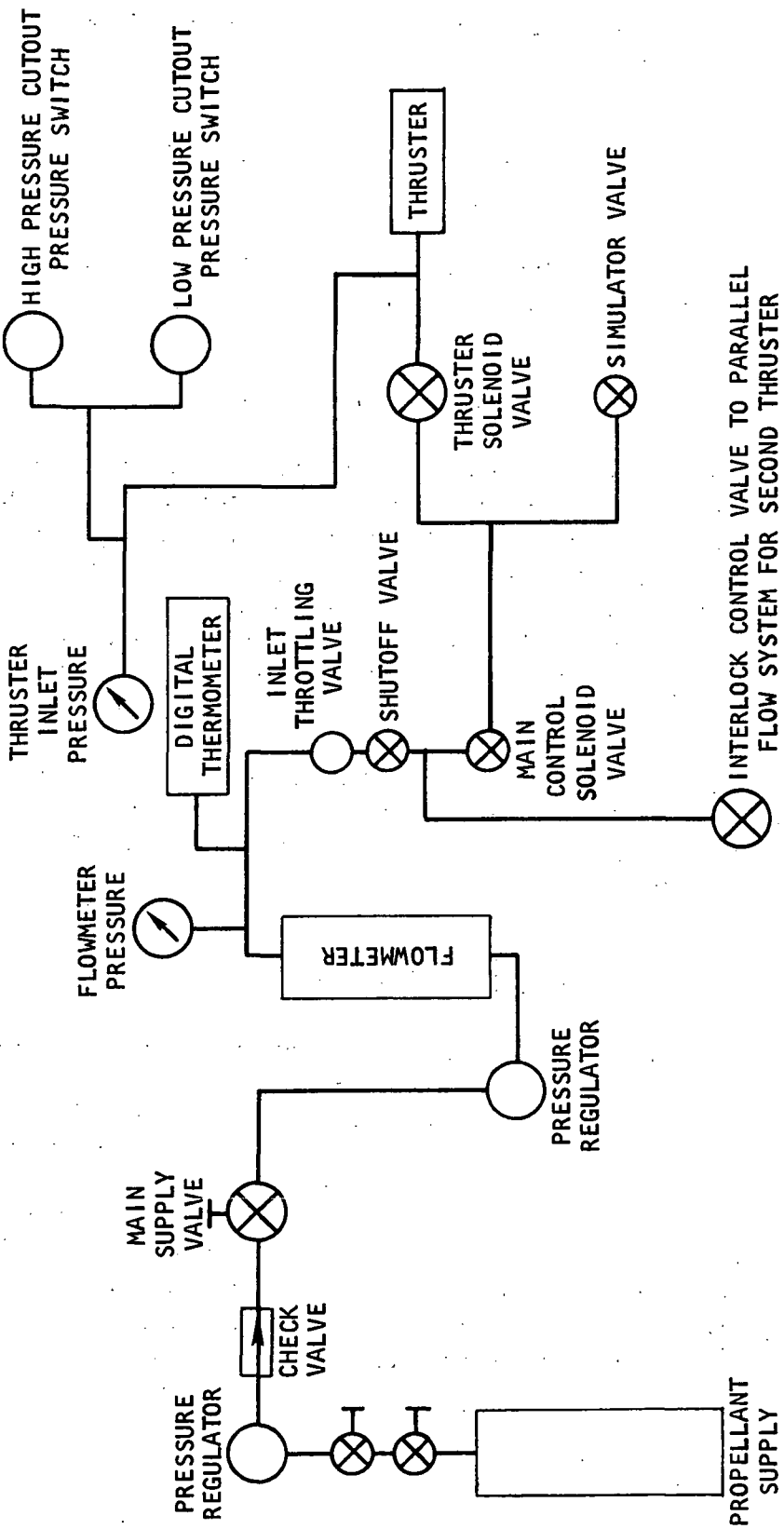

FIGURE 37.

Propellant Pressure

The propellant pressures at the flowmeter and at the thruster inlet were measured by precision Heise gauges.

Propellant Temperature

Propellant temperature was measured by a two channel digital thermometer. A sensing head was located in the propellant line at the flowmeter for accurate correction of propellant flow rates with propellant temperature variation.

Thruster Temperature

Both thrusters were instrumented at selected locations with chromel-alumel type-K thermocouples to accurately measure the temperature of the thruster. Thruster temperatures as well as the dynamometer thrust measurement arm temperature were recorded on 24 channel electronic multipoint potentiometer. In any given setup, less than 24 channels were available because an open was required on both sides of any data channel which was at a significantly higher voltage potential than the next data channel due to point contact overlap between recorder channels during channel changes.

In addition to the normal thermocouple data acquisition channels, the thruster inner heating element exterior temperature was monitored by use of an optical pyrometer sighted through an optical port in the test chamber and down the thruster vacuum jacket vent opening.

Cell Pressure Measurement

Test cell chamber pressure was measured by several instruments of different types with overlapping ranges to obtain multiple readings of cell pressures. Gage types and applicable ranges of operation are indicated in Table II. Nominal correction factors were applied, where applicable, to indicated pressure with hydrogen gas to determine actual pressure. Correlation factors were estimated for ammonia gas, with however, less success in accurate correlation. The primary cell pressure measuring device used was a Stokes, Flossdorg type McLeod gage. This instrument is insensitive to gas composition. Repeatability of the McLeod gage was significantly higher than any of the other gages used since all of the gages were sensitive to ionization potential of the cell gas mixture and required correction.

TABLE II

USEFUL RANGES OF TEST VACUUM GAUGES

Gage Type	Range
Alphatron	760 Torr to 1 x 10^{-4} Torr
Magnevac	- 500 Torr to $\approx$ 1 x 10^{-3} Torr
Thermocouple Gage	- 760 Torr to x 10^{-2} Torr
Ion Gage	- 1 x 10^{-3} Torr to 1 x 10^{-7} Torr
McLeod Gage	1 x 10^{-5} Torr to 5 Torr

Thrust Measurement

Thrust measurement was provided through the use of a Marquardt-developed thrust stand. The stand consists of a rotating vertical member mounted in Bendix flexures which allowed rotation but no vertical translation. The thrusters were mounted on a long horizontal arm attached to the rotating vertical arm. Rotation of the horizontal thrust arm about the vertical axis as a result of thruster output is resisted by the spring rate of the Bendix flexures. Moment arm position was measured by a linear variable differential transformer and exciter demodulator with the output recorded on an electric potentiometer. In this test stand, linearity and repeatability effects on thrust measurements from instrumentation lines or propellant supplies, all electrical wiring are minimized. All instrumentation wiring is transferred from the stationary part of the stand to the rotating part of the stand by long lengths of fine stranded wire. Similarly, propellant supplies are provided through a series of parallel tube arrays which completely eliminate any Bourdon tube effect due to pressure variation. Electrical power supply, requiring heavy leads, is brought into the moving portion of the stand through mercury pots. Thus the stand is virtually friction free and highly repeatable.

Calibration of the thrust output was provided by a remote calibration system. The system consisted of a servo motor which could be commanded to place known weights corresponding to thruster thrust on the stand moment arm. This system allowed frequent, in place, thrust calibrations to be made between thruster firings at vacuum conditions. General practice during the life test cycling series was to make a precision thrust calibration daily following acquisition of the first data points for the test day.

Instrumentation Summary

All instruments were calibrated in accordance with The Marquardt Company standard calibration procedure defined by TMC IDP 70-24, Class 2 (Reference 4). In the event of a shutdown caused by an instrumentation failure, the repaired or replacement instrument was calibrated prior to proceeding with the tests. Table III lists the instruments used in the test along with their ranges and accuracies.

TABLE III

INSTRUMENTATION SUMMARY

	Measurement	Instrument	Serial No.	Range	Nominal Accuracy
1.	Thrust	Thrust systems Model 128 dynamometer with Robinson-Halpern 70-3101 LVDT, Datronic 201B exciter demodulator & Honeywell Electronic 15 potentiometer.	--- --- NB6A41 V6805523001	0.1 mlbf to 1.5 lbf	± 1.0% at 10 mlbf 0.25%
2.	Propellant flow, (H_2)	Brooks Model 1110 rotameter	6802-38659/2	0.0008 to 0.008 g/sec	1.0%
3.	Propellant flow, low range (NH_3)	Brooks Model 1110 rotameter	6802-38659/1 2802-38659/2	0.0025 to 0.025 b/sec	1.0%
4.	Propellant flow, high range (NH_3)	Brooks Model 1110 rotameter	6802-38658/2 6802-38656/1	0.010 to 0.116 g/sec	1.0%
5.	Thruster voltage	Roback digital voltmeter	7002		0.1%
6.	Thruster current	Roback digital voltmeter	7002		0.5%
7.	Thruster supply pressure (H)	Heise pressure gauge	H11964 R	0 to 100 psia	0.2%
8.	Flowmeter pressure (H_2)	Heise pressure gauge	H15591 R	0 to 50 psia	0.2%
9.	Thruster supply pressure (NH_3)	Heise pressure gauge	H15613 R	0 to 50 psia	0.1%
10.	Flowmeter pressure (NH_3)	Heise pressure gauge	H15597 R	0 to 100 psia	0.1%
11.	Propellant temperature	United Systems Digitec digital thermometer	1574C	0 to 100° C	0.1%
12.	Test chamber pressure	CVC Magnevac gauge NRC Model 820 Alphatron NRC Thermocouple gauge Stokes McLeod Gauge Model 276 AC	15054 M0037 0710D1004	1 μ to atm .1μ to atm 5μ to atm .01 μ to 5000μ	±5%
13.	Thruster temperatures	Honeywell Electronic 15 multipoint potentiometer and chromel-alumel thermocouples	66B/5545	0 to 1200°C	± 2°C
14.	Element temperature	Photomatic automatic optical pyrometer, Pyrometer Instrument Company	A107	1450 to 5800°F	0.5%

Measurement Schedule

The life test system was on continuous operation except for required shutdowns for facility maintenance or repair or for analysis of apparent thruster anomalies. Normally three data points were obtained daily to monitor thruster operating condition. These data points were obtained at the start and finish of the normal working day and at approximately midnight. Most of the data points served as reference operating points since most of the test was run using the mechanical pumping system only. Nozzle performance of the thruster was lower at the higher cell pressures provided with the mechanical pumping system than when the diffusion pumps were added to the system for high vacuum periodic performance measurements at approximately 100 cycling hour intervals. The interim performance data (between major performance calibrations) did serve quite adequately to determine repeatability of thruster operation and anamolies requiring further investigation.

During cycling operation, the thrusters were operated at a 50% duty cycle, one half hour on and one half hour off power. All interim performance data was obtained during the last 400 seconds of the "on" part of the cycle. Steady state data points obtained during major calibrations at the 100 operating hour intervals were obtained after a minimum of one half hour at steady state operating conditions to obtain thruster thermal equilibrium.

THRUSTER LIFE TEST

Life Definition

Thruster life for the purposes of this test was defined as:

1. Development of a leak in the thruster structure which would result in a maximum leak rate of 0.5 milligrams/second of hydrogen at a test pressure of 50 psia, ambient temperature and at atmospheric conditions.

2. Maximum allowable resistance change of ± 8% of the initial thruster resistance prior to vibration testing for the thruster heater.

3. Deviation from the limits of the nominal performance values listed below:

Thrust	10 millipounds ± 8%
Propellant flow rate	7 milligrams/sec, ± 5% for H_2
	14 milligrams/sec, ± 5% for NH_3
Electrical power	140 watts, ± 13% for H_2
	220 watts, ± 13% for NH

4. A goal of accumulating 720 hours of cycling operation on each of the two thrusters.

Conditions

Nominal test conditions required that the test environment be at least 10^{-2}, millimeters of mercury vacuum and ambient temperature. Since the test facility had capability to develop significantly better than 10^{-2} mm Hg vacuum with the facility diffusion pumps in use, all performance calibration tests were performed at significantly lower pressures, about 1.3×10^{-3} mm mercury vacuum for the hydrogen test points and at nominally less than 1×10^{-3} mm mercury vacuum for the ammonia thruster. The major portion of the test program was performed without the use of the diffusion pumps. Under these conditions, the ammonia thruster was run at a nominal 23×10^{-3} millimeters mercury vacuum (23 microns) and the hydrogen thruster operated at a nominal 80 to 90 microns mercury vacuum. These conditions were sufficiently low in pressure to provide a good vacuum heat transfer simulation while simplifying the operation of the test facility for the majority of cycling time accrual.

Endurance Time

Endurance time was accrued during the periods when both thrusters were alternately operated in 30 minutes ON, 30 minutes OFF cycles at the nominal operating conditions established during performance calibration of the thrusters prior to start of the life test. During the life test, each test thruster accumulated one half hour of "ON" time for each hour of cycling operation. At conclusion of the life test and final calibration, the thrusters had accumulated the following total "ON" time and hours of cycling operation:

S/N 001 - Hydrogen - 720 cycling hours and
365 hours of "ON" operation

S/N 002 - Ammonia - 720 cycling hours and
392.2 hours of "ON" operation.

Chronological Summary

Life cycle testing was initiated on 13 March 1972 and completed on 30 June 1972 during which the 720 required hours of cycling operation were accumulated including final performance testing. The nominal power and flow parameters were established for the life test based on the performance calibration tests conducted prior to start of the life test and were as follows:

Parameter	S/N 001 H_2	S/N 002 NH_3
Power - watts	220	140
Mass Flow (gms/sec)	0.007	0.014
Thruster Inlet Pressure	30 psia	30 psia
Thrust at High Vacuum Conditions (millipound)	9.45	9.45

Thruster testing continued smoothly for the first 75 hours of cycling operation. On the 76th cycle, performance of the hydrogen thruster, S/N 001 indicated an anomaly in the test facility and/or thruster system. Testing was stopped at that point and a significant investigation was conducted to determine the cause of the anomaly which effectively resulted in low power being absorbed by the thruster relative to nominal conditions. Details of that study are contained in a later section. The study revealed that the anomaly was in the thruster and resulted from touching of the second heater tube by the inner heating element as a result of bending of the inner element. Basic cause of the anomaly was hypothesized to be binding within the boron nitride to third heater element system resulting in restriction of the thruster bellows to take up differential thermal growth of the heater elements.

Since the anomaly was typical of a possible mode which might occur in actual spacecraft operation with the current design thruster, and the thruster would require complete disassembly and rebuilding to repair the damage, it was decided with NASA program monitor concurrence to continue the test to determine if the anomaly could result in a catastrophic failure or whether the thruster could continue to be operated for the remainder of a mission. The only effect of the anomaly was a possible reduction in mission total impulse resulting from the degraded thruster I_{sp} performance.

The test program was resumed after completion of the investigation of the anomaly experienced on the hydrogen thruster. No further problems were experienced with thruster operation during the remainder of the test. Performance of the hydrogen thruster stabilized at an intermediate performance level after the anomaly occurred. Thruster performance remained at a nominal 460 seconds I_{sp} at about 110 watts for the remainder of the test period. Initial performance calibrations had indicated thruster performance to be about 675 seconds at 220 watts in the "new" condition. Performance of the ammonia thruster was excellent and repeatable throughout the entire test with nominal performance at 316 seconds I_{sp} at 140 watts. Initial, intermediate and final thruster performance calibrations indicated that there was no change in the thruster structure or thruster operation during the life test period. These results indicate that with the exception of minor design changes determined to be required to correct the weld deficiencies noted during the off-the limits vibration test and by the anomalous operation of the hydrogen thruster during the life test, the thrusters are sufficiently well developed to be submitted to a flight qualification test with high probability of successful completion.

Periodic Performance Calibrations

Each thruster was subjected to periodic performance calibration at the highest vacuum environmental conditions obtainable through the test program. The tests were nominally planned to be performance at 100 cycling hour intervals to document thruster thermal and specific impulse performance as a function of accrued thruster life. Although only one data point at the nominal operation point was required to document operational capability, several of the tests were extended to document thruster cold flow characteristics, thruster heater element resistance under cold conditions and thruster performance at various power conditions less than maximum operating power point. A total of eight performance calibration tests were performed on each thruster at the high vacuum conditions. These data were used to generate the performance curves shown later in this report. In addition to the periodic performance calibrations at high vacuum conditions, at least two and usually three data points were obtained at the nominal operating vacuum during each day of thruster cycling operation.

The higher environmental pressure (relatively poor vacuum) experience under the normal operation conditions (no diffusion pumps) resulted in degradation of thruster thrust because of both nozzle performance degradation and windage effects on the thrust measuring dynamometer. As a result, the daily thrust measurements were not directly correlatable with high vacuum performance thrust without correction so that intermediate calibrations were used only as monitor performance points to determine consistency of thruster operation. All required parameters, i.c., power, thruster mass flow and relative thrust were maintained within a band significantly less than the operating requirements band through the full period of the test.

Hydrogen Thruster Performance

Prior to and throughout the life test, periodic performance calibration tests were performed on both the hydrogen and the ammonia test thrusters. This section presents the results of the periodic performance tests conducted on the S/N 001 hydrogen thruster and details of an anomaly experienced in the thruster during the test.

Hydrogen thruster life testing continued smoothly for the first 75 hours (cycles) of cycling operation. On the 76th cycle, performance of the hydrogen thruster, S/N 001 indicated an anomaly in the thruster and/or facility system. Current surges of about 0.3 amp were noted as were voltage surges of 0.2 volt. In addition, thruster mean power level was down from the nominal 220 watts to about 170 to 180 watts. The life cycling was stopped and the steady state parameters recorded for subsequent investigation. All hot data indicated an anomaly in the thruster power system which could be associated with touching of the inner heater element, so the test was stopped to further investigate causes of the problem.

Cold thruster precision resistance tests and visual examination of the thruster revealed two changes. First, the small rhenium wire attached to the end of the inner heater element, for inner element voltage drop measurement had apparently migrated into the thruster stem. It was hypothesized that this wire could have snaked into the space between the inner heater element and the third heater element causing a low resistance short. To further document cause of the problem, precision resistance tests were made on the thruster to determine if a change in thruster resistance had occurred. Results of these tests were as follows:

	Inner Element Resistance (ohms)	Overall Thruster Resistance (ohms)
Before Cycle 76	0.01380	0.0183
After Cycle 76	0.00239	0.0132

A review of Figure 38, which presents the thruster resistance path schematically, shows that the only way the resistances could have changed as indicated was for the inner heater element to be touching the second tube. If only the voltage measurement wire attached to the inner element had shorted, the resistance of the inner element would have been identical to the original measurement made prior to initiating the life tests.

In order to confirm the cause of the thruster anomaly, the outer case and insulation were removed from the thruster. High intensity X-Ray photographs were made to document condition of the inner heater element assembly and the voltage pickup wire. Results of the X-Ray studies are shown in Figure 39, a photograph of the thruster inner structure in the undisturbed condition. In this photo, it can clearly be seen that the inner heater element is bowed and resting against the inner wall of the second heater tube and the voltage pickup wire is also bent and possibly touching the third tube.

The phenomenon of the inner heater element touching against the second tube inner wall was determined to bea problem worth further detailed investigation since other resistojet thrusters of similar construction have shown the same operational problem (Reference 2).

In attempting to determine the cause of the bent inner heater element of the hydrogen thruster, it appeared that there could be two possible basic causes. One potential mode could be through thermal transient differential part growth rates; i.e., if the inner element could heat up and grow at a rate significantly higher than the second, third, and outer tubes, the inner heater element could be put in column compression. The second potential mode could occur through binding of the boron nitride spacers between the third and fourth tubes.

Inner element thermal compression could occur if the inner element differential growth was significant enough to exceed the full takeup capabilities of the bellows assembly during startup. The bellows can absorb approximately 0.008 to 0.009 inches of inner element relative growth before the pressure area tension force exerted on the bellows by the inlet gas is exceeded at 30 psia inlet pressure. At this deflection the tube is compressed at the spring rate of the bellows (120 lb/in.) against the pressure force exerted by the run gas (approximately 0.9 lb). To determine if compression of the inner tube could be the only problem, thermal transients of each of the thruster parts which could be instrumented were measured under controlled power application conditions as well as under step power input conditions. These tests were intended to determine if the differential growth rate of the thruster parts could be the problem, and if it were, whether the differential growth rate could be controlled by application of power at a rate consistent with ability of the thruster to thermally respond to the changes in power.

RUGGEDIZED RESISTOJET ELECTRICAL SCHEMATIC

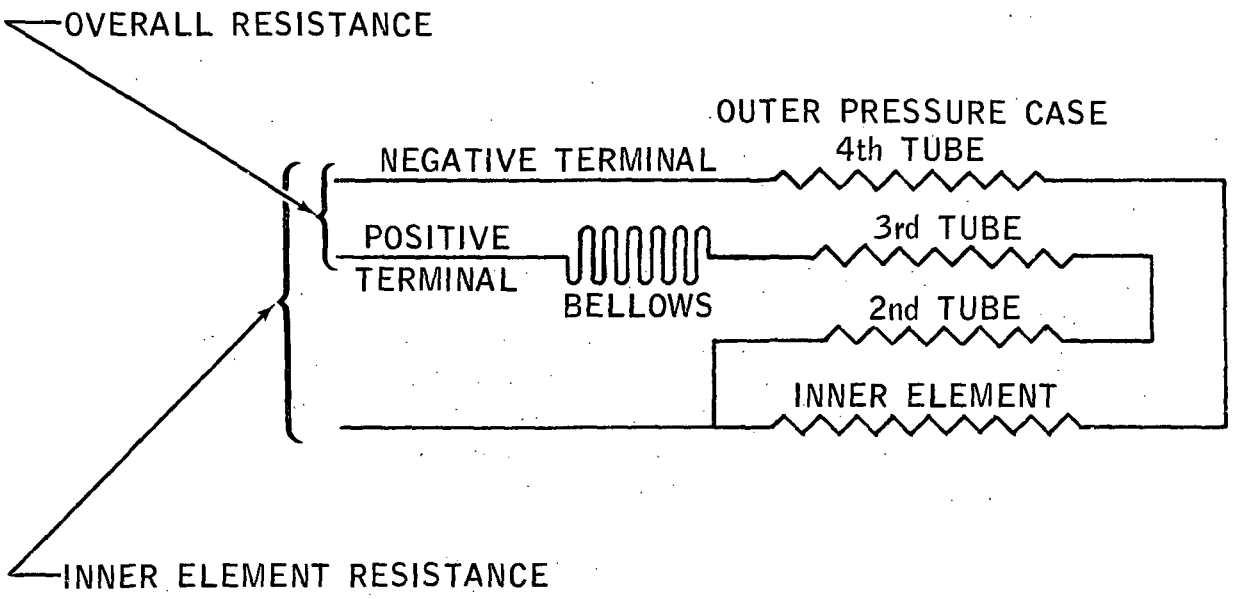

FIGURE 38.

X-RAY OF S/N 001 RUGGEDIZED THRUSTER

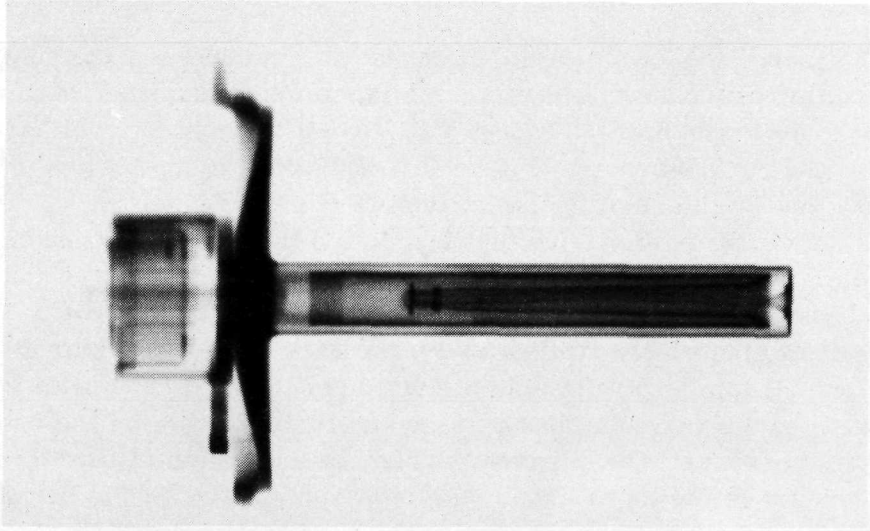

FIGURE 39.

Thermal transients were measured for four types of run conditions using the S/N 002 NH_3 thruster which appeared to be in good condition. First, "normal" start conditions; i.e., step current input, was run and critical transient temperatures recorded. Second, a current input ramp was attempted; however, this procedure was not significantly successful in controlling rate of power input since the voltage drop increase resulting from rising thruster temperatures was not fast enough to keep up with a controlled two-minute current ramp. The third and fourth tests conducted were voltage control ramps where voltage was controlled to provide either a two or a four-minute voltage rise ramp. This technique did result in control of power input on a roughly linear slope ramp.

Since the inner element absorbs most of the power input and the length of the inner element is a critical parameter in the problem, the thermal transient temperatures of all parts which could be measured were related to inner element length. This parameter is most easily related to the inner element resistance since inner element temperature and thus length is directly related to the resistance.

Figure 40 shows thermal response of the center of the outer pressure case as a function of the inner element resistance for three cases of power application; a step input, a two-minute voltage ramp and a four-minute voltage ramp. The fact that the curves practically overlay each other indicated that there was virtually no difference in the relationship of the functions irrespective of the power input rate. Other temperatures similarly plotted showed the same relationship with regard to inner element temperature. These results plus observation of tubes being tested in the bell jar facility indicated that the thruster tube temperatures are almost directly responsive to power absorption by the thruster with only minor differences in transient times to final temperature being a function of the heat capacities (thus heating time constants) of the various tubes and the additional heating of the outer tubes through conductivity from the center tube. Thus, except for the above minor differences in time constant of the tubes under ohmic heating, there should be relatively small differential growth between the inner and outer tubes during a step input power transient. Thus, unless the steady state temperature distribution could cause enough differential growth to cause the inner element tube to become an unstable column, the probability of thermal transients being directly responsible for the bending of the inner tube appeared to be very unlikely.

In order to check both the possibility of high column loads on the center heater element and the possibility of binding of the boron nitride spacers between the third and fourth tubes, a second series of tests were run to document relative movement ofthe inner element during starting of the thruster. These tests consisted of starting the thruster in both a step power input mode and a voltage ramp input mode while measuring the movement of the forward end of the bellows assembly. Movement of the bellows assembly relative to the thruster structure was accomplished by attaching the slug of a linear variable differential transformer (LVDT) to the positive thruster connector and the coil or core of the LVDT to the thrust stand so that its position did not vary relative to the thruster structure. Thus, any movement of the bellows could be accurately measured.

A72-7-290-49

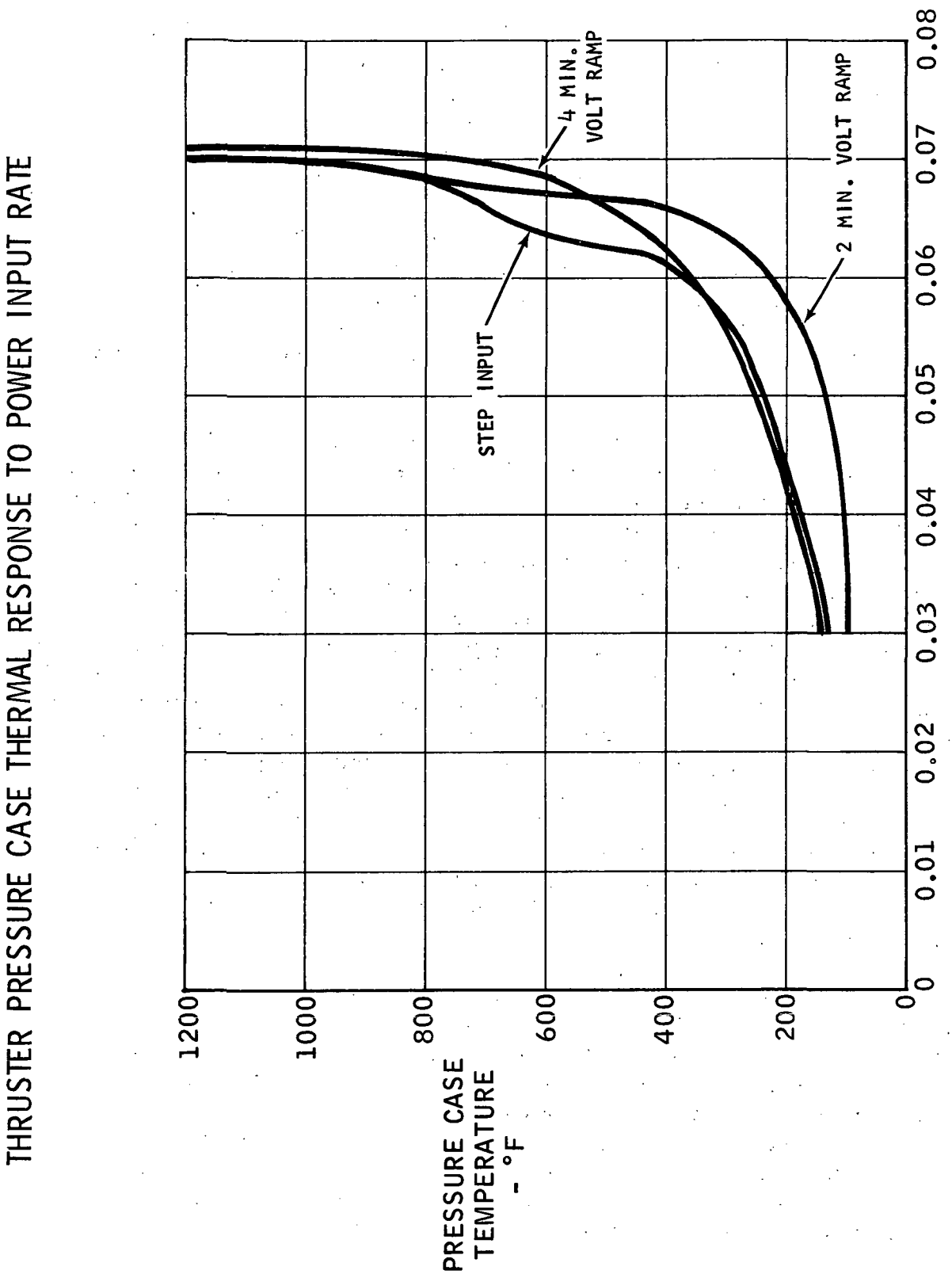

FIGURE 40.

Since the S/N 002 NH_3 thruster appeared to be operating normally, it was used as the baseline for testing with both NH_3 and H_2 as propellant gases. The first test consisted of measuring relative bellows movement for steady state conditions at progressively increasing power levels using H_2 as the propellant gas. Figure 41 shows the results of these tests. It can be seen that the bellows progressively retracts at higher and higher power levels until at 220 watts power, about 0.0063 inches deflection was obtained. These data are in good agreement with the analytically predicted position at 220 watts. After steady state data were obtained, the thruster was started in a normal step power input start with H_2 and then NH_3. Thermal growth was immediately responsive to power application with the majority of change occurring in the first few seconds of operation. Total deflections for a normal start on H_2 and NH_3 were 0.0068 and 0.0075 inches, respectively. This deflection is within the capability of the bellows to maintain a tension load on the center heater element. Based on the data obtained, it appears that the thruster is fully capable of being started in a normal step power input mode with no danger of bending the center heater element through compressive column loading.

The test data obtained using both H_2 and NH_3 on the S/N 002 thruster indicated that the problem in causing the bending of the center heater element was not associated with the start transient per se. To check the only other remaining possibility, the S/N 001 thruster was reinstalled in the thrust stand with the LVDT attached to the center element to determine if binding was occurring in the boron nitride spacer area which prevented the bellows from maintaining a tension load on the center tube during thruster startup. These tests revealed that there was only about 0.001 inches of movement of the bellows during starting of the thruster. Since the thrusters are supposed to be identical, these data strongly indicated the third tube was not capable of sufficient movement to allow the bellows to absorb relative growth of the inner heater element, probably as a result of binding between the boron nitride spacers and the outer tube. The boron nitride spacers are retained in position by milled flats on the third tube. This method of retention could result in slight circumferential movement of the spacers off of the flat during dynamic environment testing. This could cause the spacers to act as a wedge between the third tube and the outer tube and thus prevent relative longitudinal movement between these tubes. This apparent anomaly can be easily eliminated on future designs by positively keying the spacers to prevent circumferential movement.

Repair of the thruster would require extensive disassembly and rework of the thruster not within scope of the current contract. The decision was consequently made to continue testing the thruster under conditions which would duplicate the anomaly in the spacecraft system. These test conditions consisted of operating the thruster at the same regulated inlet presure as it had been operating at and at the same current control level as during normal operation. The remainder of the tests provided data on the life expectancy of the thruster under the anomalous condition. The only effect of the anomalous condition on thruster performance was to reduce thruster consumed power and consequently lower thruster temperatures. While

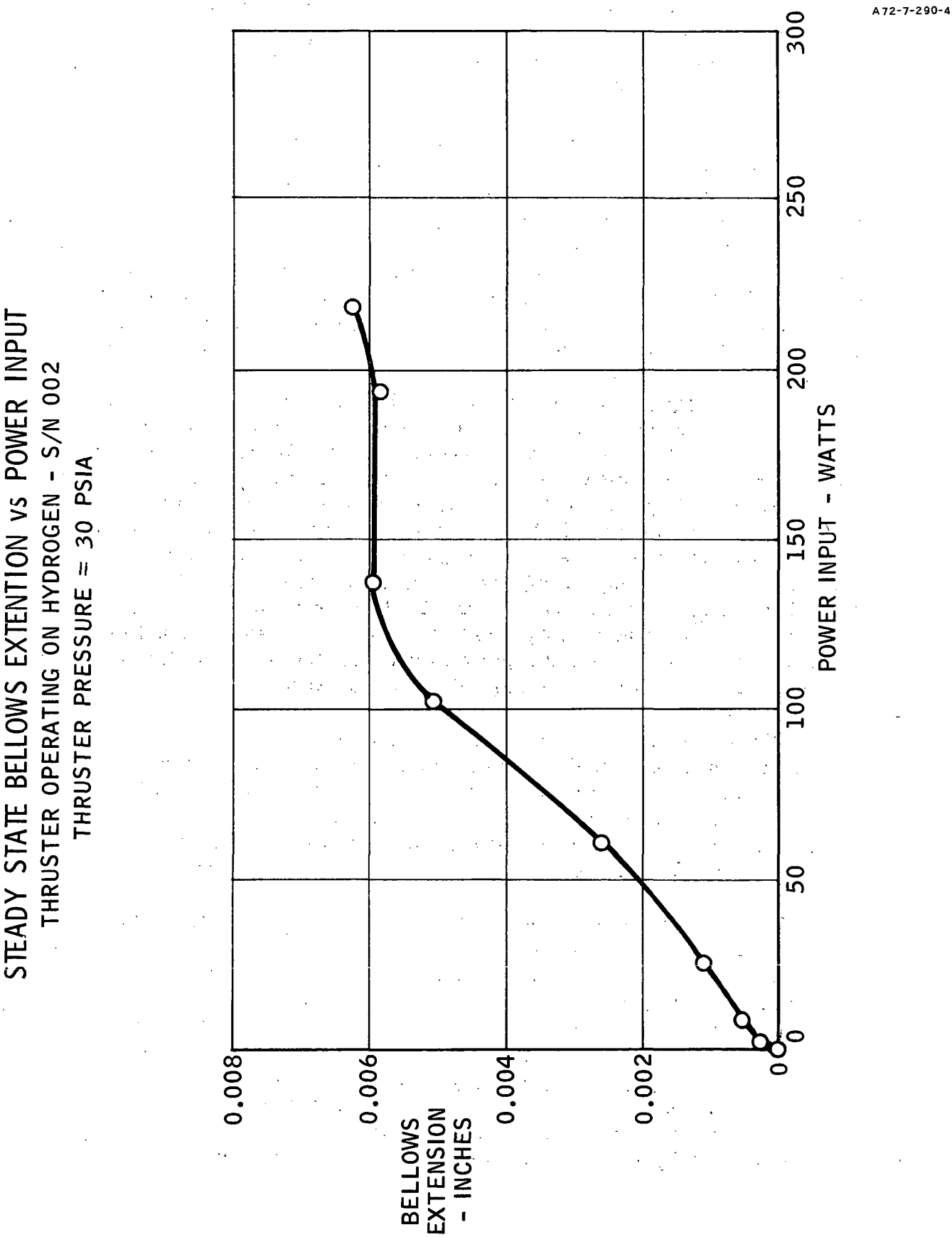
STEADY STATE BELLOWS EXTENTION vs POWER INPUT
THRUSTER OPERATING ON HYDROGEN - S/N 002
THRUSTER PRESSURE = 30 PSIA
A72-7-290-48
BELLOWS EXTENSION - INCHES
0.008
0.006
0.004
0.002
0
0
50
100
150
200
250
300
POWER INPUT - WATTS

FIGURE 41.

thruster temperatures and performance were reduced because of the lower power level and higher mass flow of propellant, thus reducing the total system impulse available, the thruster could continue to operate in the reduced power mode and still provide the required mission functions.

After completion of the life test program, the thruster was again examined using high intensity X-Ray techniques. As expected from the thruster data, no further significant change had occurred in the hydrogen thruster. The post-test X-Ray of S/N 001 thruster is shown in Figure 42 with a similar X-Ray of S/N 002. This photograph shows the S/N 002 tube to be in good condition (straight) and the S/N 001 thruster to be approximately as it was after initial occurrence of the touching anomaly. As shown in Figure 43, post-test teardown of S/N 001 thruster did verify that a wedged spacer was the cause of the touching anamaly that was experienced on this thruster during the life test program.

Specific impulse performance. - Initial acceptance test of the thruster (conducted prior to the vibration test) and the majority of the pre-life calibration tests on this thruster were conducted at conditions slightly different than the selected life test operating conditions. Pre-life and acceptance tests were run with a thruster inlet pressure of 32 psia. Analysis of these data plus additional limited tests indicated that the thruster mass flow at the acceptance test level was higher than desirable to maintain work statement operating conditions so an inlet pressure of 30 psia was picked for performing the life test. Figure 44 shows the effect of inlet pressure (mass flow) on I_{sp} at nominal input power levels. Figure 45 shows specific impulse performance of the thruster at the life test 30 psia inlet pressure condition as a function of power. It can be seen that performance was consistent as a function of power level even after the anomaly causing reduced power occured.

Thruster performance at the life test operating power level is shown in Figure 46 as a function of accrued thruster cycles. Initial performance measurements indicated a specific impulse of approximately 675 seconds at 220 watts of input power. After the inner element touching anomaly, performance degraded as a function of the percentage of the inner element assembly no longer carrying power. After about 300 hours, performace stabilized at a mean level of about 470 seconds I_{sp}.

Thruster overall efficiency. - Figure 47 presents all of the periodic performance calibration data taken during the program in terms of overall efficiency as a function of thruster input power. As with the specific impulse performance data, performance repeatability was good, especially considering the anomalous operating condition of the thruster.

Effect of windage on thruster performance. - Previous testing of resistojet thrusters had revealed (Reference 2), that increased test cell pressure had a deleterious effect on the measured thrust. The phenomena of increased performance at lower cell environmental pressures could partially be attributed to cell flow recirculation

X-RAY INSPECTION OF MODEL R-110 RUGGEDIZED RESISTOJETS FOLLOWING COMPLETION OF LIFE TEST

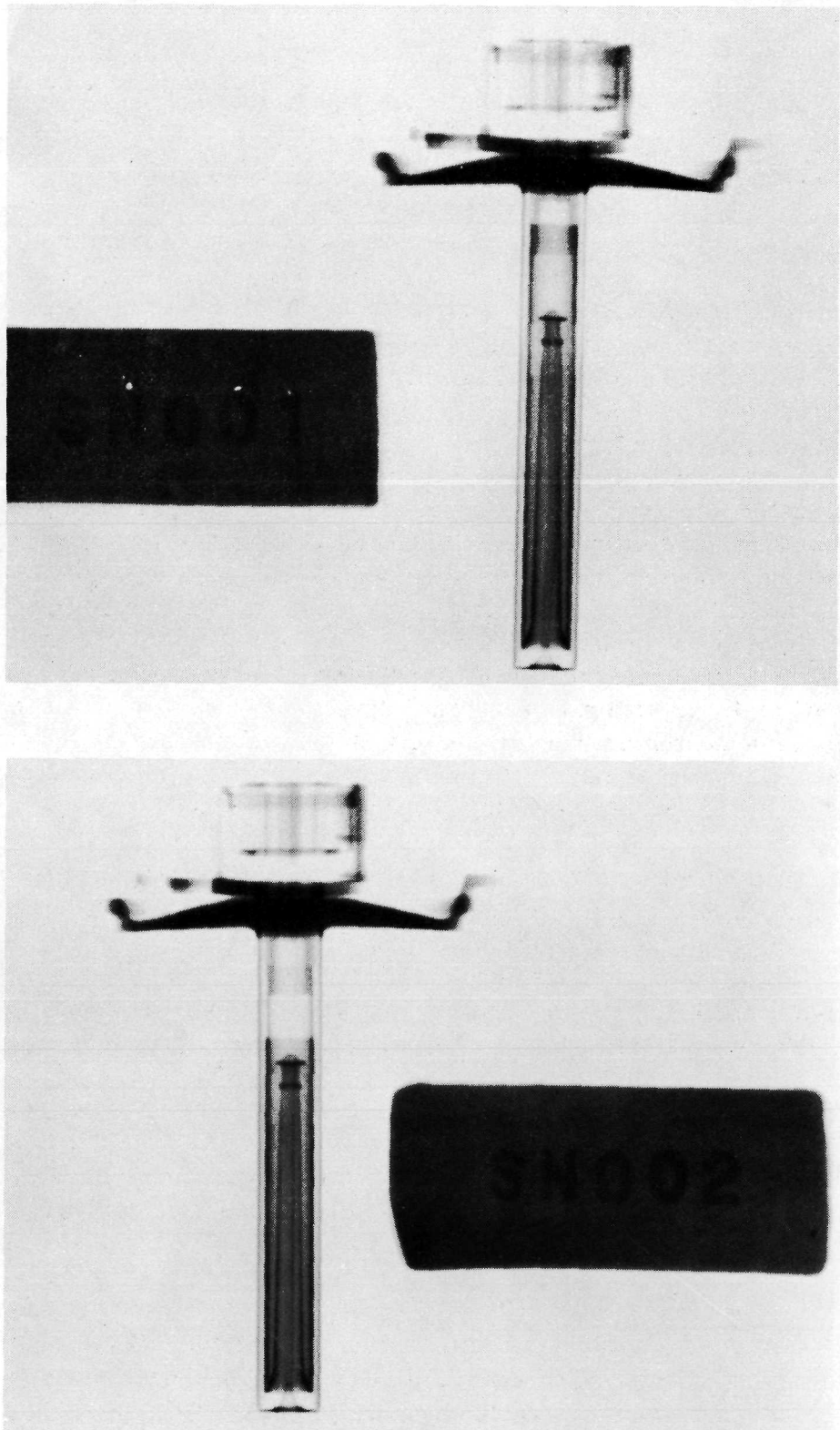

FIGURE 42.

POSITION OF P/N 232607 SPACER ON S/N 001 RESISTOJET AS FOUND DURING POST-TEST TEARDOWN INSPECTION

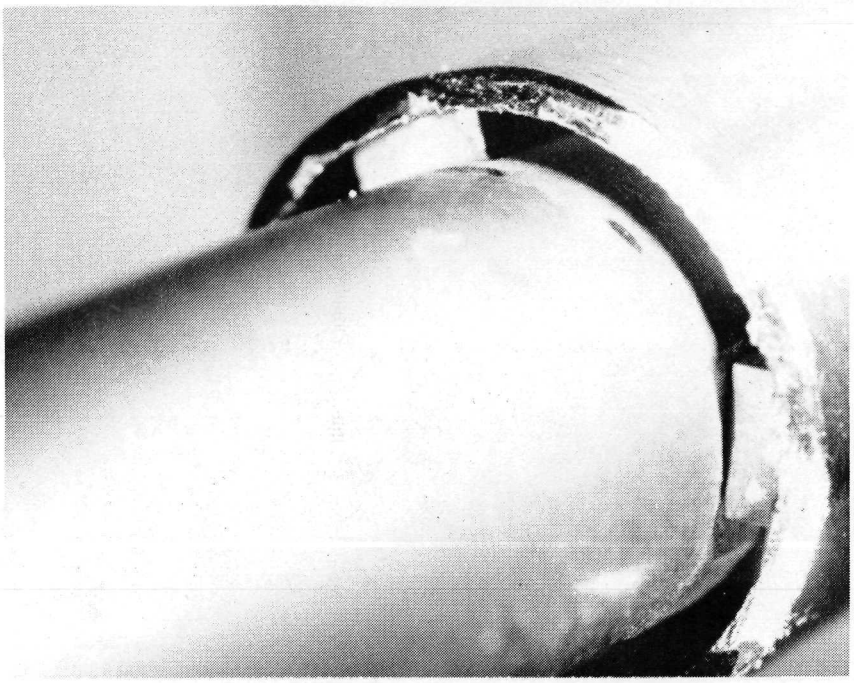

WEDGED SPACER

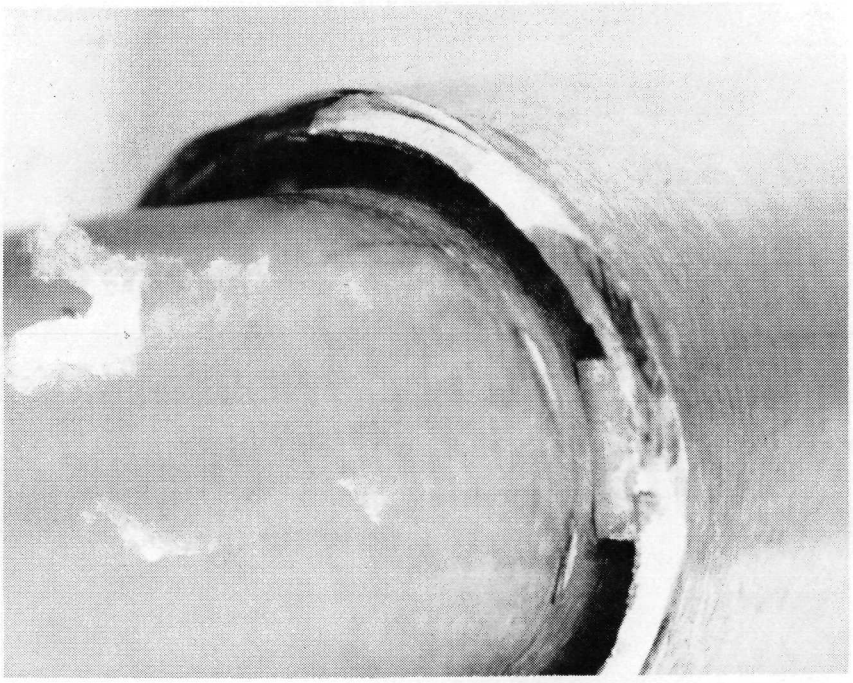

NORMAL SPACER INSTALLATION

FIGURE 43.

SPECIFIC IMPULSE vs HYDROGEN MASS FLOW RATE

HYDROGEN THRUSTER - S/N 001

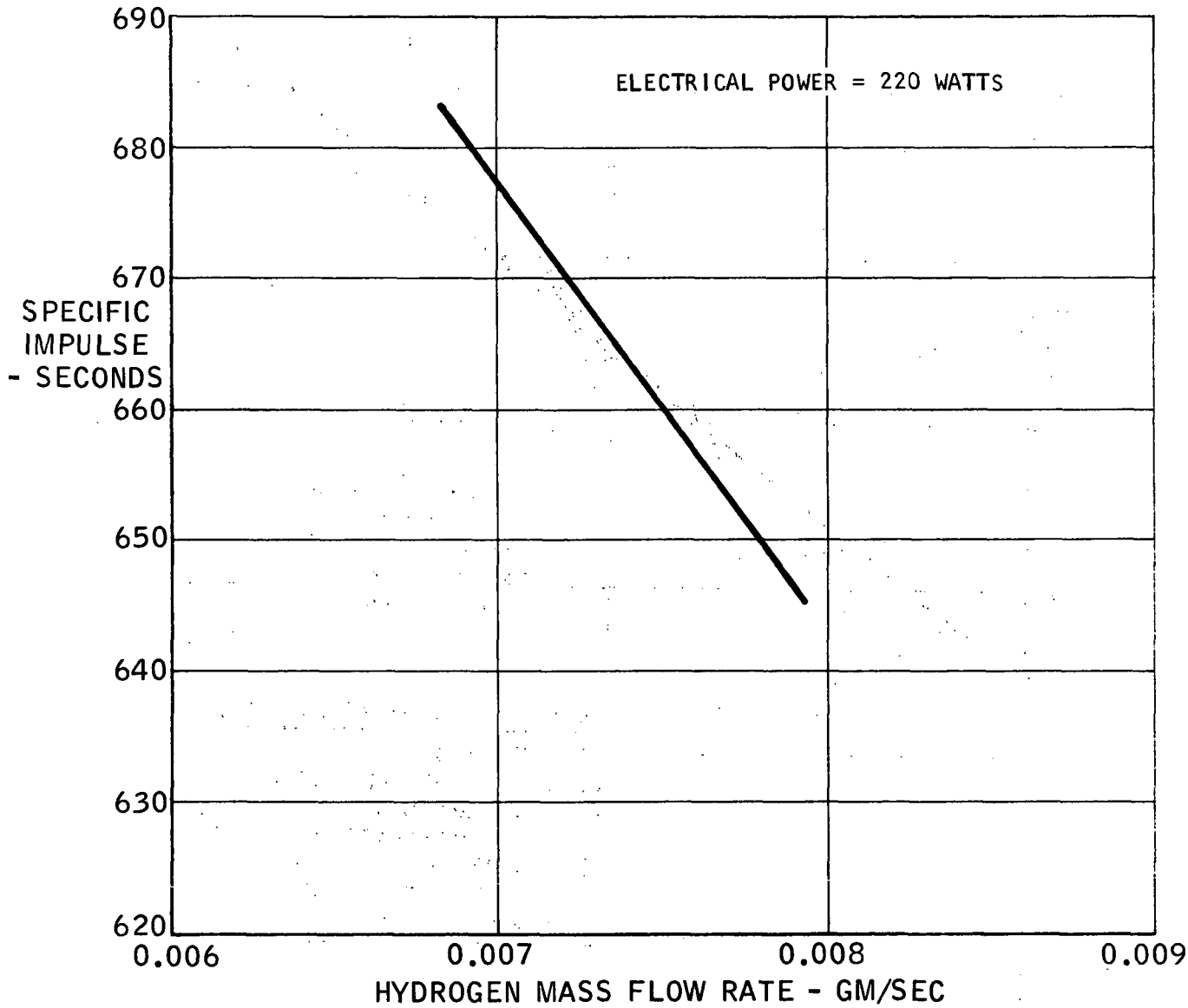

FIGURE 44.

SPECIFIC IMPULSE vs ELECTRICAL POWER
HYDROGEN THRUSTER, S/N 001, LIFE TEST RESULTS

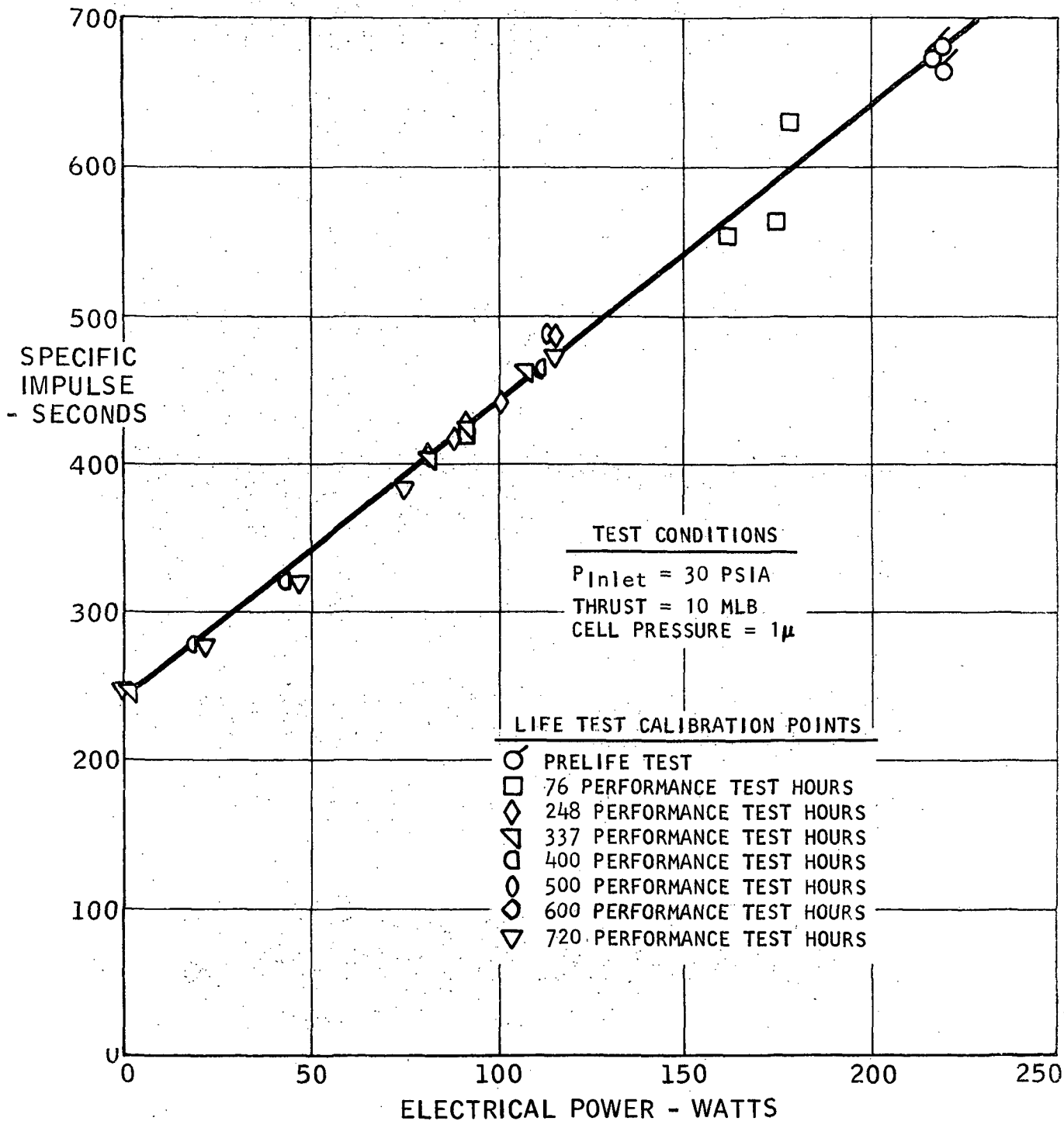

FIGURE 45.

SPECIFIC IMPULSE vs ACCRUED LIFE
HYDROGEN THRUSTER - S/N 001

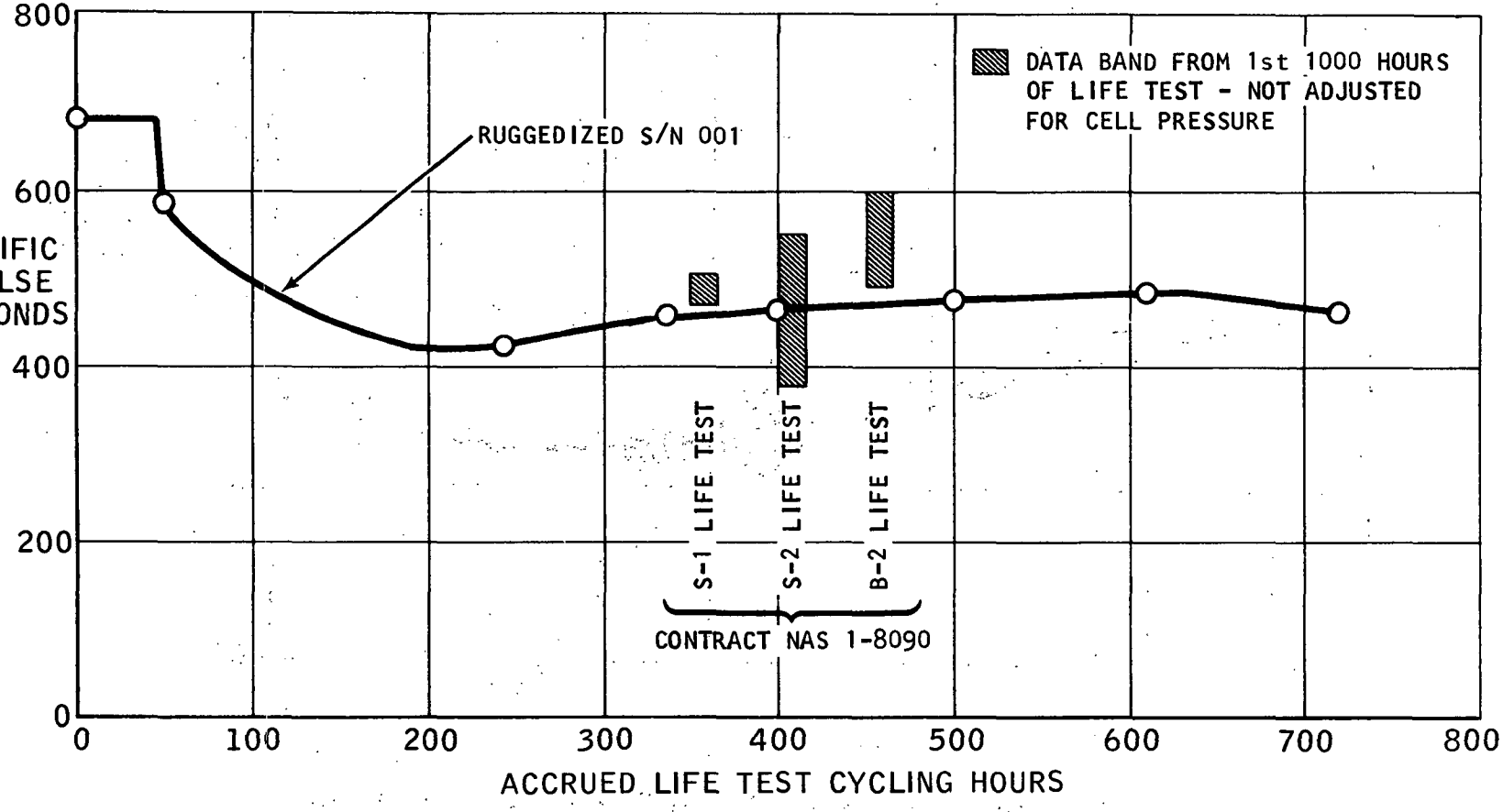

FIGURE 46.

A72-7-290-30

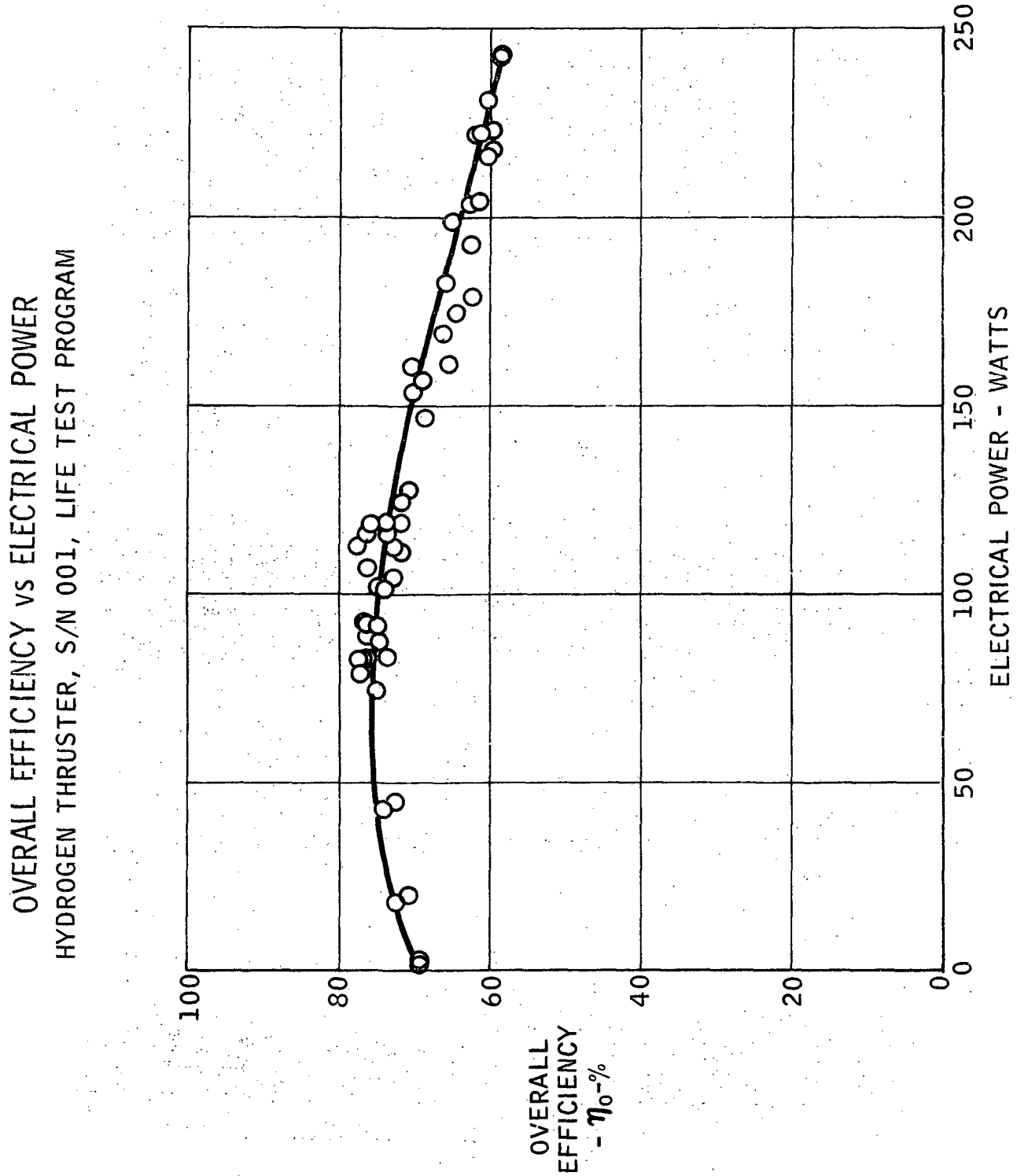
OVERALL EFFICIENCY vs ELECTRICAL POWER
HYDROGEN THRUSTER, S/N 001, LIFE TEST PROGRAM
OVERALL EFFICIENCY - η_o-%
100
80
60
40
20
0
0
50
100
150
200
250
ELECTRICAL POWER - WATTS

FIGURE 47.

or "windage". The effect is dependent of both the cell pressure and mass flow rate through the thruster. As cell pressure is increased either through higher mass flow through the thruster or degradation of available vacuum from the pumping system, more molecules become available to recirculate within the chamber and react with the thruster and thrust stand. In effect, the thrust stand and associated moving wires, etc., act like a boat sail as shown in Figure 48.

Since the windage effect is directly affected by the sail area available, the effect must be measured for each individual installation. Windage effect was measured by installing a 0.020 inch diameter fixed orifice close to and in the same plane as the thruster exit but independent of the thrust measuring system. The test gas is then flowed through the same measuring system as used during the thruster tests and routed through the simulator orifice. Each mass flow variation resulted in a different thrust correction. Performance of the pumping system was extremely repeatable for a given flow rate of hydrogen as shown in Figure 49. This fact resulted in an extremely repeatable effect on the measured thrust. Measured windage effect for hydrogen thruster testing is shown in Figure 50. The curve shown includes points from all of the periodic calibrations and demonstrates the repeatability of the pumping system. In order to assure that the pumping performance (windage effect) did not change throughout the test, a windage point was measured for each test mass flow at the resultant cell environment pressure.

The windage effect discussed above results in lower apparent thruster I_{sp} at higher cell environmental pressures. A cross check against performance effects measured during the Reference 2 tests was made indicating that windage effect of thruster performance for the two specific tests was similar considering the thrust stand differences between the two tests. The windage correction, however, does not account for all of the difference in I_{sp} performance between operation of the thruster at high and low cell environmental pressures. The difference in operating performance measured at high versus low cell environmental pressures (even with windage effects corrected for) shown in Figure 51 is attributed to degradation of the viscous flow of the nozzle. The 10 mlb resistojet thruster nozzle operates at Reynolds numbers below 1,000 with hot hydrogen and ammonia. Nozzle flow is viscous and laminar with a significant subsonic flow boundary layer along the nozzle walls. When the cell pressure is raised, it is believed that the increased pressure is propagated upstream through the subsonic flow layer to affect the internal flow characteristics of the nozzle. Increasing cell pressure is believed to thicken the boundary layer, thus effectively reducing the nozzle expansion process, reducing exit gas velocity with resultant lower specific impulse.

Thruster thermal performance. - Thruster temperatures were measured throughout the test to provide input for further thermal analysis of the thruster structure. In general, thruster temperatures were reasonably repeatable. Variations in measured temperature resulted primarily in differences in the time the thruster was allowed to remain at the operating power level at which the temperature was

FLOW RECIRCULATION IN ELECTRICAL PROPULSION LABORATORY TEST CHAMBER

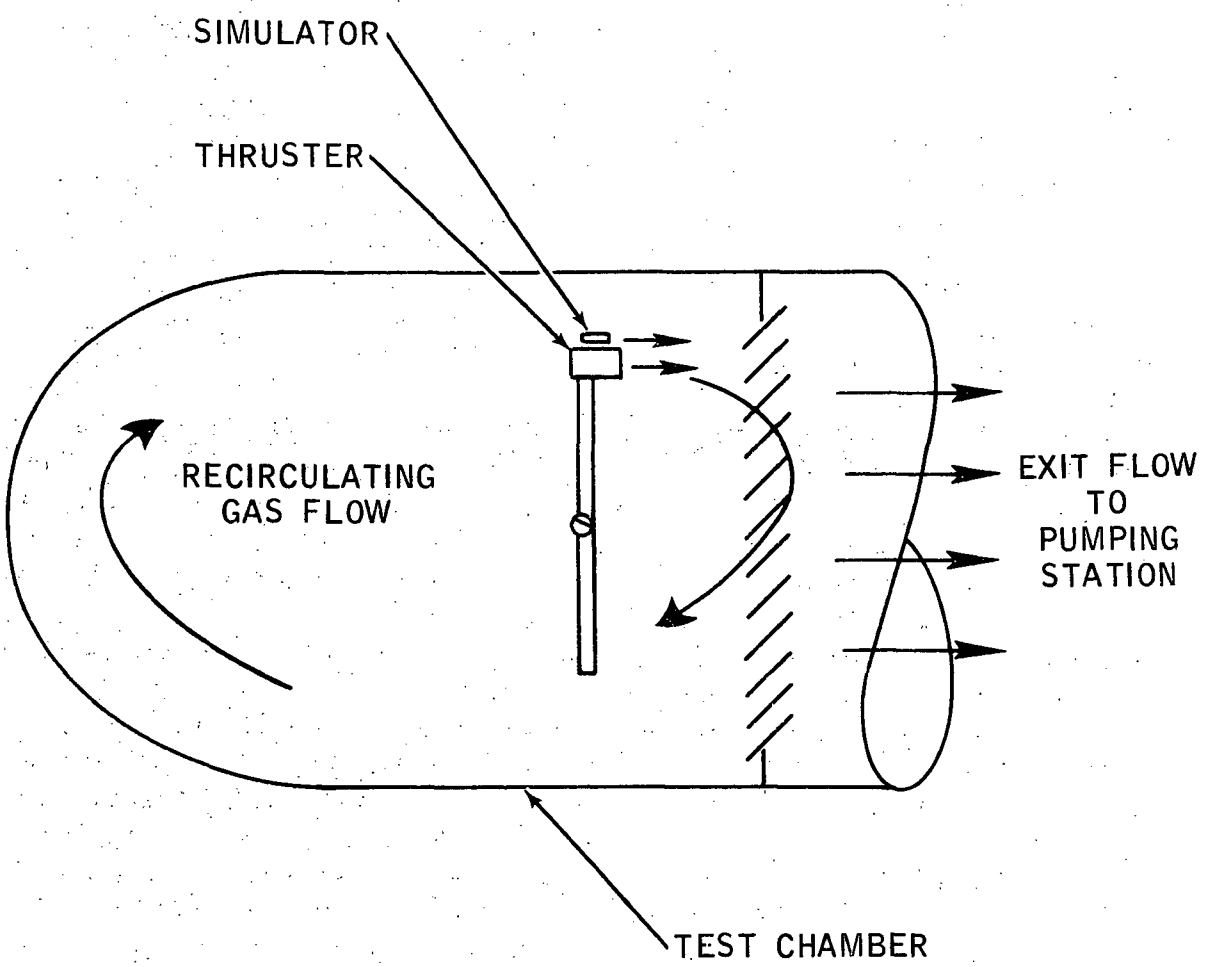

FIGURE 48.

CELL PRESSURE vs HYDROGEN FLOW RATE

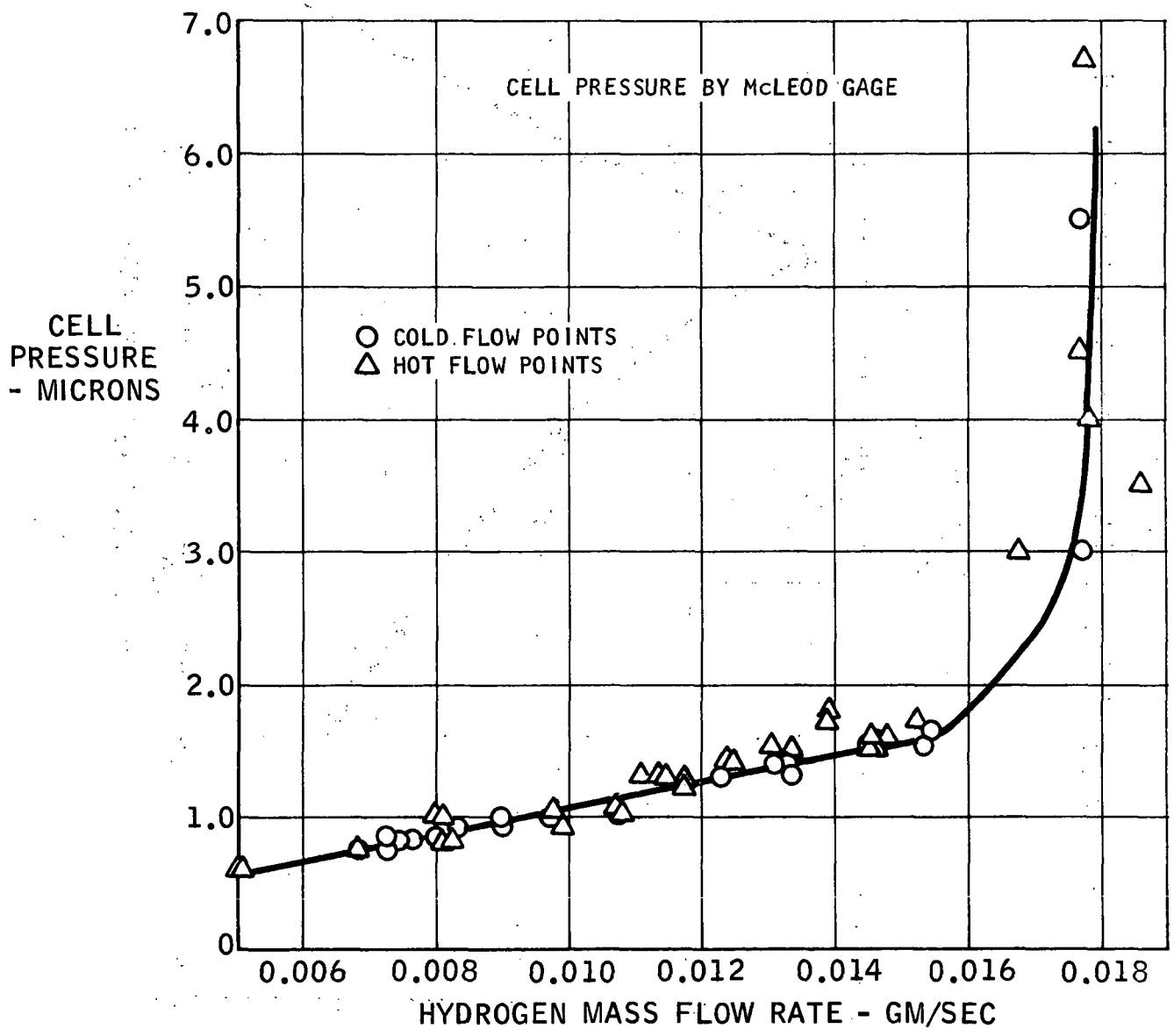

FIGURE 49.

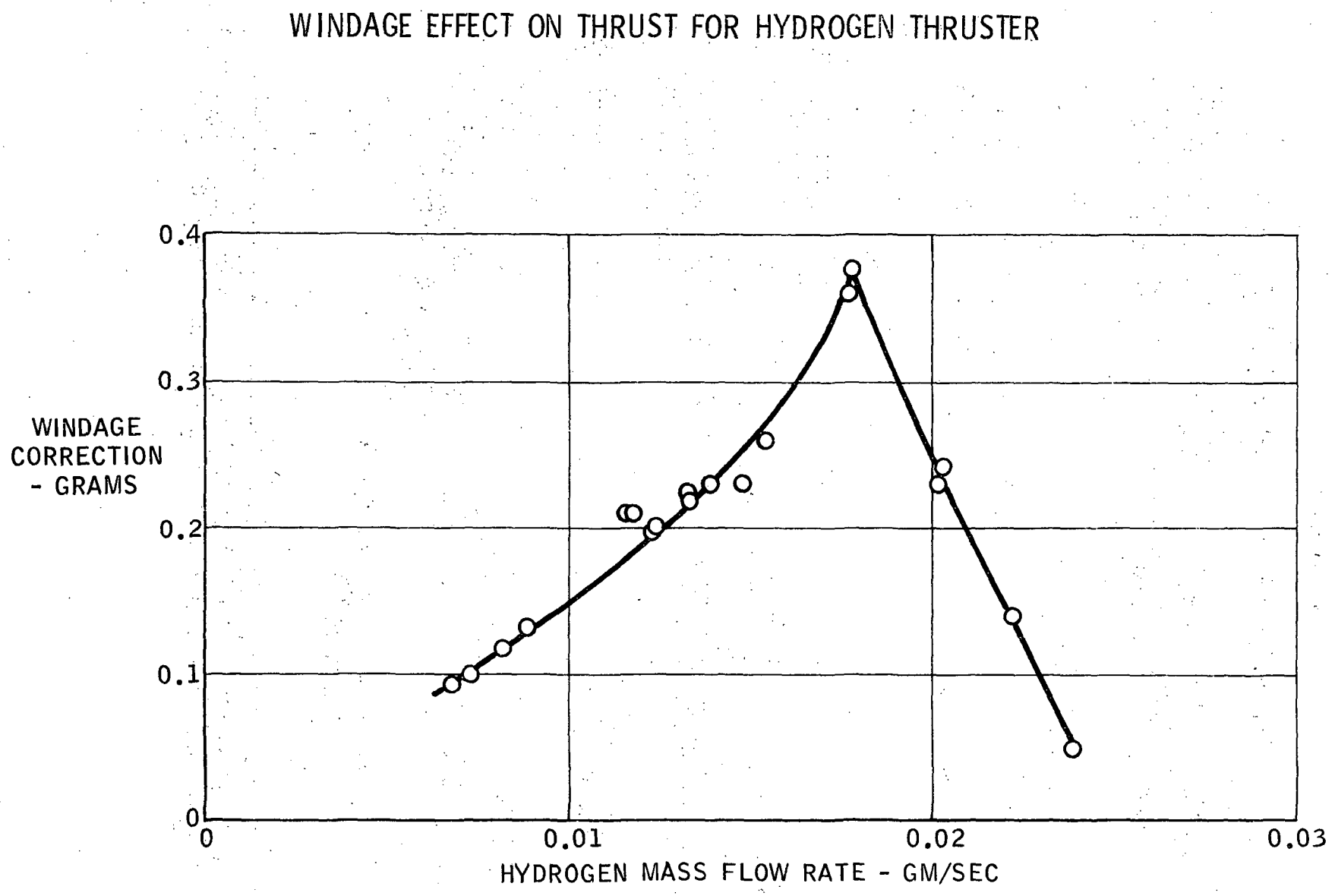
WINDAGE EFFECT ON THRUST FOR HYDROGEN THRUSTER
WINDAGE CORRECTION - GRAMS
0.4
0.3
0.2
0.1
0
0
0.01
0.02
0.03
HYDROGEN MASS FLOW RATE - GM/SEC

FIGURE 50.

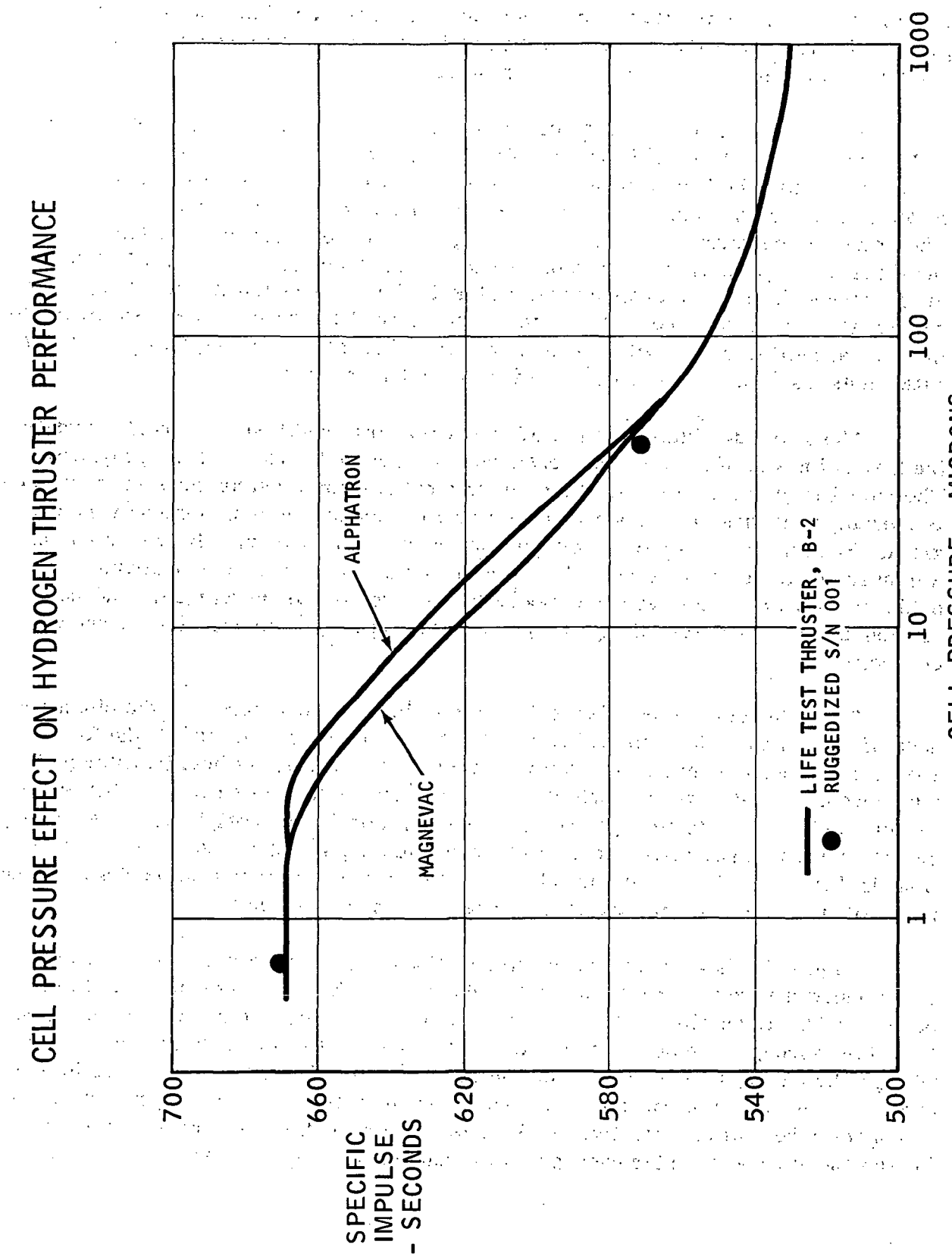
CELL PRESSURE EFFECT ON HYDROGEN THRUSTER PERFORMANCE
SPECIFIC IMPULSE - SECONDS
700
660
620
580
540
500
1
10
100
1000
CELL PRESSURE - MICRONS
ALPHATRON
MAGNEVAC
LIFE TEST THRUSTER, B-2
RUGGEDIZED S/N 001

FIGURE 51.

measured. The hydrogen thruster was initially intended to be most heavily instrumented for maximizing information to update the thermal model of the thrusters prepared early in the program. However, after occurrence of the touching anomaly previously discussed, the majority of the available thermocouple channels were redirected to usage with the ammonia thruster.

Locations of temperatures periodically measured during the test are shown in Figure 52. Not all of the locations were monitored for all of the tests. The temperature distributions at nominal life test operating conditions of 220 watts measured during the periodic performance calibrations are shown in Table IV. The dropoff in performance after the touching anomaly occurred is reflected in the thruster temperatures measured. It can be seen from Table IV that all of the temperatures dropped to levels corresponding to the lower performance level generated during later portions of the tests. Some of the critical temperatures measured on the thruster are shown as a function of input power in Figure 53, for a typical set of run data points taken prior to occurrence of the touching anomaly.

Thermal data obtained at the life test operating conditions was used to update the thermal model of the thruster constructed during early phases of the program. The model required minimal modification to obtain thermal distributions which agreed reasonably well with the temperature data obtained during the test portion of the program. For this thermal model, the thermal conductivity and emissivity of rhenium was assumed to be constant over the operating temperature range as available evidence indicates. However, the model does include the temperature dependence of rhenium electrical resistivity, propellant heat capacity, and propellant thermal conductivity.

The principal unknown factor in the resistojet thermal design is the effectiveness of the foil radiation shields between the first and second passes. If the foil sheets have good thermal contact with each other, the conductive heat transfer path may negate the radiative heat shield effect. To determine the extremes of the temperature distributions to be expected, two thermal models were originally constructed, one assuming five perfectly effective radiation shields, the other assuming no radiation shields at all. The latter model, it was found, predicts temperature distributions in excellent agreement with available temperature measurements.

Figure 54 shows temperature distributions in the four concentric tubes predicted using the thermal model without radiation shields operating with 0.0072 grams per second hydrogen flow and 240 watts input power. Temperature data points taken from thermocouple and optical pyrometer measurements show excellent agreement with predicted results. The complete thermal model is discussed in detail in Reference 5. Resistivity of rhenium was taken from Reference 6 . Hydrogen conductivity and specific heat were taken from Reference 7 . Convective heat transfer coefficients for the annular and circular passages were calculated using Reference 8 results.

THERMOCOUPLE LOCATIONS ON HYDROGEN RESISTOJET THRUSTER

A72-7-290-53

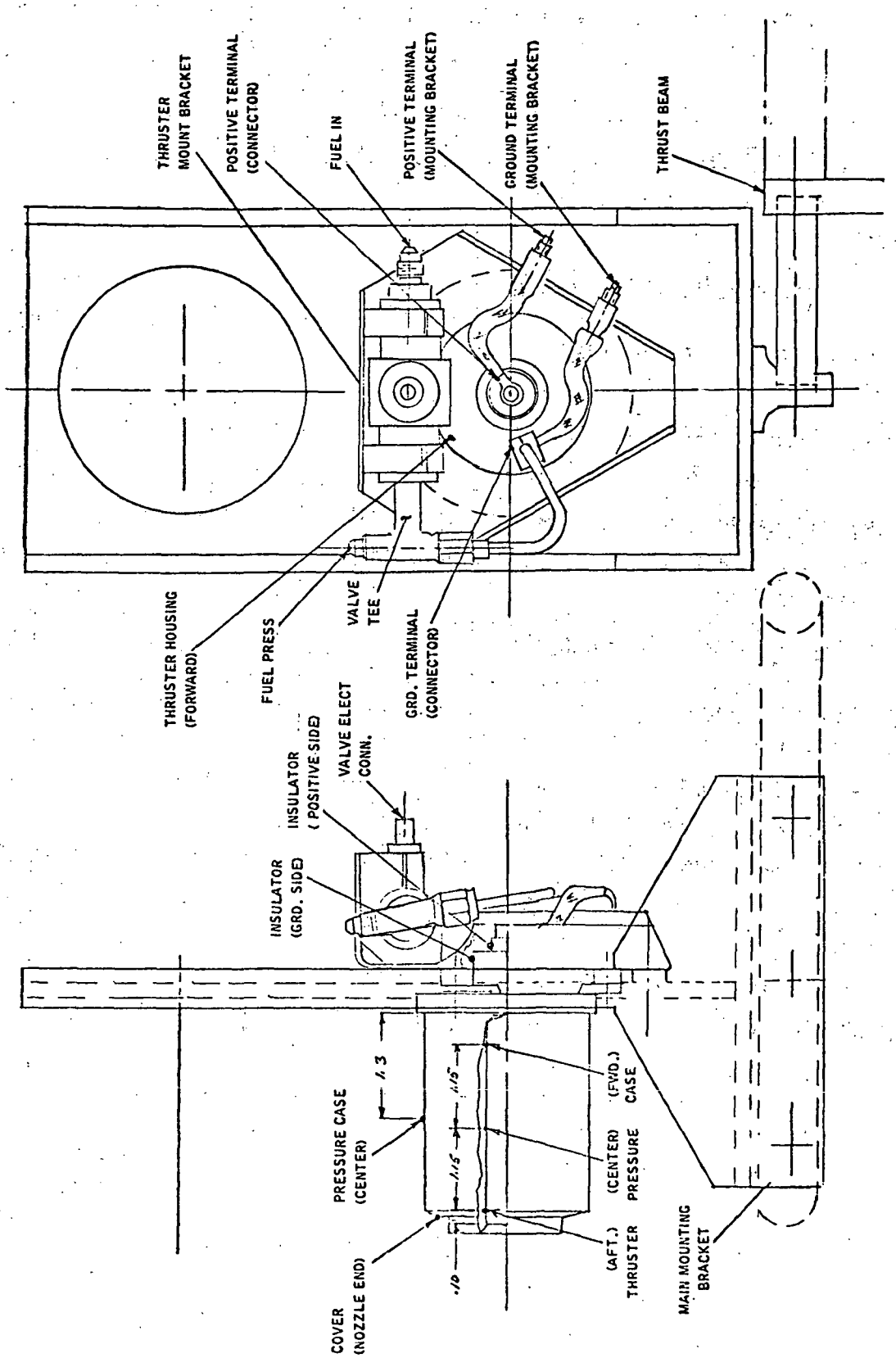

FIGURE 52.

TABLE IV

HYDROGEN THRUSTER TEMPERATURES MEASURED DURING LIFE TEST

Location	Life Test Point - Hours							
	0	100	200	300	400	500	600	700
Power-Watts	222.3	179	95.2	107.8	111.8	112.4	115.5	115.4
Thruster Pressure Case (Aft), °K	1199	898	369	381	381	389	397	389
Thruster Pressure Case (Center), °K	1065	-	-	-	-	-	-	-
Thruster Housing (Forward), °K	-	378	314	316	313	318	317	318
Cover (Nozzle End), °K	518	-	-	-	-	-	-	-
Cover (Center), °K	468	-	-	-	-	-	-	-
Insulator (Ground Side), °K	403	384	317	318	316	321	319	322
Ground Terminal Connector), °K	360	344	308	310	310	311	316	313
Ground Terminal (Mounting Bracket), °K	354	-	-	-	-	-	-	-
Positive Terminal (Connector), °K	448	423	360	360	360	369	371	364
Positive Terminal (Mounting Bracket), °K	393	-	-	-	-	-	-	-
Insulator (Positive Side),°K	-	388	316	318	315	319	325	319
Mount Bracket Above Valve, °K	336	-	-	-	-	-	-	-
Thrust Beam, °K	289	-	-	-	-	-	-	-
Main Mounting Bracket, °K	308	295	-	294	-	-	-	-
Valve Tee, °K	323	-	-	-	-	-	-	-

THRUSTER TEMPERATURE DISTRIBUTION vs ELECTRICAL POWER FOR HYDROGEN OPERATION

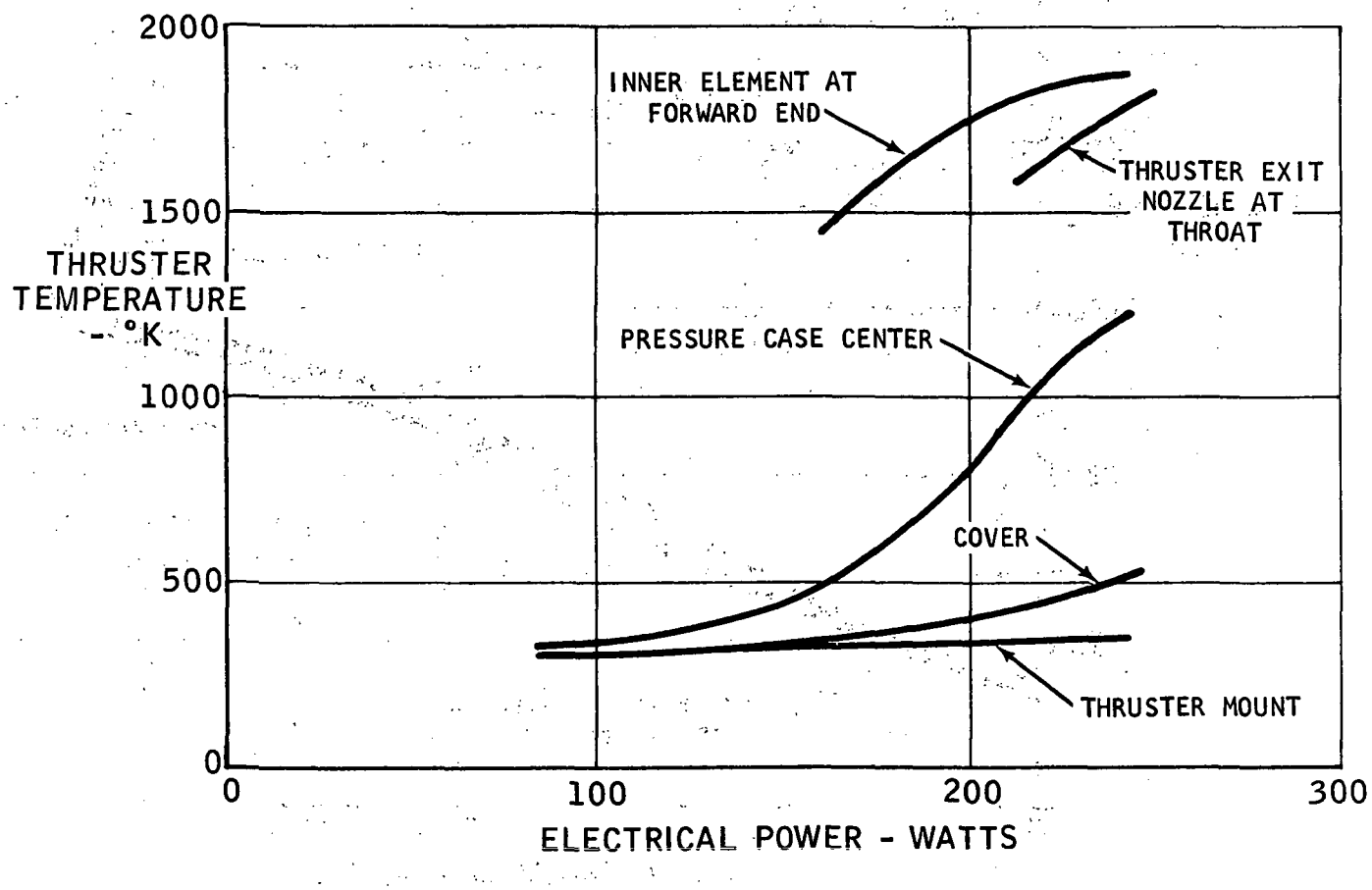

FIGURE 53.

MODEL 110 RUGGEDIZED RESISTOJET WALL TEMPERATURES

H_2 PROPELLANT - 240 WATTS

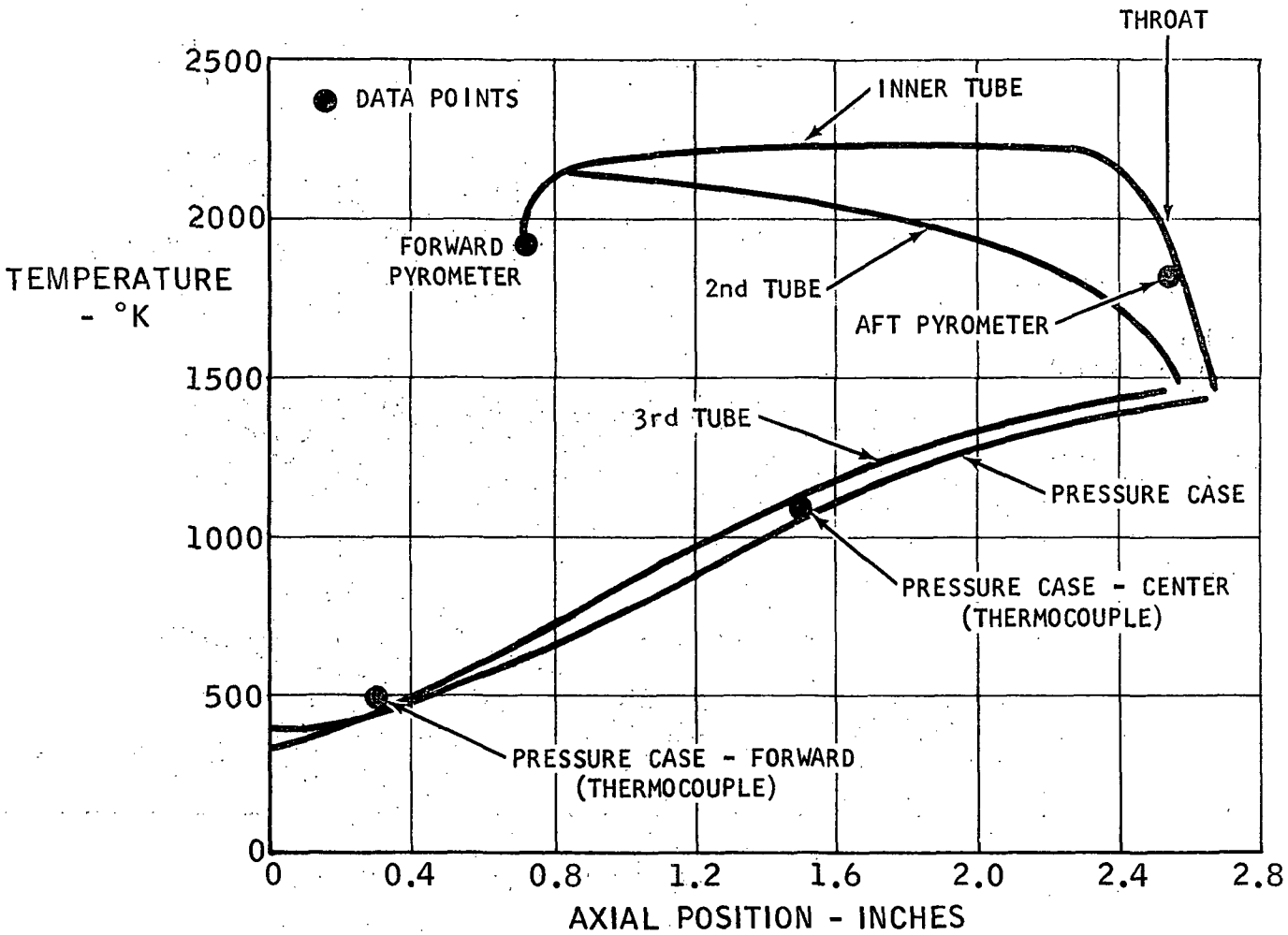

FIGURE 54.

The maximum metal temperature of about 2170°K occurs in the middle of the inner tube. The expansion bell and the forward dome are considerably cooler due mainly to radiative cooling. The exit gas temperature is 2090°K which implies the power transferred to the gas is about 220 watts. About 20 watts are lost from the system. Table V is an accounting of power losses estimated using empirical temperature data. The main losses are by conduction through the power cables and thruster mounts and by radiation from the nozzle and nozzle end plate.

Thruster resistance. - After the initial period of variable operation resulting from inner element touching, the thruster exhibited relatively stable performance. Thruster resistance is shown as a function of developed I_{sp} in Figure 55. The operating characteristic during touching resulted in variation of the thruster resistance and consequently the power absorbed by the thruster. The touching phenomena was a make and break phenomena, i.e., the current path would be normal until the inner element heated up sufficiently to contact the second tube as a result of thermal growth. At that time, the thruster resistance would drop significantly and the inner tube would cool slightly breaking the shorted current path. The upper line of Figure 55 shows the normal resistance characteristic of the thruster, and the lower point, shorted resistance level. Figure 56 shows thruster current-voltage characteristics of the thruster, demonstrating the spread in operating voltage in the touching operational mode.

Thruster resistance was measured with a precision measurement device periodically throughout the program. Results of those measurements are shown in Figure 57, as a function of test program activity.

It is apparent that there was quite a variation in measured thruster resistance after the touching anomaly was first observed at 76 hours of life test cycling. Other following resistance points show data scatter depending upon the degree of contact of the inner tube with the second heater element tube at the time of measurement.

Thruster pressure drop characteristics. - Significant change was observed in the pressure drop/mass flow characteristics of the S/N 001 hydrogen thruster during the course of the test program. The thruster was calibrated for hydrogen mass flow rate as a function of thruster inlet pressure prior to conduct of any functional tests. Repeated testing following the initial hot operation acceptance test did not indicate the same pressure drop characteristics. As shown in Figure 58, the pressure drop characteristics of the thruster were significantly different after the initial performance acceptance test and vibration tests were completed. No further change was noted in thruster pressure drop characteristics throughout the entire life cycling test even after the touching of heater elements anomaly was observed. There is no ready explanation for the apparent change in thruster pressure drop characteristics during the test program. It may be that a small particle entered the thruster when new and partially logged the thruster throat. The particle then was either burned out in the initial tests or was dislodged during subsequent testing.

TABLE V

SUMMARY OF THERMAL LOSSES

MODEL 110 RUGGEDIZED RESISTOJET

H_2 PROPELLANT

POWER IN = 220 WATTS

Source of Loss	Power Loss (Watts)
Radiation from Cover	1½
Radiation from Nozzle and Nozzle End Plate	8½
Conduction Down Power Cables	5½
Conduction through Thruster Mounts	4½
TOTAL LOSS	20 watts

HYDROGEN THRUSTER RESISTANCE AS A FUNCTION OF DEVELOPED SPECIFIC IMPULSE

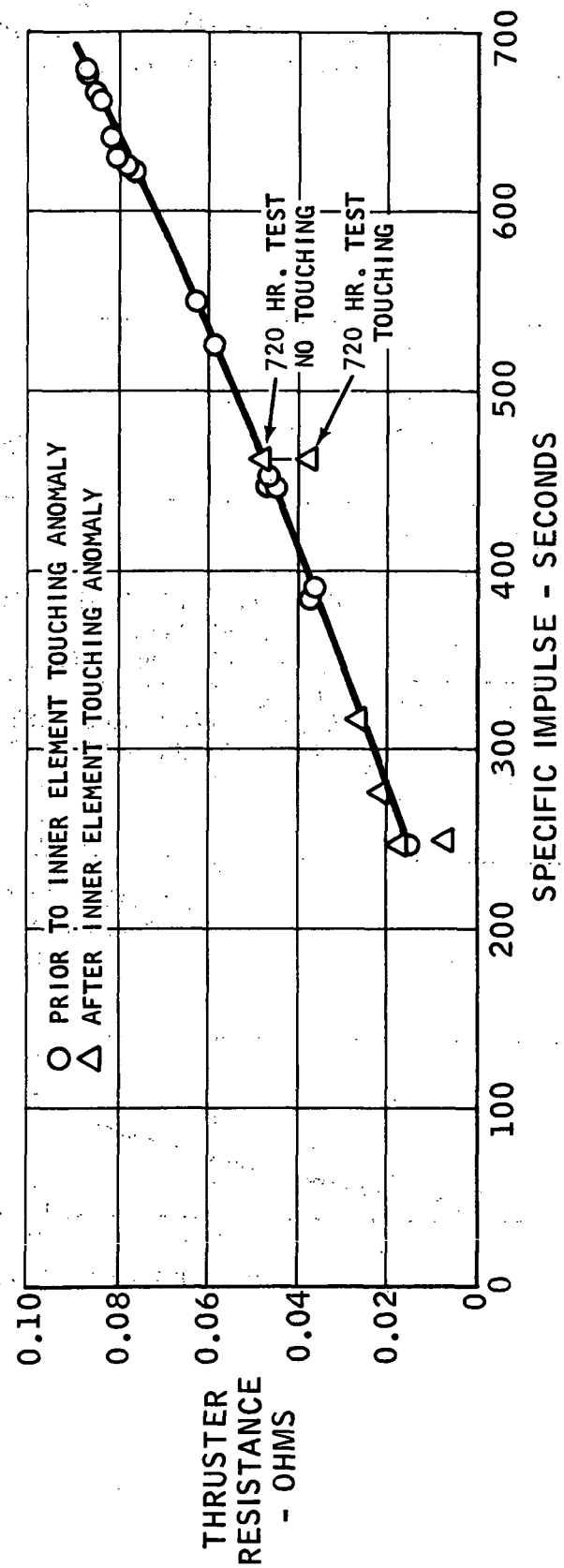

FIGURE 55.

TERMINAL CURRENT vs TERMINAL VOLTAGE
HYDROGEN THRUSTER S/N 001

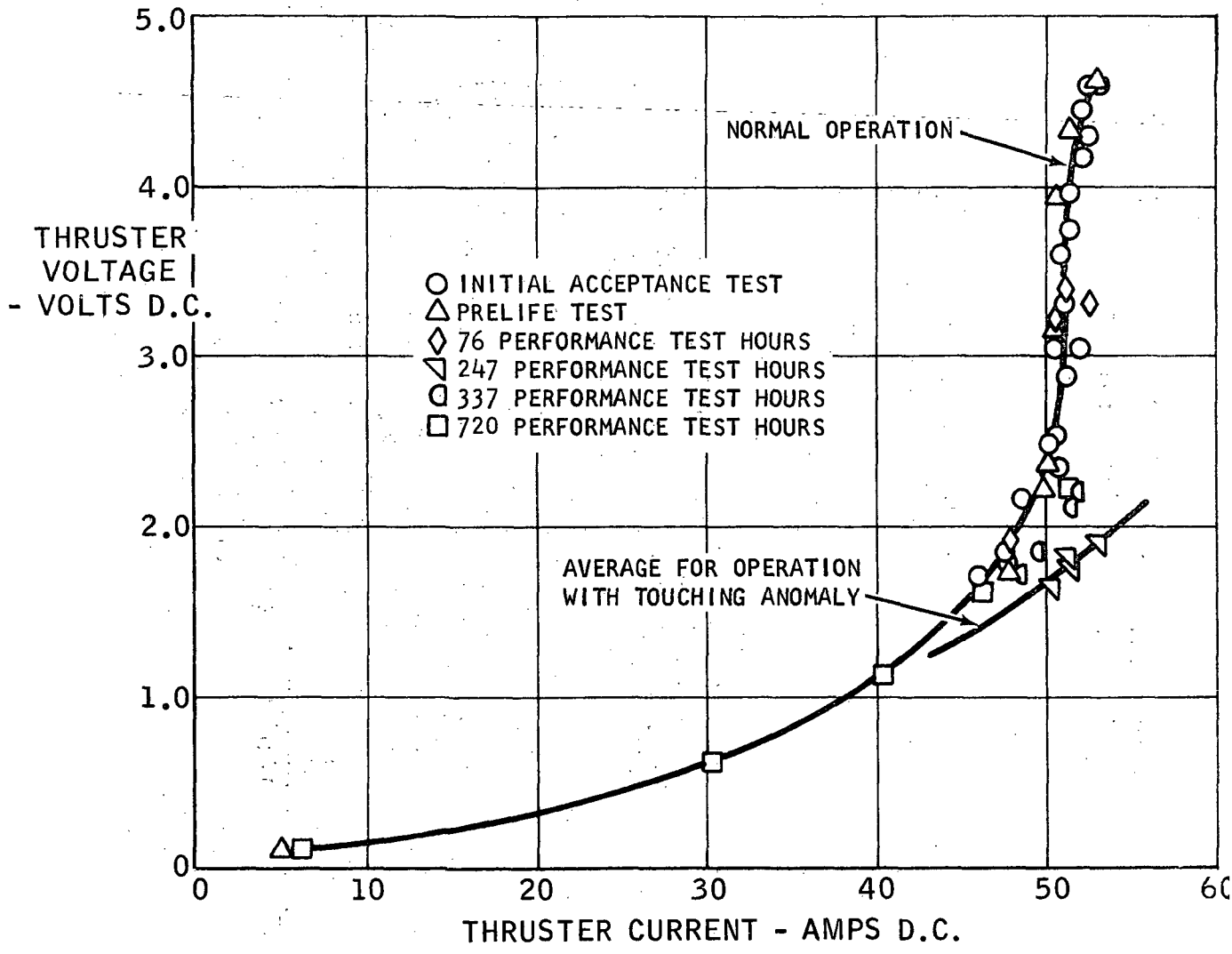

FIGURE 56.

CHRONOLOGICAL RESISTANCE SUMMARY
HYDROGEN THRUSTER - S/N 001

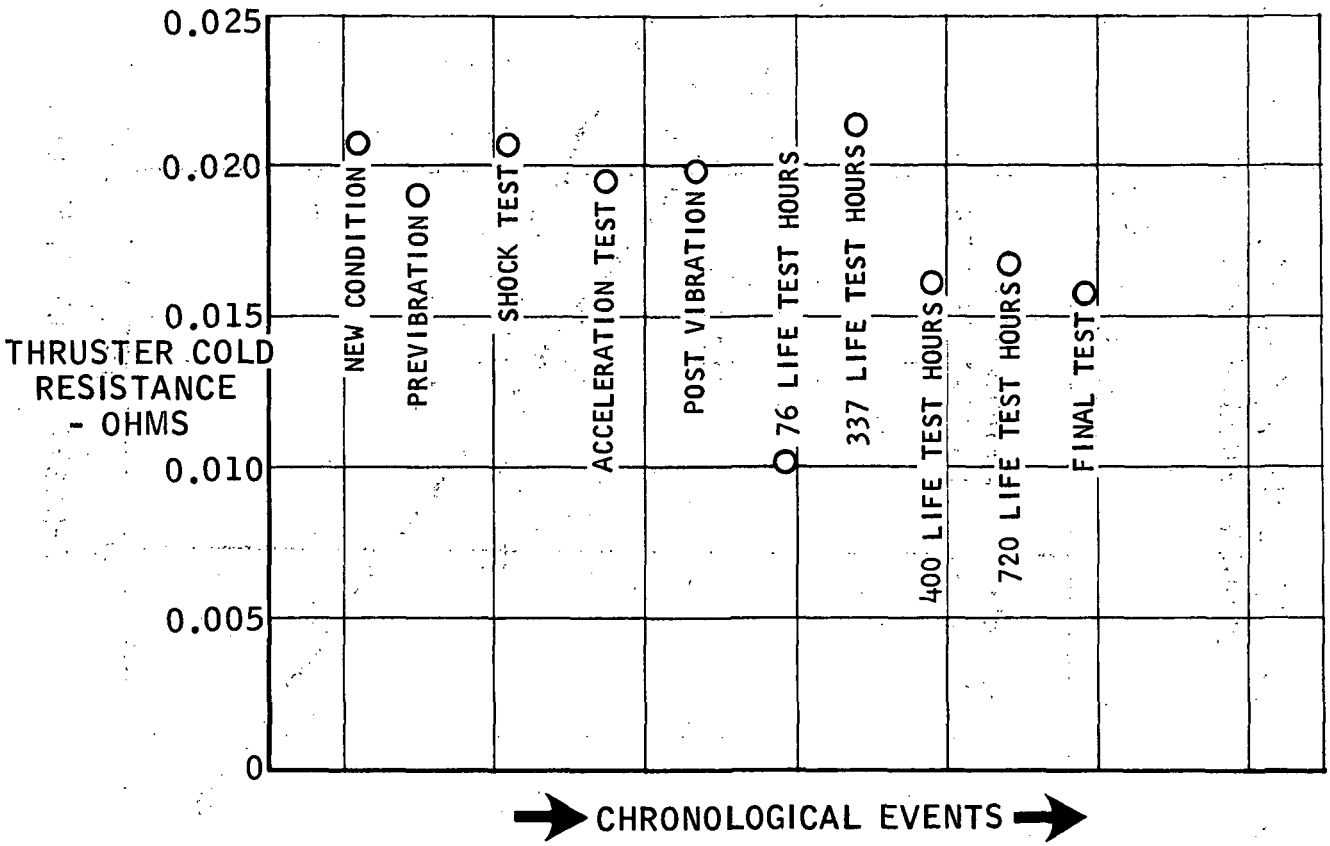

FIGURE 57.

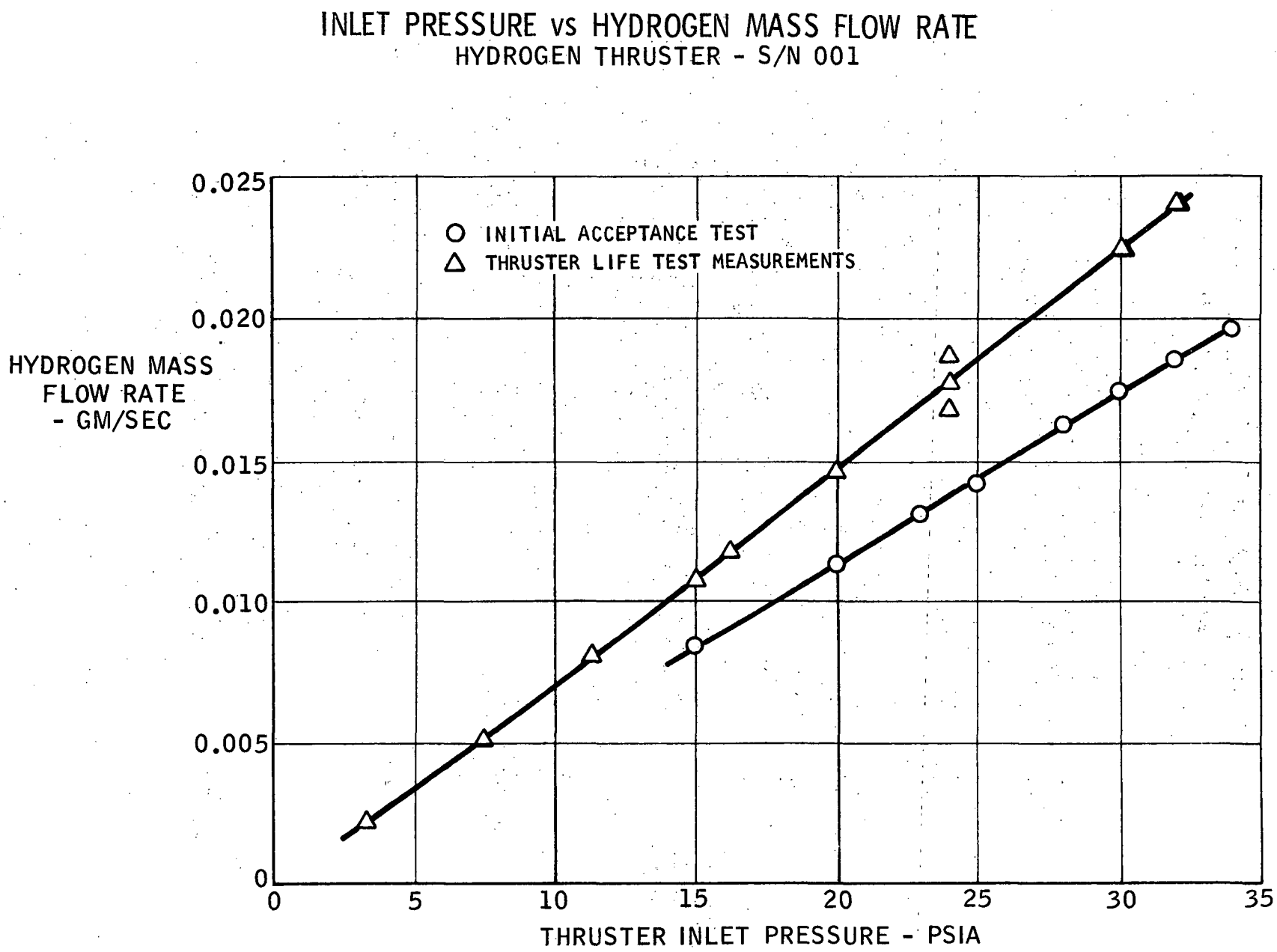
INLET PRESSURE vs HYDROGEN MASS FLOW RATE
HYDROGEN THRUSTER - S/N 001
INITIAL ACCEPTANCE TEST
THRUSTER LIFE TEST MEASUREMENTS
HYDROGEN MASS FLOW RATE - GM/SEC
0.025
0.020
0.015
0.010
0.005
0
0
5
10
15
20
25
30
35
THRUSTER INLET PRESSURE - PSIA
A72-7-290-37

FIGURE 58.

Thruster leakage. - Structural leakage tests were made at three points through the thrusters useful life to determine structural integrity of the thruster. Two types of tests were performed. The first consisted of a Veeco helium leak check. This procedure involves pressurizing the interior of the thruster structure and checking for the presence of helium around the exterior of the thruster with a sensitive electronic detector. The procedure is good for detecting extremely small leaks undetectable using other means. The second technique used for determining leakage consisted of a locked volume system which included a sensitive Heise gage (0.2%) accuracy and the thruster with associated lines. The drop in system pressure at a constant temperature is then equated to thruster pressure loss. This technique is accurate in detecting leaks on the order of 1 SCCH of helium leakage.

The hydrogen S/N 001 thruster was leak tested using both of the above techniques prior to initiation of any other testing on the thruster, after the acceptance test, and after completion of all planned tests. Both of the initial tests indicated an integral thruster structure. The final test, after completion of all other tests did indicate a small leak to be present in the thruster structure. Magnitude of the noted leak was 2.2 SCCH of helium at 25 psig thruster inlet pressure. The leak apparently originated in the basic heater element structure since a bubble check indicated that the gas was escaping from the port used to view the back of the inner heater element. This magnitude of leakage was not significant and would not affect thruster pressure drop characteristics, however, it does indicate a deficiency in the thruster structure resulting from the thruster operation during the life test.

Ammonia Thruster, S/N 002 Performance

Performance of the ammonia thruster was extremely consistent throughout the entire test period. There were virtually no changes in thruster operating performance during any portion of the test. Consistency of the thruster has demonstrated that from an operational standpoint, the thruster design is ready for qualification and usage on space systems.

Specific impulse performance. - The S/N 002 ruggedized thruster selected for operation on ammonia during the life test sequence demonstrated extremely repeatable operational performance. Figure 59 shows specific impulse performance of the thruster as a function of input electric power level. For comparison, the S/N 003 performance measured during acceptance test is shown in Figure 60. Data points shown include all of the calibration test points recorded during the periodic calibrations performed on the thruster during the life test period. Repeatability at the 140 watt life test power level is best shown in Figure 61, showing I_{sp} at 140 watts as a function of accrued test cycle life in hours. Mean specific impulse at the life test power level was 316.6 seconds with a total indicated data spread of 11 seconds. This minimal data spread is remarkable considering the time period covered during data acquisition and potential data spread due to instrumentation accuracy along. The measured data spread is significantly within the ± 12 second data spread potentially possible just due to measurement accuracy.

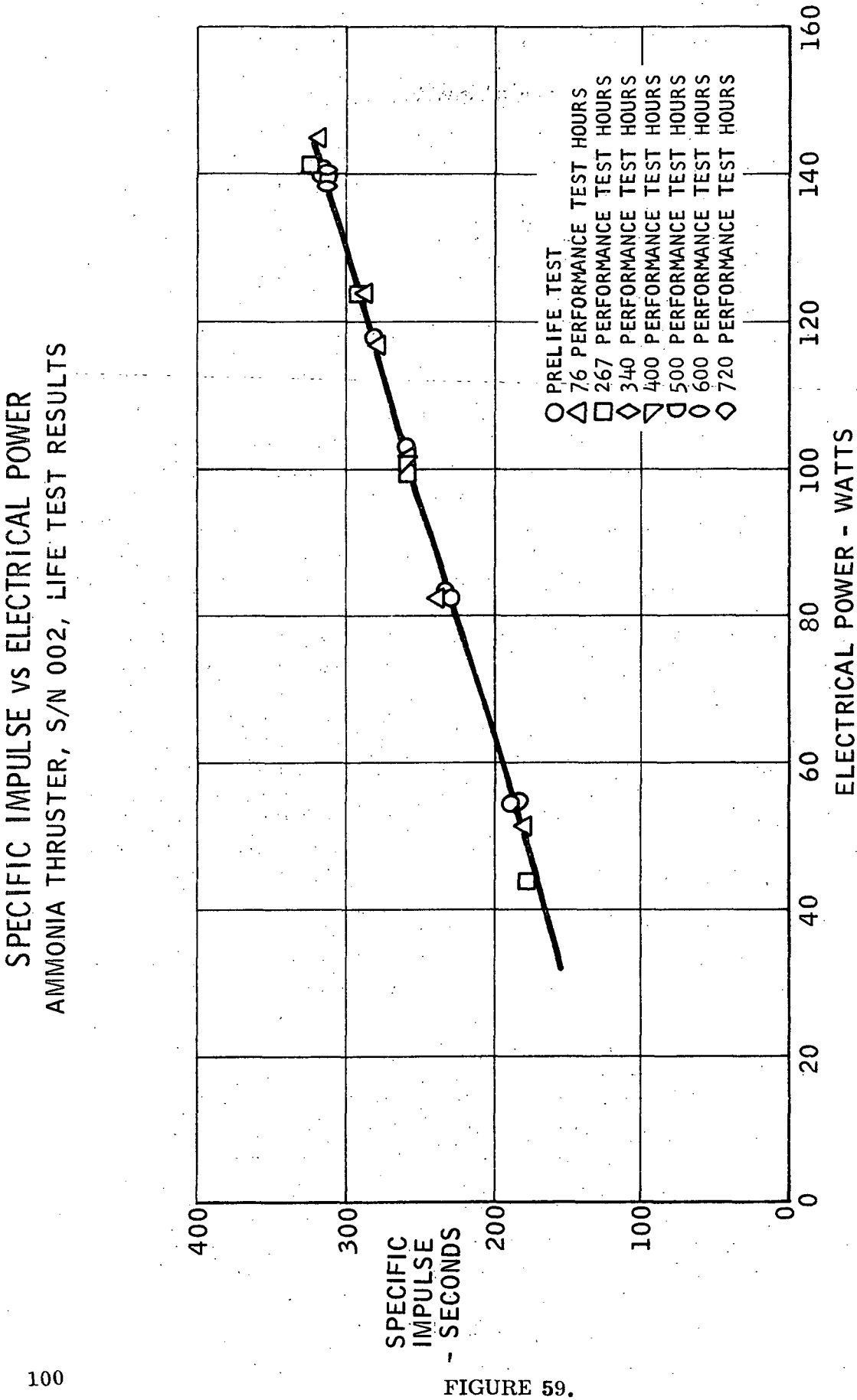
SPECIFIC IMPULSE vs ELECTRICAL POWER
AMMONIA THRUSTER, S/N 002, LIFE TEST RESULTS
A72-7-290-32
SPECIFIC IMPULSE - SECONDS
400
300
200
100
0
ELECTRICAL POWER - WATTS
0
20
40
60
80
100
120
140
160
PRELIFE TEST
76 PERFORMANCE TEST HOURS
267 PERFORMANCE TEST HOURS
340 PERFORMANCE TEST HOURS
400 PERFORMANCE TEST HOURS
500 PERFORMANCE TEST HOURS
600 PERFORMANCE TEST HOURS
720 PERFORMANCE TEST HOURS

FIGURE 59.

SPECIFIC IMPULSE vs ELECTRICAL POWER
AMMONIA THRUSTER, S/N 003, ACCEPTANCE TEST RESULTS

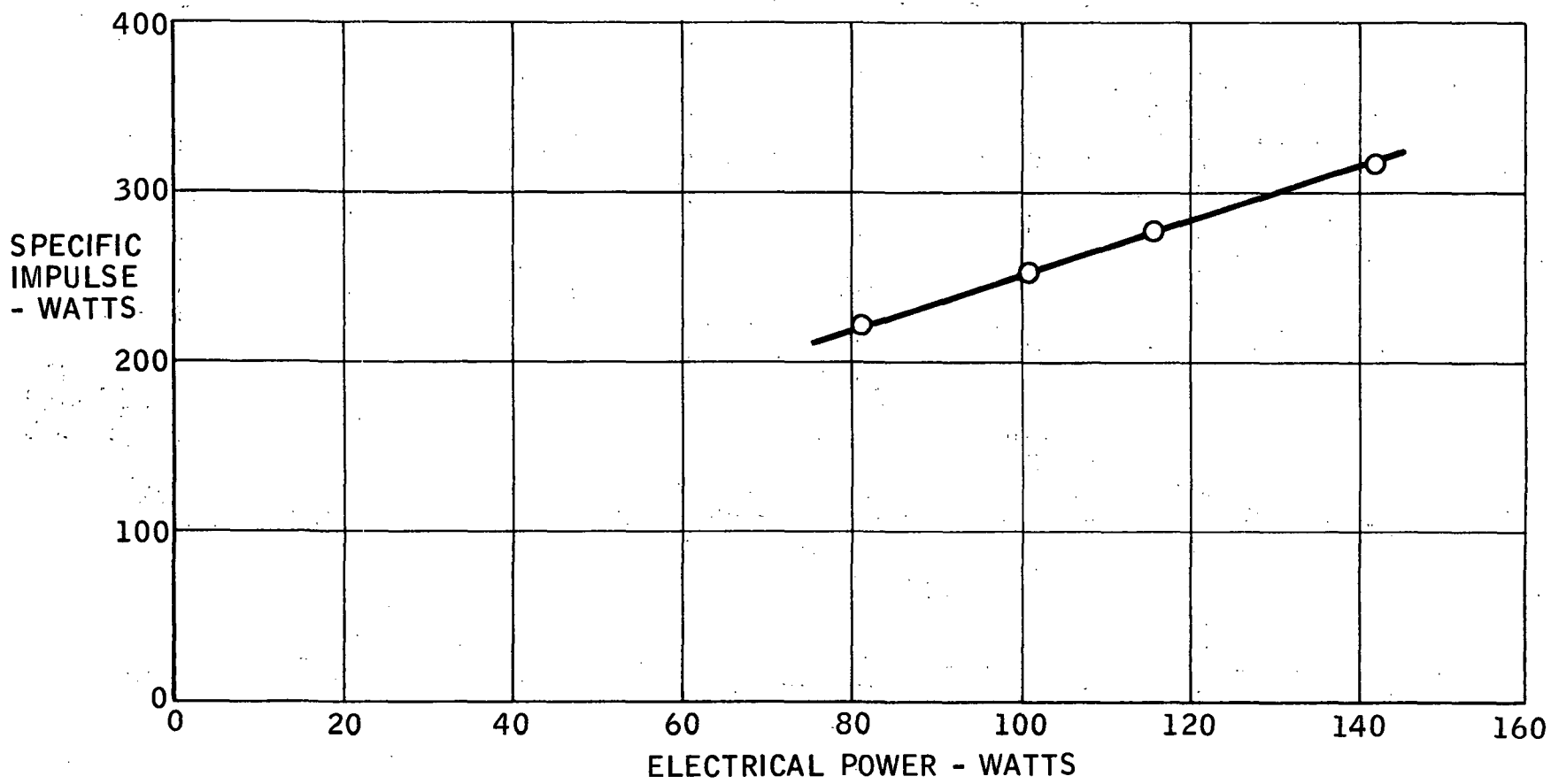

FIGURE 60.

A72-7-290-17

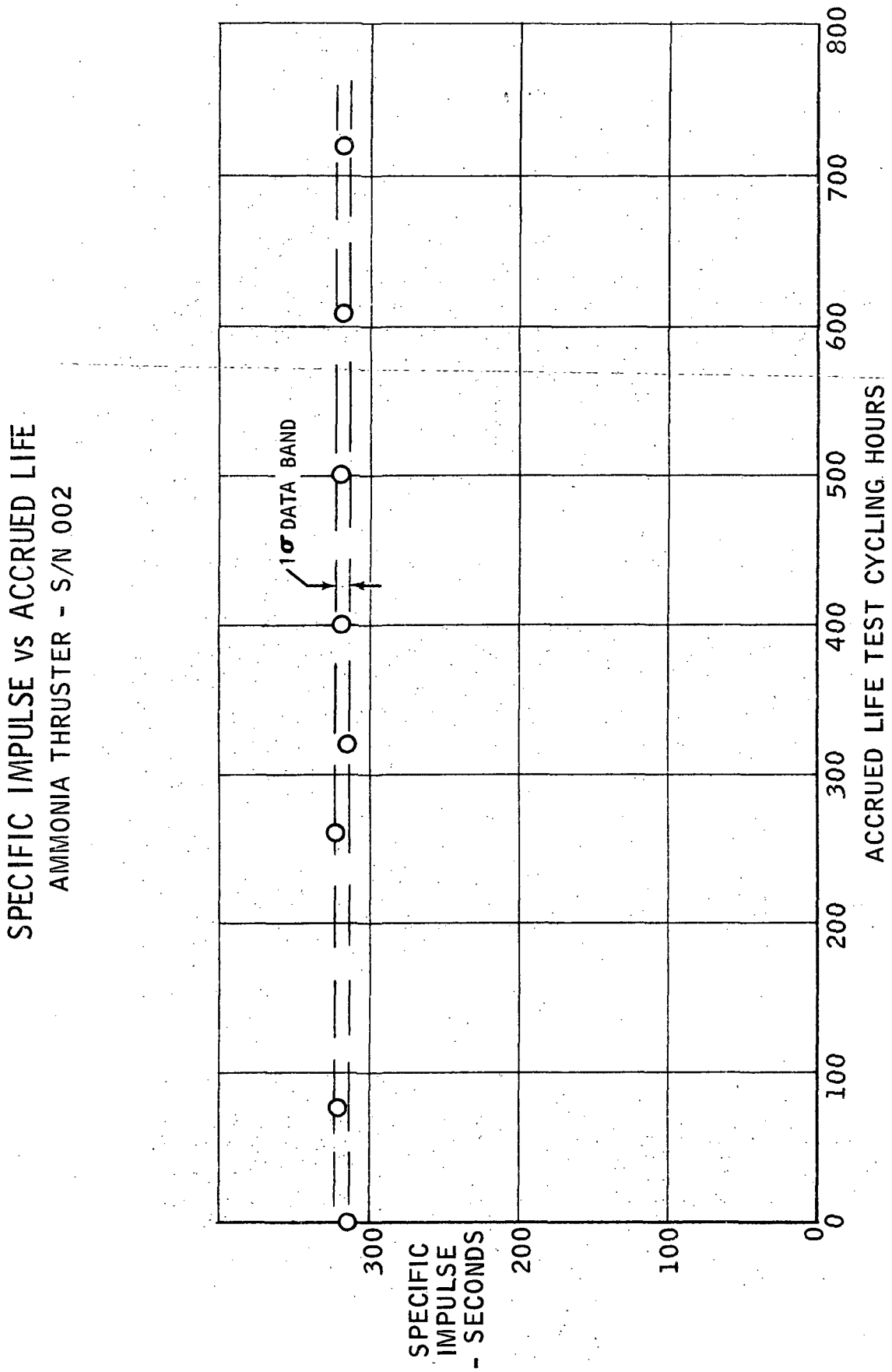
A72-7-290-29
SPECIFIC IMPULSE vs ACCRUED LIFE
AMMONIA THRUSTER - S/N 002
1σ DATA BAND
SPECIFIC IMPULSE - SECONDS
300
200
100
0
0
100
200
300
400
500
600
700
800
ACCRUED LIFE TEST CYCLING HOURS

FIGURE 61.

Overall efficiency. - Thruster overall efficiency was quite good over the test period with a mean average of 47% overall system efficiency being demonstrated at the life test power level. Overall efficiency of the thruster is shown in Figure 62. This figure shows the data points obtained during the periodic high vacuum performance calibrations and again demonstrates consistency of the thruster operating characteristics during the life test period. Figure 63 shows overall performance of the thruster at the life test power level as a function of accrued life test cycling hours. Again, only about a 3% spread was noted in measured thruster operating efficiency over the entire test operating period.

Effects of test cell windage on ammonia thruster performance. - The factors previously discussed regarding windage effects on thruster apparent specific impulse performance also affected measured performance from the ammonia test thruster. With ammonia as the thruster propellant, one additional effect had to be considered in correcting for the windage effects. The hydrogen flow rate effect on cell pressure was relatively constant, whether the flow was hot or cold. With ammonia as the test propellant, this was not the case.

Measured cell pressure was higher when the thruster was operated under powered up conditions than when the same mass flow was flowed through either the thruster or the windage simulator orifice as cold gas. The difference in operating cell pressure resulted from the dissociation of the ammonia into hydrogen and nitrogen at the hot conditions. The degree of dissociation was directly related to the demanded exit gas temperature or I_{sp}. Figure 64 shows the windage correction data obtained during the thruster life test calibrations for the ammonia thruster. Since the propellant did dissociate thus raising the cell pressure above the cold flow cell pressure, each hot flow point was duplicated during the windage tests to provide not only the same mass flow rate as the test point but also the identical cell pressure as the test point. Cell pressure was raised by introducing nitrogen gas downstream of the thruster exit until a match was obtained between the test data point and the cell pressure during the windage test. The McLeod gage was used as the primary cell pressure reference since it was not sensitive to gas composition as were the other electronic vacuum pressure measurement devices available.

As with the hydrogen thruster, even when windage corrections were taken into account, the measured performance of the thruster was lower at high cell pressures than at the lowest cell pressures available. Figure 65 shows the cell pressure effect defined during the previous Reference 2 testing and two typical points measured during the ruggedized thruster life test. These data indicate the effect on nozzle performance of higher cell pressure to be of the same magnitude during the ruggedized thruster tests as was measured on the development life test units previously reported in Reference 2.

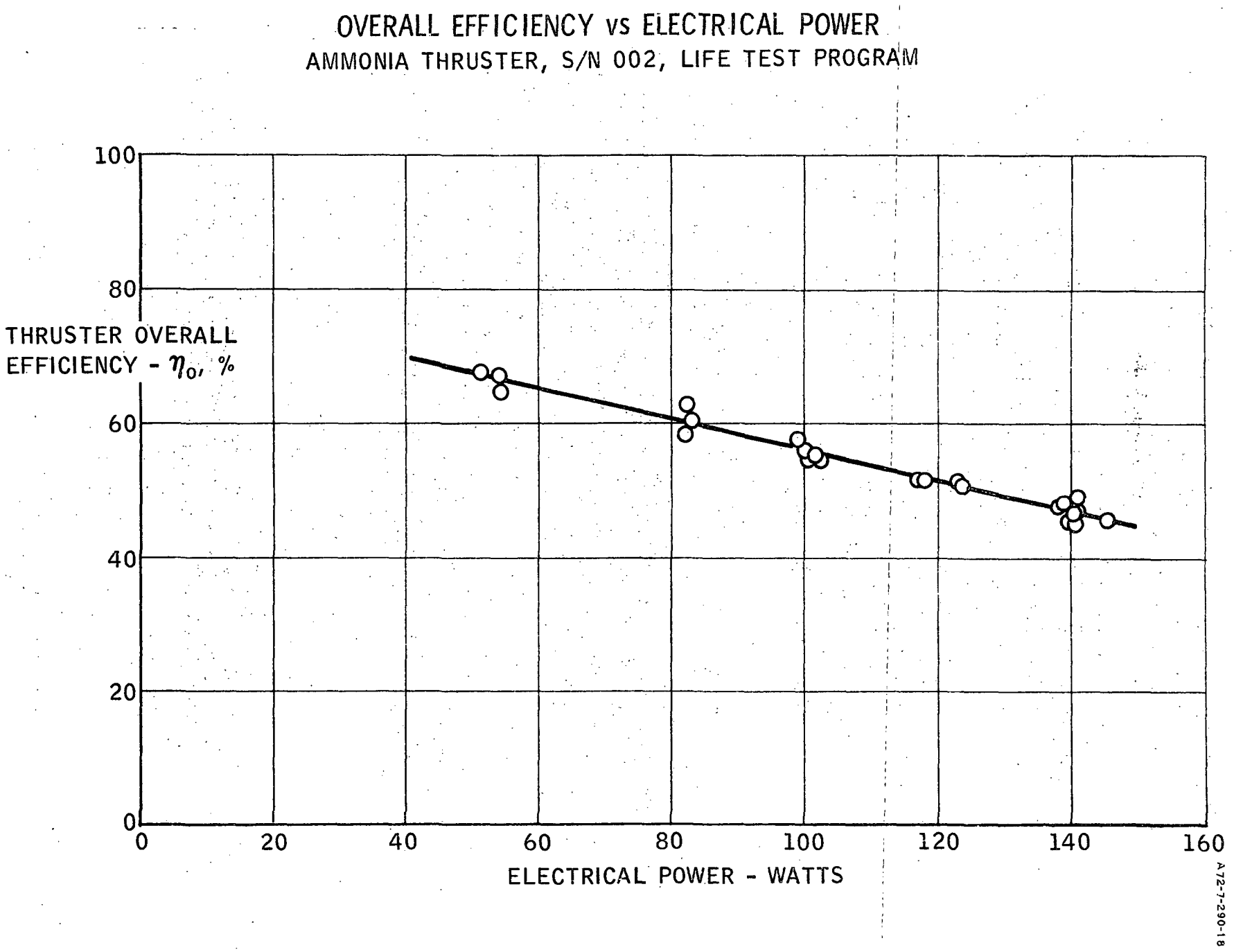
OVERALL EFFICIENCY vs ELECTRICAL POWER
AMMONIA THRUSTER, S/N 002, LIFE TEST PROGRAM
THRUSTER OVERALL EFFICIENCY - η_o, %
100
80
60
40
20
0
0
20
40
60
80
100
120
140
160
ELECTRICAL POWER - WATTS
A72-7-290-18

FIGURE 62.

A72-7-290-28

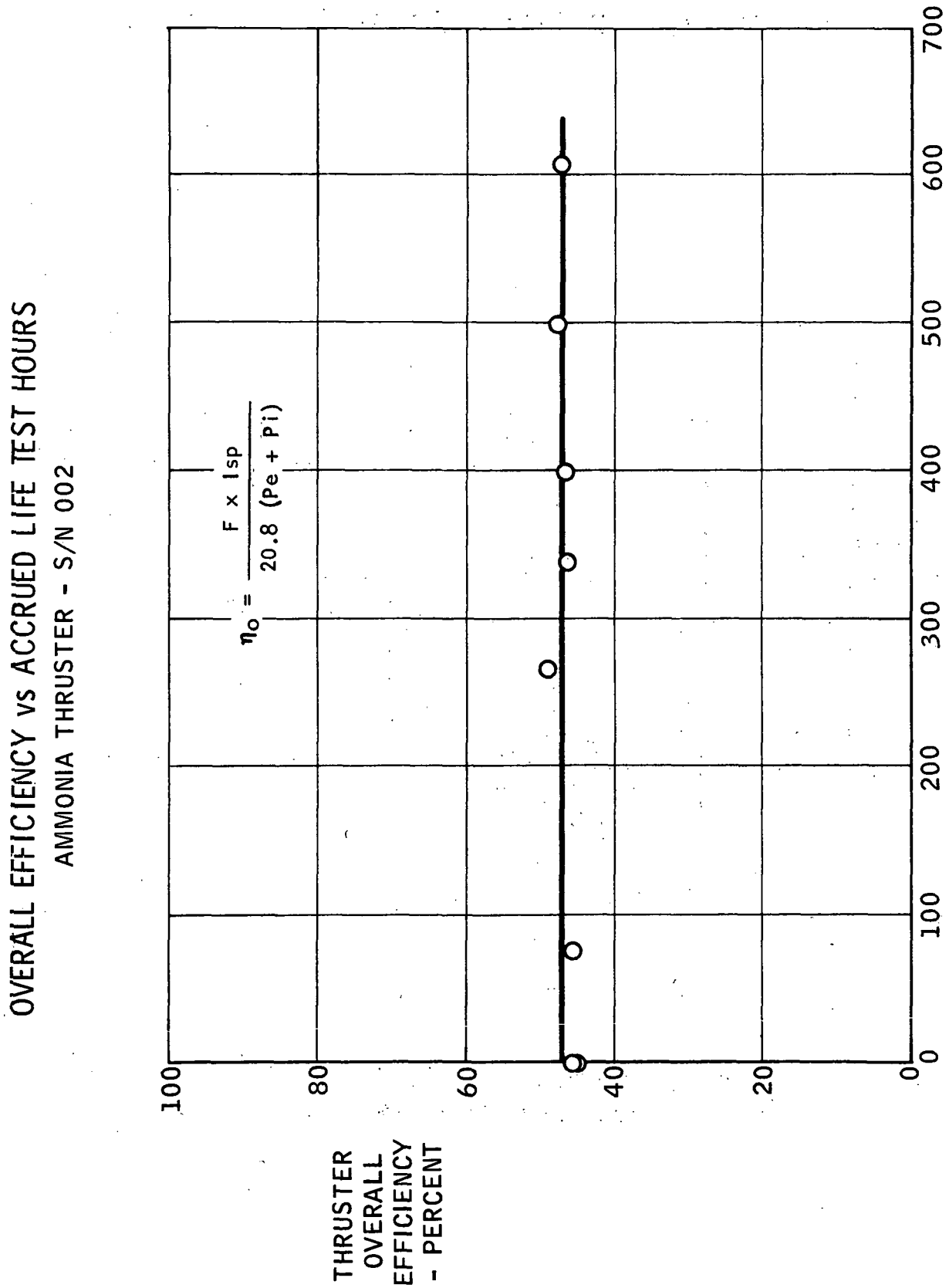

FIGURE 63.

WINDAGE EFFECT ON THRUST FOR AMMONIA THRUSTER

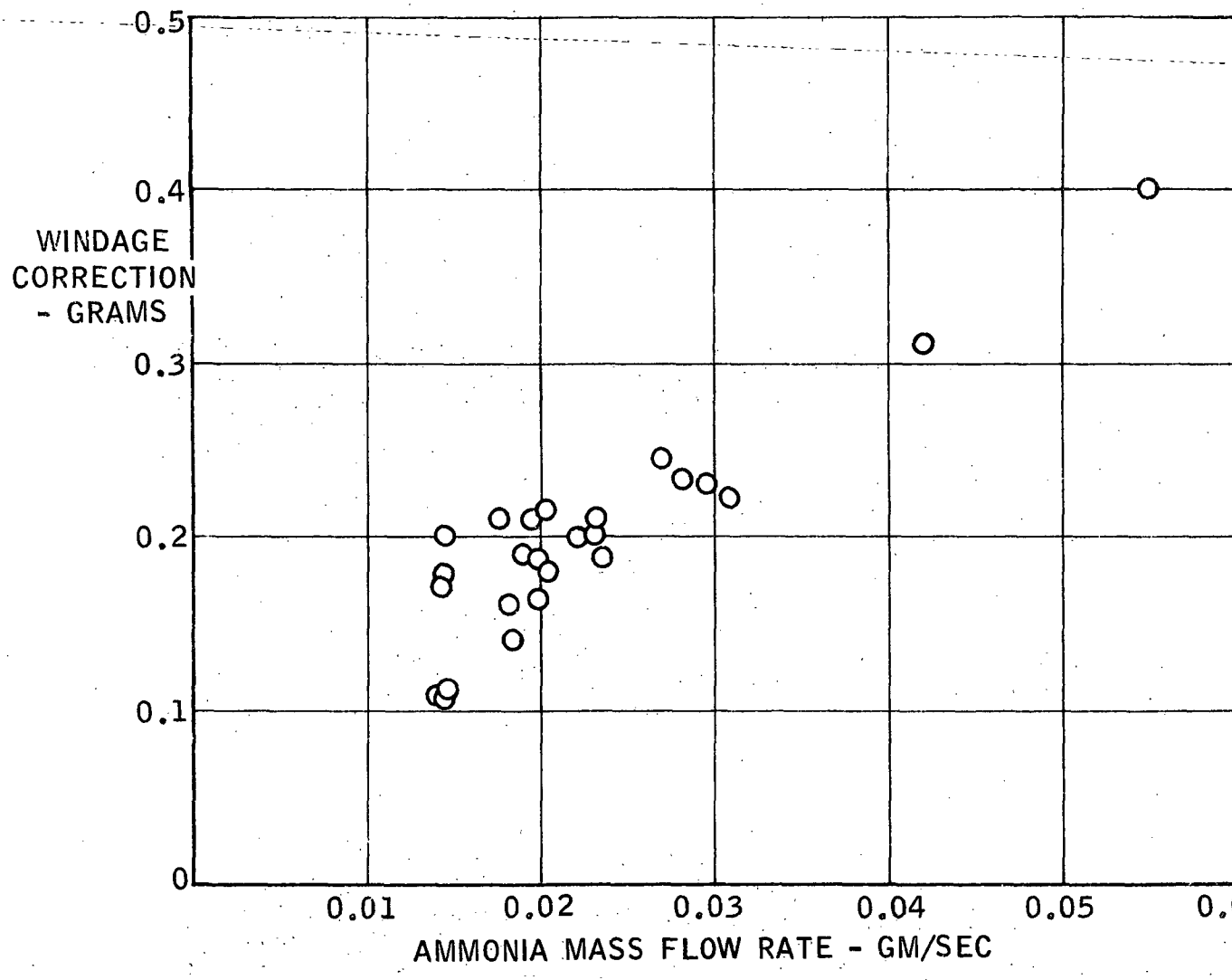

FIGURE 64.

A72-7-290-20

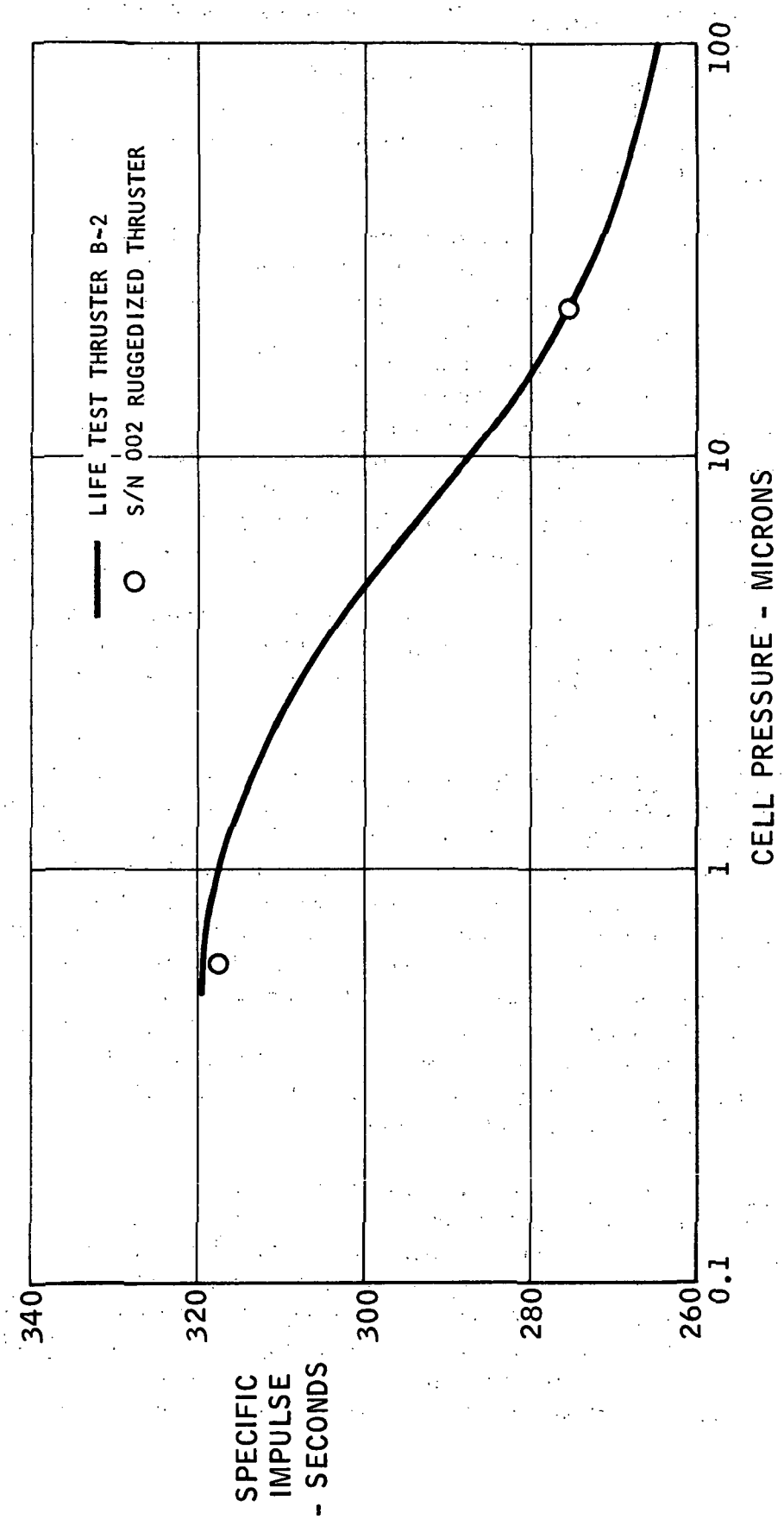

FIGURE 65.

Thruster Resistance. - Thruster resistance measurements were made periodically through the life test program. Initial and final measurements were made using a precision instrument designed specifically for the purpose of measuring the low thruster resistances with precision. All other measurements were made using the same instrumentation used to monitor power absorbed by the thruster during the life test.

Thruster resistance showed repeatability within the expected operating band and within the accuracy of repeatable measurement. Thruster resistance measurements were reasonably repeatable throughout the test period. Total spread in measurement repeatability was about 5%, as good as could be expected considering the extremely low resistances being measured. Thruster resistance is shown as a function of specific impulse in Figure 66. These data include all data points obtained during the thruster operational tests and shows the excellent repeatability obtained in the data during the thruster life test. Resistance under cold (ambient) conditions is shown in Figure 67 as a function of chronological life. All data repeats quite well except for the last point which was obtained after operating the thruster at high performance levels on both hydrogen and ammonia as propellants.

The repeatable operating characteristics of thruster resistance as a function of developed power or specific impulse was reflected in the thruster current - voltage characteristics. Thruster terminal voltage is shown as a function of thruster terminal current in Figure 68.

Thruster pressure drop characteristics. - Both of the thrusters subjected to the life cycling test showed some change in pressure drop characteristics under cold flow conditions. The only changes noted, however, were between the new, as received, condition and subsequent tests after power had been applied to the thruster. The change noted in the ammonia thruster was not as significant as the change measured in the hydrogen thruster. Figure 69 shows the thruster pressure drop measurements made during the life tests to determine changes in characteristics. After the first change was noted, no further change in pressure drop characteristics were measured through the remainder of the test. Also shown in Figure 69 for reference, are pressure drop characteristics of the S/N 003 thruster. The data are reasonably similar considering the extremely small dimensions involved and the accuracy of making and measuring the parts.

Thruster leakage. - Structural leakage tests were made at two points during the thruster operational life to determine deterioration of the thruster structure as a result of the life testing performed. Both Veeco helium leak tests and closed volume leakage tests indicated no leaks present in the thruster structure prior to the test. After completion of the test, a Veeco test indicated the presence of a leak in the thruster structure. Magnitude of the leakage was 74.4 SCCH of helium at 25 psig thruster inlet pressure as measured by the closed volume, pressure drop leakage tester which is sensitive to about one SCCH minimum leakage. Location of

AMMONIA THRUSTER RESISTANCE AS A FUNCTION OF DEVELOPED SPECIFIC IMPULSE

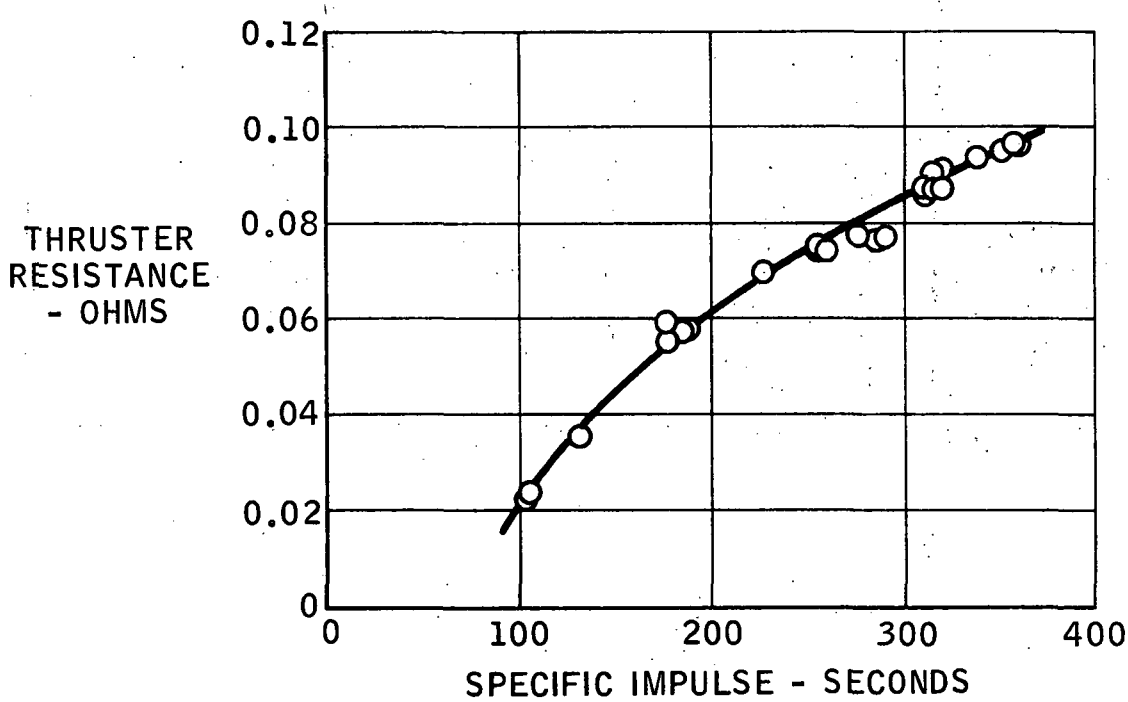

FIGURE 66.

CHRONOLOGICAL RESISTANCE SUMMARY
AMMONIA THRUSTER - S/N 002

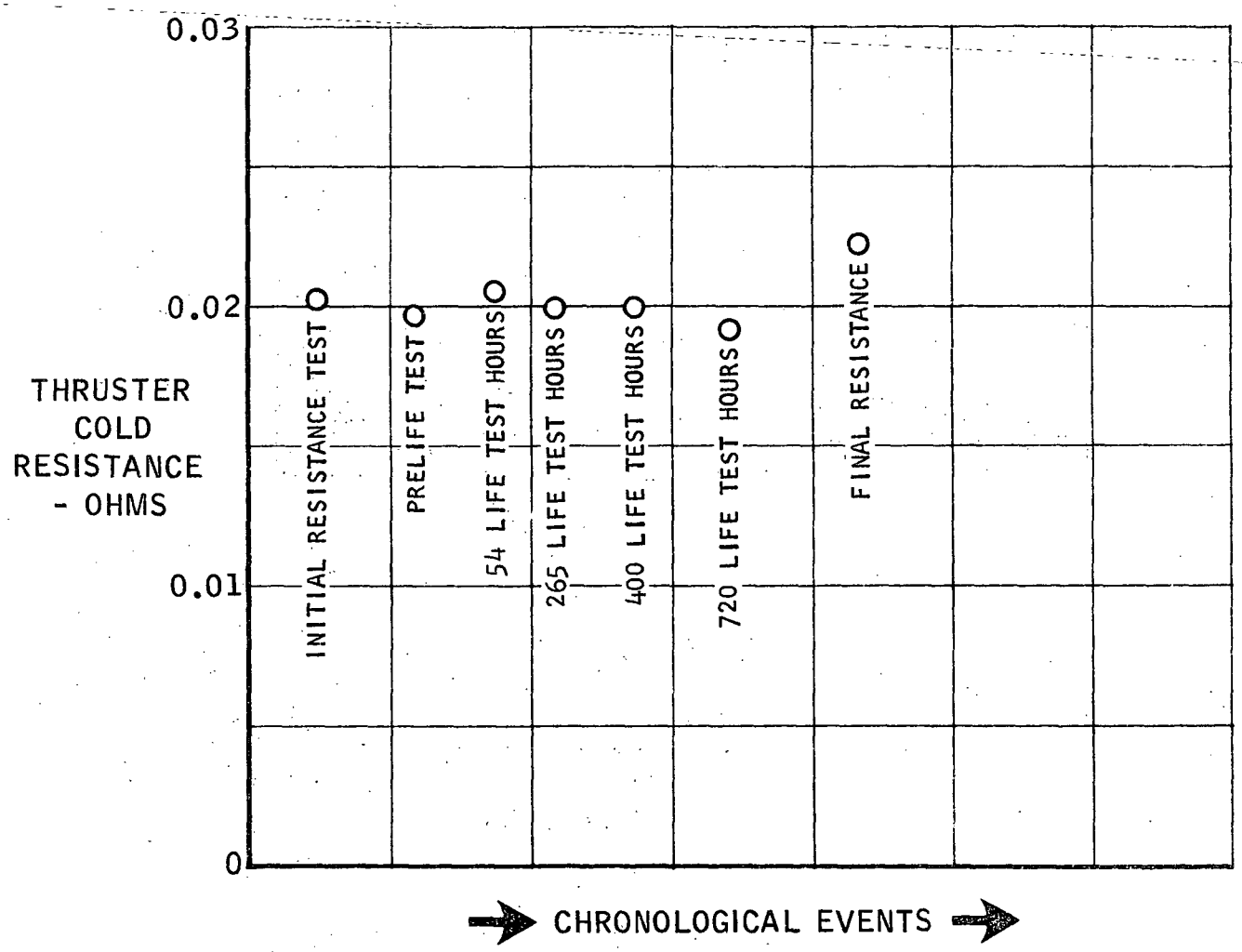

FIGURE 67.

TERMINAL CURRENT vs TERMINAL VOLTAGE

AMMONIA THRUSTER - S/N 002

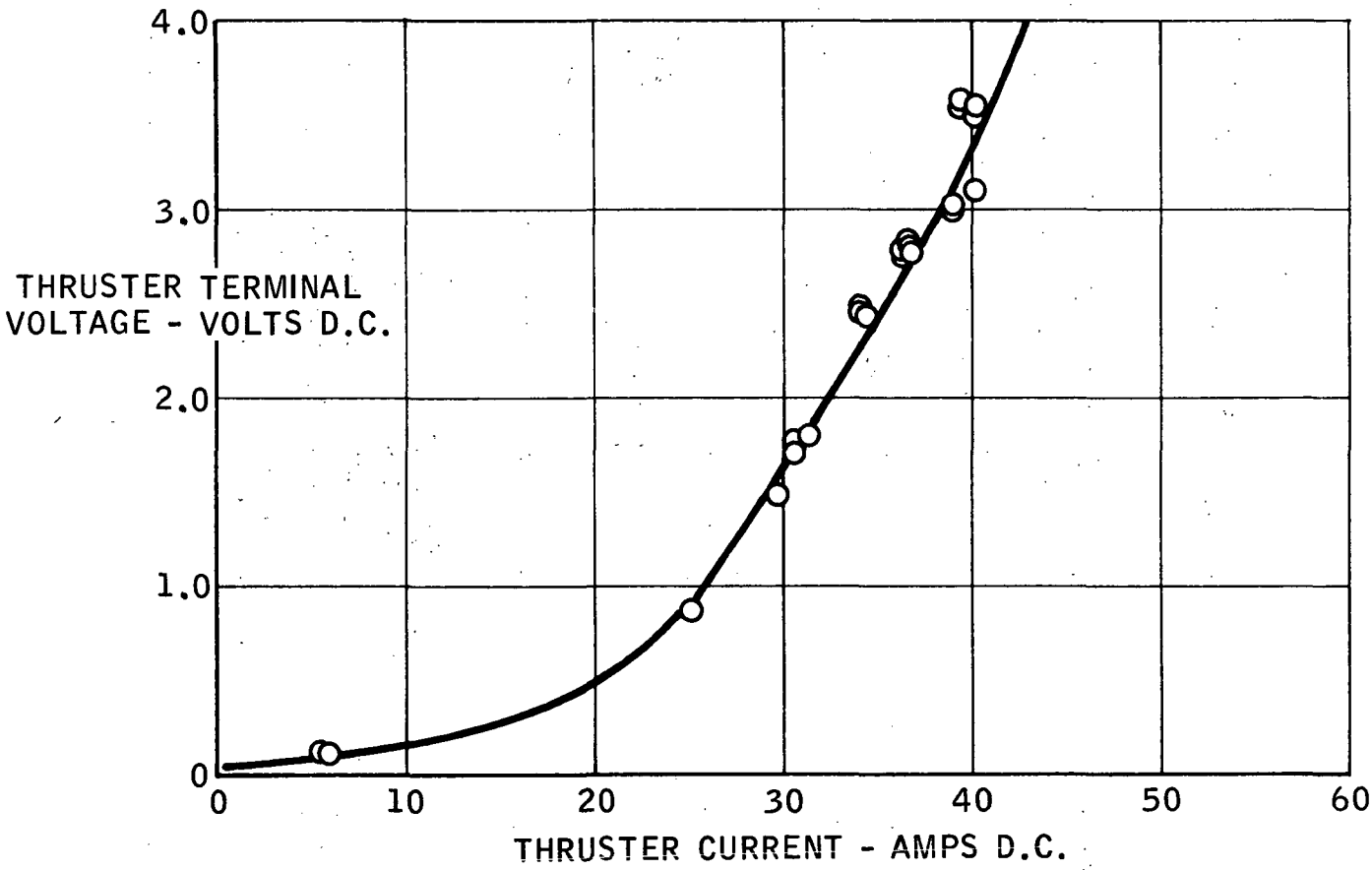

FIGURE 68.

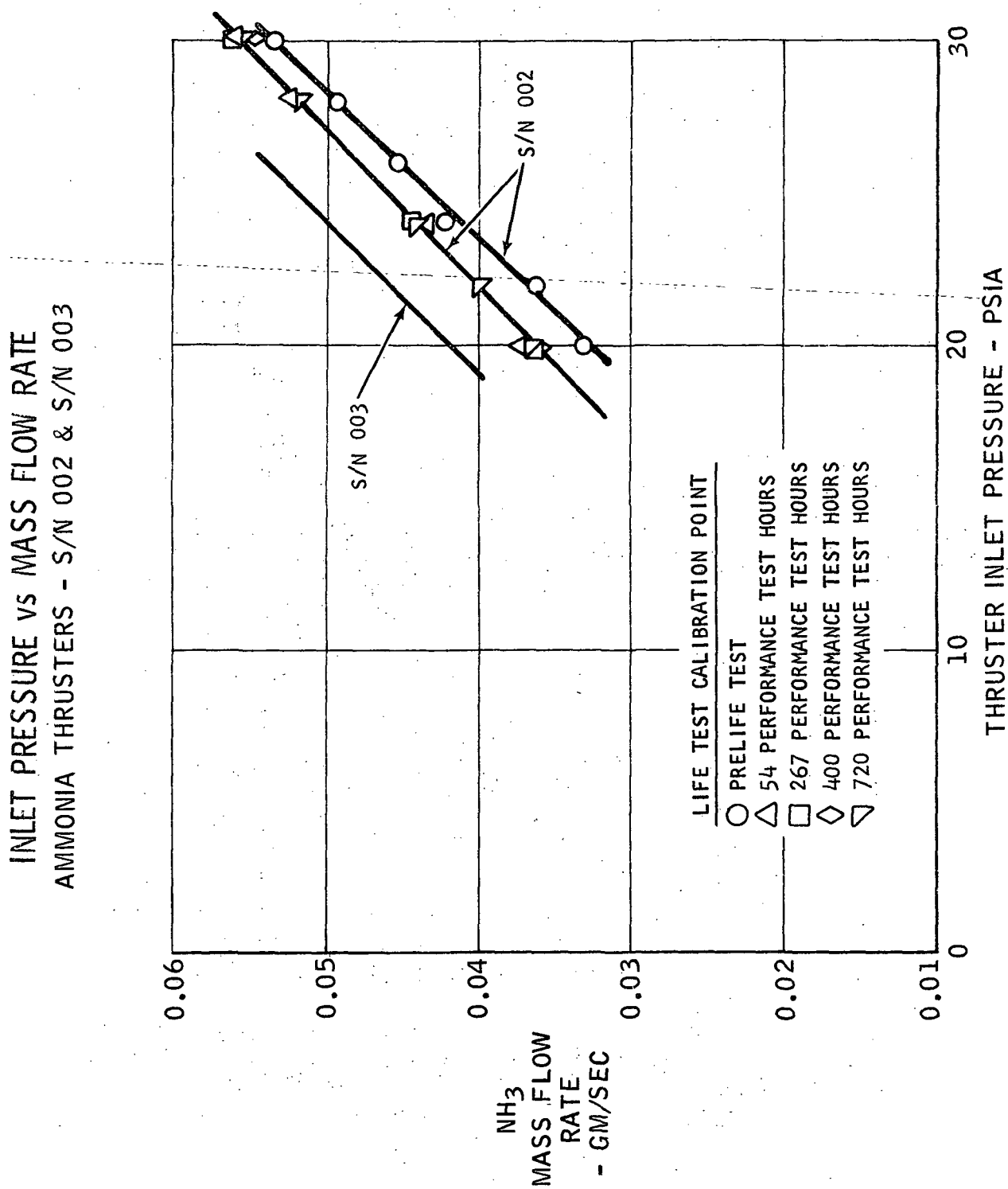
INLET PRESSURE vs MASS FLOW RATE
AMMONIA THRUSTERS - S/N 002 & S/N 003
S/N 002
S/N 003
LIFE TEST CALIBRATION POINT
PRELIFE TEST
54 PERFORMANCE TEST HOURS
267 PERFORMANCE TEST HOURS
400 PERFORMANCE TEST HOURS
720 PERFORMANCE TEST HOURS
0.06
0.05
0.04
0.03
0.02
0.01
NH3 MASS FLOW RATE - GM/SEC
0
10
20
30
THRUSTER INLET PRESSURE - PSIA

FIGURE 69.

the leakage as indicated by "Snoop" leak detector fluid applied to the exterior of the thruster structure was around the joint where the thruster expansion bellows is welded to the thruster structure to provide a pressure tight seal. Exact location of the weld failure was not determined since the thruster was not disassembled and metallographically examined. The magnitude of the leak, while considered significant, was not big enough to have deleteriously affected the thruster pressure drop measurements discussed in another report section. Also, it is felt that the thermal data obtained is representative since the total gas loss is not significant in terms of lost energy of available cooling to distort the thermal distribution.

Thruster thermal performance. - Measured thruster temperatures on the ammonia thruster were reasonably consistent throughout the test period. Locations of measured temperatures are shown in Figure 70. Temperature distributions measured during the periodic performance calibrations are shown in Table VI for the data obtained at the nominal 140 watt operating point and typical thruster temperatures are shown as a function of power in Figure 71. The only major change in thermal data obtained during the test was a noticeable reduction in thruster external case temperature. This was due to amalgamation of the gold cover surface with mercury vapors from the power transmitting pots which overheated periodically during the test.

As with the hydrogen thruster, the thermal data obtained at the nominal operating point of 140 watts was fed back into the data analysis loop to revise and update the thruster thermal model. Rationalization of data obtained from operation using ammonia is considerably more difficult than data obtained on hydrogen. The complicating factor is that of dissociation of the ammonia at high temperature as it passes through the thruster heater network. The factors associated with high percentage dissociation of ammonia result in a high specific impulse because of the lower molecular weight of the exhaust product, and lower than expected metal temperatures, however, a significant increase in power is required to accomplish the dissociation.

The thermal model approach is similar to that discussed previously for the hydrogen thruster except for those changes necessitated because of propellant differences. A flow rate of 0.0144 grams/sec and a power input of 140 watts matches test conditions. As Figure 72 shows, good agreement was obtained with experimental data, except in the expansion bell. The extreme thermal gradient in this area makes precise point temperature measurement by optical pyrometer quite difficult, and the discrepancy is not surprising.

The thermal analysis shows that the inner tube reaches a maximum temperature of 2310^{o}K using ammonia propellant. The exit gas temperature is 2090^{o}K.

THERMOCOUPLE LOCATIONS ON AMMONIA RESISTOJET THRUSTER

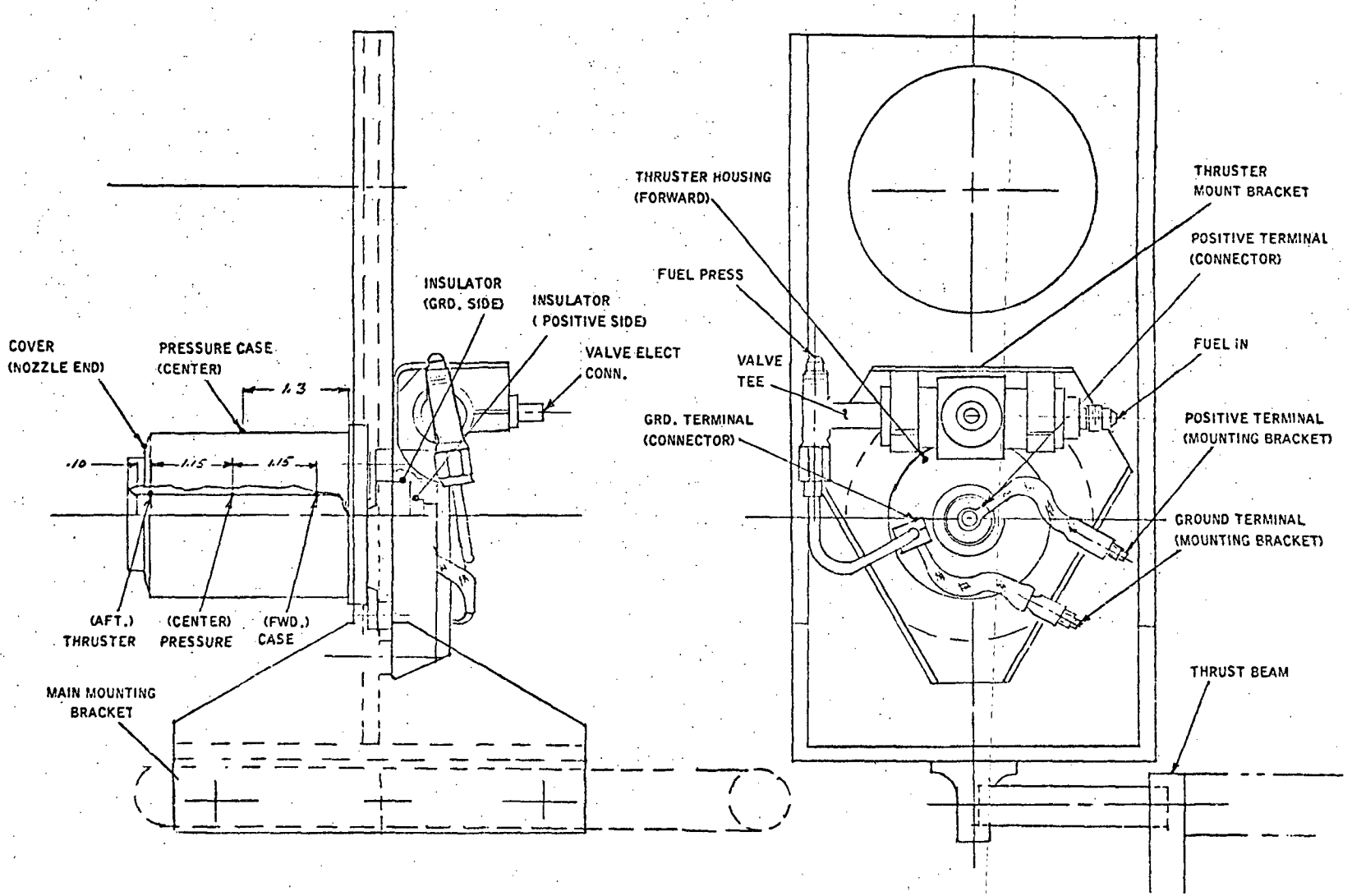

FIGURE 70.

A-72-7-290-54

TABLE VI

AMMONIA THRUSTER TEMPERATURES MEASURED DURING LIFE TEST

LOCATION								
Test Accrued Life - Hours	0	54	267	340	400	500	600	720
Thruster Pressure Case - Forward ^{o}K		628	611	608	609	591	602	589
Cover - Forward End - ^{o}K		461	456	463	468	452	464	452
Insulator - Ground Side - ^{o}K		327	466	486	489	476	486	473
Ground Terminal - Mount Bracket ^{o}K		363	358	363	364	358	366	361
Positive Terminal - Mount Bracket ^{o}K		422	413	416	416	413	416	409
Positive Terminal - Connector - ^{o}K	286	508	488	491	491	485	489	481
Insulator - Positive Side - ^{o}K		518	511	508	511	497	506	494
Thruster Mount Bracket - ^{o}K		343	338	346	346	339	346	341
Main Mount Bracket - ^{o}K		297	291	288	299	-	324	326
Cover - Nozzle End - ^{o}K	387	476	466	476	485	461	479	454
Pressure Case - Center - ^{o}K	1023	1046	999	972	971	941	1011	998
Ground Terminal - Connector - ^{o}K	434	436	431	426	418	419	426	428
Valve Tee - ^{o}K		333	328	336	335	334	337	331
*Inner Element Forward End - ^{o}K	1658	1732	1616	1615	1700	1682	1662	1640
*Thruster Nozzle Near Throat - ^{o}K		1450					1399	1360
Thruster Housing - Forward - ^{o}K	368	481	473	478	481	466	478	496

*Temperatures measured by optical pyrometer

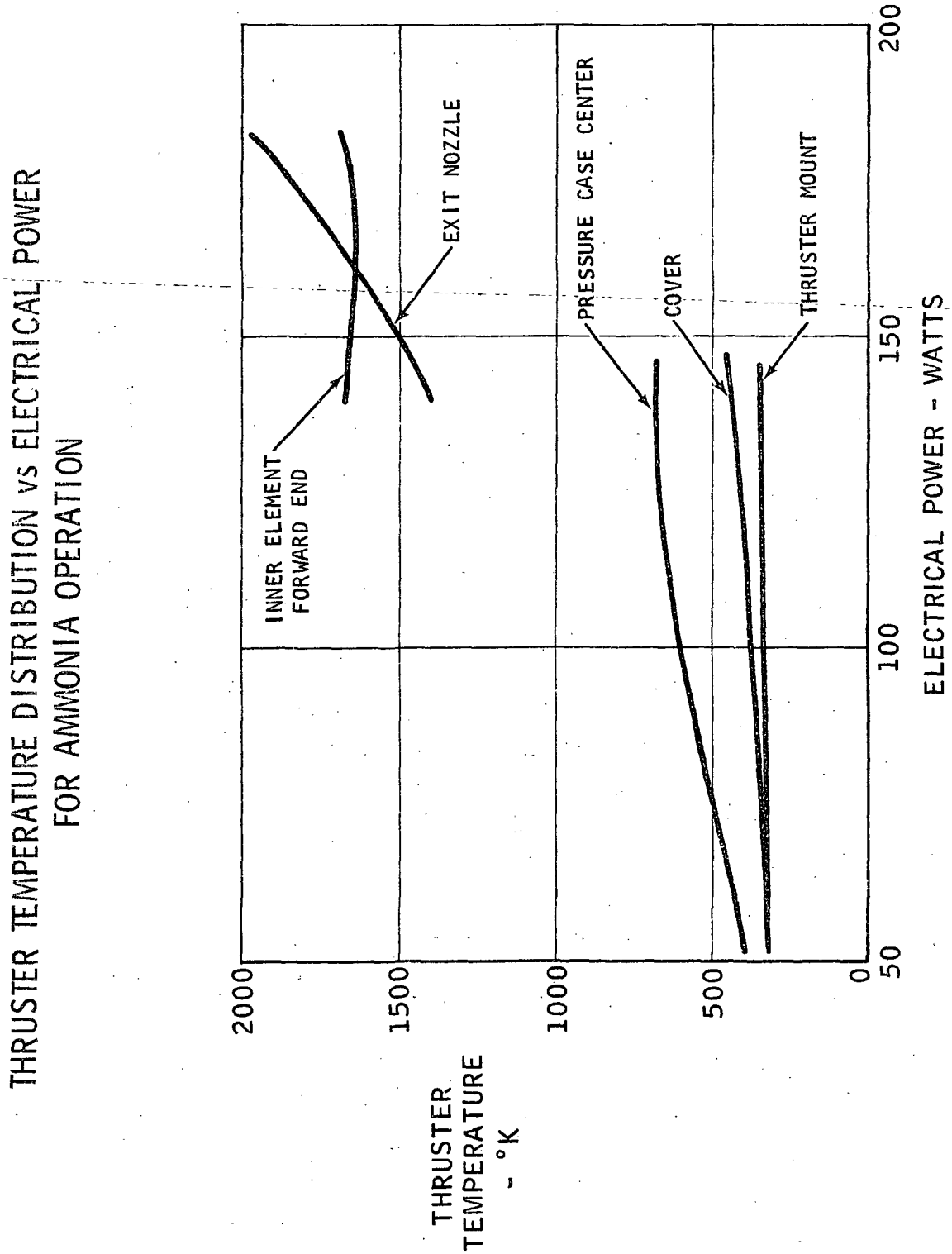
THRUSTER TEMPERATURE DISTRIBUTION vs ELECTRICAL POWER
FOR AMMONIA OPERATION
INNER ELEMENT
FORWARD END
EXIT NOZZLE
PRESSURE CASE CENTER
COVER
THRUSTER MOUNT
THRUSTER
TEMPERATURE
- °K
2000
1500
1000
500
0
50
100
150
200
ELECTRICAL POWER - WATTS

FIGURE 71.

MODEL 110 RUGGEDIZED RESISTOJET WALL TEMPERATURES

NH_3 PROPELLANT - 140 WATTS

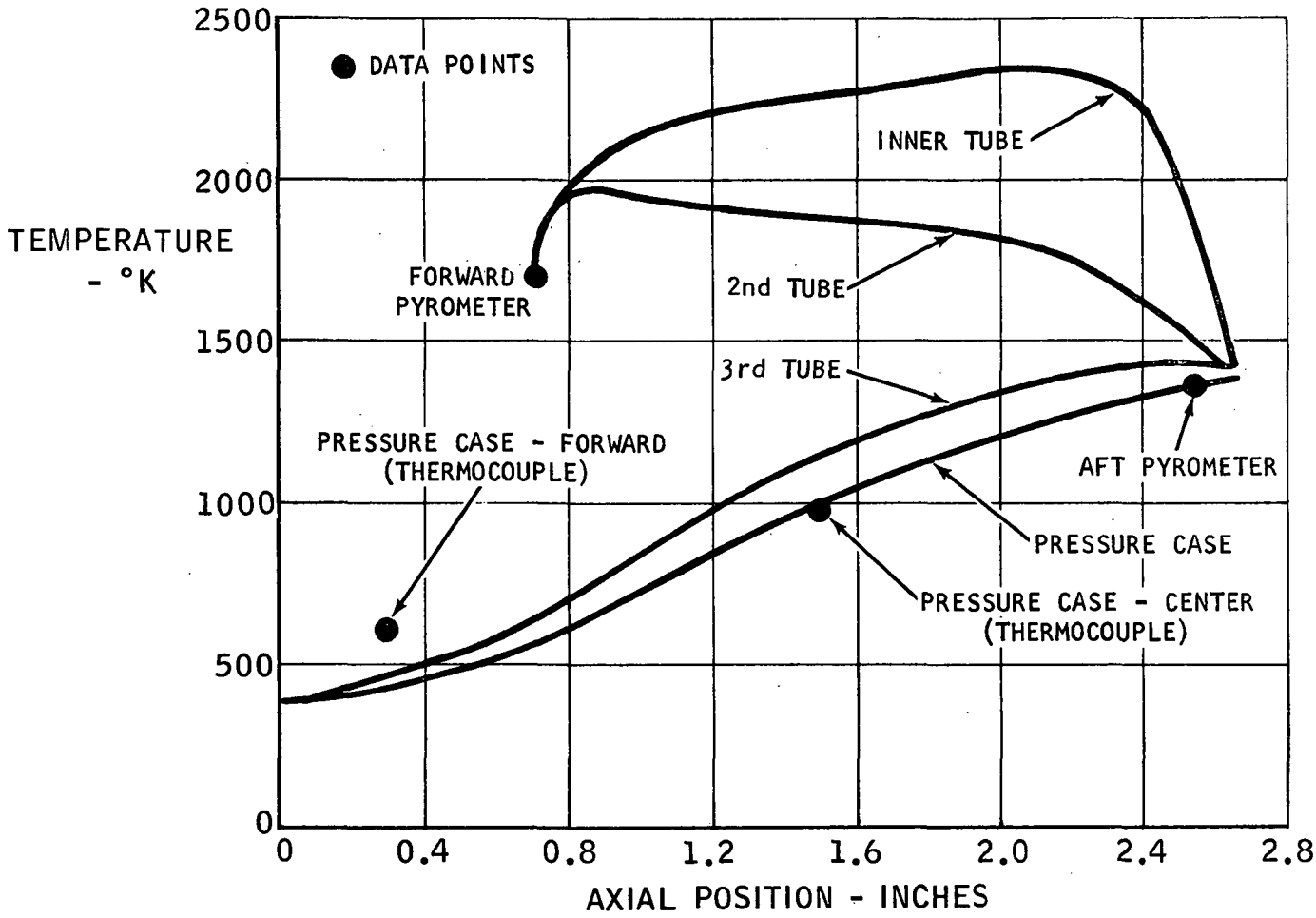

FIGURE 72.

The high metal temperatures reflect the poor thermal conductivity of ammonia when compared to hydrogen. A greater thermal potential is required to achieve equivalent energy transfer from the thruster structure to the ammonia than is the case when hydrogen propellant is used.

The thermal conductivity of ammonia gas was estimated from Reference 9 data. Ammonia enthalpy was taken from Reference 10 assuming chemical equilibrium.

EXTENDED RANGE PERFORMANCE TESTS

Following completion of all other required tests and determination that the basic thruster structure had not significantly degraded as a result of the 720 hours of cycling operation already completed, it was decided to demonstrate high performance levels on both propellants. The S/N 002 thruster was chosen to perform the high specific impulse tests. Goals were to demonstrate 700 seconds I_{sp} using hydrogen propellant and a nominal 350 seconds I_{sp} using ammonia propellant. A second objective was to demonstrate extended operational life capability of the thruster valves.

Specific impulse performance goals were met easily without exceeding 2400°K exterior metal temperatures. Demonstrated performance on hydrogen was 703.7 seconds I_{sp} and performance on ammonia was 359.0 seconds I_{sp} as shown in Figure 73. As expected, the thruster temperatures were quite hot during the high performance hydrogen tests. Maximum measured metal temperature was 2120°K measured just downstream of the thruster throat with the micro optical pyrometer. The forward or dome end of the inner heating element was measured to be 1855°K. This data infers that the redesign of the inner heating element to progressively reduce the wall thickness toward the nozzle throat thus increasing ohmic heating in that location was successful. Exact temperature just upstream of the throat or at the throat was impossible to determine since there was no acceptable view angle for the pyrometer to determine the temperature. Surprisingly, the metal temperatures measured during the high performance tests on ammonia with the same thruster demonstrated significantly lower temperatures than expected for the performance generated. Maximum metal temperature measured during the 359 second ammonia run was 1980°K at the nozzle location. The reduced temperatures undoubtedly resulted from dissociation of the ammonia into its nitrogen/hydrogen components. Although exterior temperatures measurable with the existing instrumentation, were reasonably low for the power condition, interior temperature of the inner heating element had to be in excess of 2400°K to generate the measured performance. Results of the tests were encouraging in that it would appear that the thruster is capable of being operated at the high power conditions on either ammonia or hydrogen for a significant period.

After all operational performance tests were completed on the thruster assemblies, the valves were subjected to extended life testing in ammonia and hydrogen. The valves had each accrued about 100 operational cycles in propellant as part of the thrusters during the life test. Extended range of operation tests were performed to determine valve operational life characteristics.

Examination of the valves at conclusion of the thruster life test indicated that the valves were in excellent condition and leak free. The valves were reinstalled in the propellant system and cycled for 100,000 additional cycles. The valve from S/N 001 was cycled using hydrogen as the propellant and the valve from S/N 002

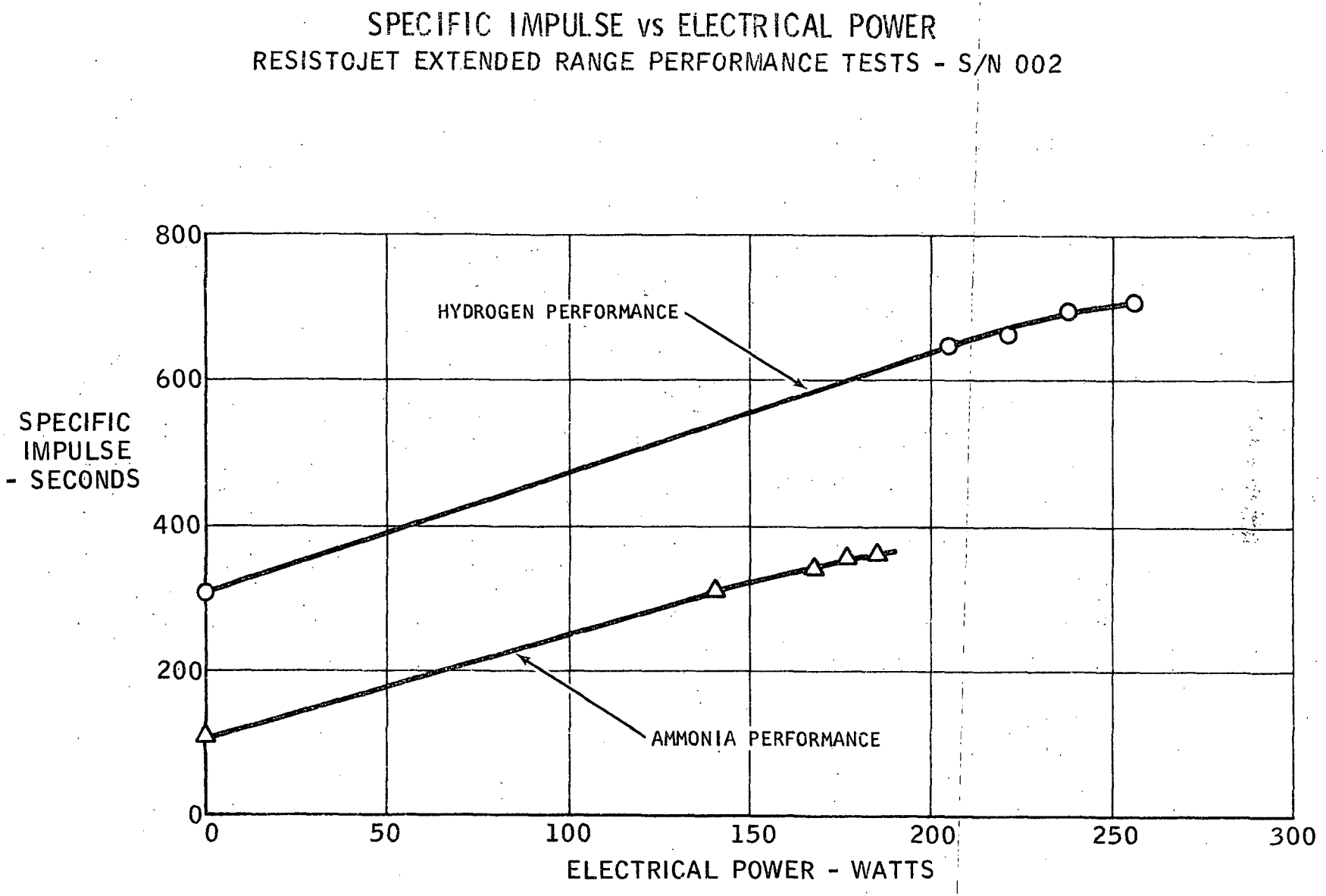
SPECIFIC IMPULSE vs ELECTRICAL POWER
RESISTOJET EXTENDED RANGE PERFORMANCE TESTS - S/N 002
SPECIFIC IMPULSE - SECONDS
800
600
400
200
0
HYDROGEN PERFORMANCE
AMMONIA PERFORMANCE
0
50
100
150
200
250
300
ELECTRICAL POWER - WATTS
A72-7-290-47

FIGURE 73.

as cycled using ammonia as the test propellant. Leakage checks were performed at 10,000, 20,000, 50,000, 75,000 and 100,000 accrued cycles to assure valve seat integrity. Cycling was performed at a pulse repetition rate of about 50 cycles per second.

Both valves performed in an excellent manner throughout the test. No leakage was detected during any of the leakage tests within the accuracy of the leak test setup. Minimum leakage which can be recorded reasonably accurately using the test setup was approximately 0.5 SCCH of helium leakage.

Successful completion of the additional life cycling tests demonstrated conclusively that the valve design is ready for flight qualification tests. Additional information regarding basic design of the valve and the results of other successful bench testing conducted using the valves can be found in Reference 11.

CONCLUSIONS

Completion of the Ruggedized Resistojet life test program covered in this report has resulted in significant state of the art advancement in the development technology of production of a flight qualification capable thruster. Important outputs from the program included:

- Demonstration of significant thruster life capability both at nominal performance values and under extended range operation. During this program, 720 hours of cycling operation was demonstrated on both the hydrogen and the ammonia thrusted operation. The ammonia thruster accrued approximately 350 "on-off" cycles and 392.2 hours of operation.

- Extended range operational tests were performed using the S/N 002 thruster to demonstrate 704 seconds I_{sp} using hydrogen as propellant and 359 seconds I_{sp} using ammonia as propellant.

- Detailed documentation of response characteristics of the resistojet structure to environmental loads including vibration, shock and acceleration.

- Successful completion of significant environmental test loads without structural damage. Passage of these tests demonstrated the increased capability of the resistojet structure to withstand expected launch and other environmental loads.

- Documentation that the thruster structure is satisfactorily designed to withstand pressure and thermal differential growth loads under step input starting conditions. Output of this test series alone can result in significant reduction of the required support equipment required for space operation of the resistojet.

- Increased capability with regard to maximum required operating temperature was shown. Maximum metal temperatures measured during steady state performance testing indicated that the nominal life test operating conditions could be maintained with an approximate 500°K margin in operating temperature gained over previous development units fabricated and tested.

- A valve suitable for operation with either hydrogen or ammonia was developed and successfully operated during the program for in excess of 100,000 operational cycles with less than 1 SCCH measured helium leakage. This valve has demonstrated excellent capability for multi-application operation where requirements including high response, capability for extended operation with extremely low power draw and high reliability are required.

- Vendors were developed for producing complex shaped, miniature parts through vapor deposition techniques. In addition, metal to ceramic seal technology was developed, improving capability and ultimately reliability of the thruster.

In summary, the program resulted in conversion of an essentially research and development status piece of hardware to a producible, operational thruster capable of flight qualification with only minor changes.

Minor problem areas were uncovered where increased quality control will be required, however, in general, considering the difficulty of conversion from a hand made development unit to a production capable thruster, the program was highly successful.

RECOMMENDATIONS

The favorable results obtained during this program indicate the Model 110 Ruggedized Resistojet Thruster to be nearly ready for qualification and flight experimental testing. It is accordingly recommended that design efforts be continued to accomplish the following:

a. Further evaluate and refine electron beam weld schedules used to control the assembly of the welded rhenium parts.

b. Fabricate typical weld sections incorporating the required weld schedule changes, test in high temperature vacuum environment and metallographically examine the weld specimens to determine final weld configuration adequacy.

c. Incorporate minor redesign elements required to avoid the touching phenomena experienced on the hydrogen thruster during the test program.

d. Fabricate at least three qualification configuration thrusters to the revised drawings and subject them to a flight qualification program to document readiness for incorporation into a space experiment system. The qualification program should include at the minimum, environmental tests typical of maximum environments, calibration under expected operating conditions and off limits testing to determine and document thruster operating margins.

Continuation of the program as indicated above would complete the transition of the resistojet concept from development status to flight ready hardware with a minimum of development risk.

REFERENCES

1. Page, R. J., and Short, R.A., "Definition of a Resistojet Control System for the Manned Orbital Research Laboratory", Final Report, Addendum to Volume V, 720-Hours Resistojet Life Test, NASA CR-66604A, September 1968

2. Yoshida, R.Y., Halbach, C.R., Page, R.J., Short, R.A. and Hill, D.S., "Resistojet Thruster Life Tests and High Vacuum Performance", NASA CR-66970, July 1970

3. Yoshida, R.Y., "Technology Development and Demonstration of a Low Thrust Resistojet Thruster", Sixth Monthly Progress Report, The Marquardt Company PR 5078-6, October 1970

4. Anon: "Calibration and Maintenance of Test Instrumentation and Test Equipment", IDP 70-24, The Marquardt Company, June 1967

5. Wilson, M.S., "A Thermal Model of the Ruggedized Resistojet", Marquardt MIR #381, August 1970

6. Sims, C.T., "Investigation of Rhenium", WADC Tech. Report 54-371, 1954

7. Grier, N.T., "Calculation of Transport Properties and Heat Transfer Parameters of Dissociating Hydrogen", NASA TN D-1406, 1962.

8. Summary, R.W., "Variable Properties Laminar Gas Flow Heat Transfer and Pressure Drop", Arizona University Press, 1969

9. Gambill, W.R., "Estimating Engineering Properties", Reprint from Chemical Engineering, 1957.

10. Bennett, AVCO 1st Quarterly Progress Report, Contract NAS 3-5908

11. Lynch, R. A., "The Design and Development of a Miniature Bi-Stable Latching Solenoid Valve for Low Thrust Resistojets", NASA CR-112160, June 1972.

APPENDIX A

DATA ACCURACY AND DEFINITION OF PERFORMANCE PARAMETERS

Accuracy of the data acquisition system was completed based on the system components in use for the resistojet thruster test facility. For the purposes of the analysis, the following terms apply:

Standard deviation, σ. -- If a parameter is measured n times and each measurement differs from the average by an amount δ n then

$$\sigma = \sqrt{\frac{\sum_{m=1}^{k} (\delta_n)^2}{k - 1}}$$

Probable error, p. -- The probable error is that magnitude of deviation whose probability of being exceeded is one-half. It can be shown that:

$$p = 0.6745\ \sigma$$

Manufacturers stated accuracy. -- It will be assumed that manufacturers stated accuracy is $\pm 3\ \sigma$ which means that the probability of finding a deviation outside this band is .003.

Rules for combining errors. -- Where $v = x \pm y$

$$\sigma_v = \sqrt{\sigma_x^2 + \sigma_y^2}$$

where $v = x^m y^q$

$$\sigma_v = v \sqrt{m^2 \left(\frac{\sigma_x}{x}\right)^2 + q^2 \left(\frac{\sigma_y}{y}\right)^2}$$

These definitions and rules were used in determining the probable errors, for the various measured and calculated parameters of interest, shown in Table A-I. The percentages shown are calculated at normal operating conditions. These calculated quantities $3\ \sigma$ and p are the ones used for evaluation of the precision with which measurements are made.

TABLE A-I

Measured parameters	3σ	p
Thrust	1.4%	0.3%
Mass flow	3.0%	0.7%
Thruster cover temperature	3.0%	0.7%
Cell pressure	11.7%	2.6%
Voltage	0.25%	0.06%
Current	0.3%	0.07%
Calculated parameters	**3σ**	**p**
Specific impulse	3.3%	0.7%
Electric power	0.4%	0.09%
Resistance	0.04%	0.09%
Overall efficiency	4.3%	1.0%
Chamber gas temperature	7.4%	1.7%
Chamber pressure	6.9%	1.6%

Definition of Performance Parameters

Specific impulse, I_{sp}, seconds

$$I_{sp} \triangleq \frac{F}{\dot{m}} \tag{1}$$

where F = measured thrust by dynamometer, g

$\dot{m}$ = propellant mass flow, $g\text{-}sec^{-1}$

Electric power to terminals, P_e, watts

$$P_e = E_t \times I_t \tag{2}$$

E_t = electric voltage difference between thruster terminals, v

I_t = electric current passing between terminals, a

Resistance, R, ohms

$$R = \frac{E_t}{I_t}$$

Efficiency - total power overall, η_o

$$\eta_o \triangleq \frac{F \times I_{sp}}{20.8\ (P_e + P_i)} \tag{3}$$

Initial power in gas, P_i, watts

$$P_i = \dot{m}\ h\ 4.186 \tag{4}$$

h = enthalpy of an ideal gas above absolute zero, cal/gm

Note: $\triangleq$ means "definition"

Power in the jet, P_j, watts

$$P_j = P_e + P_i - P_1 \tag{5}$$

P_1 = heat lost from the thrustor prior to the exhaust jet, w

Heater efficiency, η_H

$$\eta_H \triangleq \frac{P_j}{P_e + P_i} \tag{6}$$

Nozzle efficiency, η_n

$$\eta_N \triangleq \frac{F \times I_{sp}}{20.8\, P_j} \tag{7}$$

or

$$\eta_N = \frac{\eta_o}{\eta_H} \tag{8}$$